

8-2012

Investigating the Role of Mechanosensitive Ion Channels in Urothelial Cell Pressure Mechanotransduction

Shawn Olsen

Clemson University, solsen@clermson.edu

Follow this and additional works at: https://tigerprints.clemson.edu/all_dissertations

 Part of the [Biomedical Engineering and Bioengineering Commons](#)

Recommended Citation

Olsen, Shawn, "Investigating the Role of Mechanosensitive Ion Channels in Urothelial Cell Pressure Mechanotransduction" (2012). *All Dissertations*. 982.

https://tigerprints.clemson.edu/all_dissertations/982

This Dissertation is brought to you for free and open access by the Dissertations at TigerPrints. It has been accepted for inclusion in All Dissertations by an authorized administrator of TigerPrints. For more information, please contact kokeefe@clermson.edu.

INVESTIGATING THE ROLE OF MECHANOSENSITIVE
ION CHANNELS IN UROTHELIAL CELL
PRESSURE MECHANOTRANSDUCTION

A Dissertation
Presented to
the Graduate School of
Clemson University

In Partial Fulfillment
of the Requirements for the Degree
Doctor of Philosophy
Bioengineering

by
Shawn Martin Olsen
August 2012

Accepted by:
Dr. Jiro Nagatomi, Committee Chair
Dr. Martine Laberge
Dr. C. Ken Webb
Dr. P. Darwin Bell

-Abstract-

Overactive bladder (OAB) is a bladder disorder that is characterized by bladder storage symptoms of urgency with or without urge incontinence, frequency, nocturia, and, as of 2003, affected approximately 16.5% of adults in the United States with an annual treatment cost of over \$65 billion. While therapies are available to mitigate the symptoms of OAB, there are no treatments for the cause of OAB, due to the lack of understanding of the etiology of the disorder. Recent research has provided evidence that the bladder urothelium is not just a passive barrier, but is also sensitive to various chemical and mechanical stimuli and responds by releasing neurotransmitters (NO, ATP) to participate in the sensory function of the bladder. Thus, it has been suggested that overactive bladder is caused, at least in part, by altered sensitivity to bladder fullness by urothelial cells (UCs). While previous research has demonstrated that the urothelium responds to tissue stretch induced by elevated pressure, the role of hydrostatic pressure alone in the cellular events was unclear. Therefore, this doctoral thesis sought to decouple the two stimuli and investigate the effects of pressure on UCs, especially the role of select ion channels in UC pressure mechanotransduction. Overall, the objective of this project was to test the hypothesis that UCs sense hydrostatic pressure via activation of membrane-bound ion channels, and that these cells respond by releasing ATP. In order to test this hypothesis, multiple *in vitro* studies were performed in which UCs were

subjected to controlled hydrostatic pressure while monitoring their response to the stimulus.

First, using a custom-made pressure chamber, rat bladder UCs were exposed to sustained hydrostatic pressure (5–20 cmH₂O) for up to 30 min. When compared to the control, the supernatant culture media of UCs exposed to hydrostatic pressure (10-15 cmH₂O) exhibited a significant increase in ATP. In the absence of extracellular calcium, ATP release due to hydrostatic pressure was attenuated. Pharmacologically blocking transient receptor potential (TRP) channels, stretch-activated channels (SACs), and the epithelial sodium channel (ENaC) all abolished the hydrostatic pressure-evoked ATP release. These results provided evidence for the first time that cultured UCs are sensitive to physiologically relevant levels of hydrostatic pressure and that one or multiple mechanosensitive ion channels play a role in the mechanotransduction of hydrostatic pressure. These findings support the view that not only tissue stretch or tension, but also pressure is an important parameter for the sensing of bladder fullness.

Second, UCs loaded with a fluorescence dye, calcein-AM were exposed to hydrostatic pressure up to 20 cmH₂O while fluorescence intensity was measured in real-time. UCs exposed to hydrostatic pressure exhibited a sharp decrease in fluorescence intensity, indicative of a cell volume increase. These observations were confirmed by confocal imaging of primary UCs, which displayed a 7.7% volume increase when exposed to 20 cmH₂O. Exposing the cells to Na-free solution and blocking of ENaC during pressure application resulted in a significantly lower change in cell volume. These

results provided part of a novel mechanism involving cell swelling for mechanotransduction of hydrostatic pressure and an explanation for the previously reported ENaC-dependent, pressure-evoked ATP release by UCs.

Finally, UCs were exposed to hydrostatic pressure while monitoring the kinetics of ATP release. UCs exposed to pressure (10 cmH₂O) exhibited a sharp increase in ATP release that slowly decreased over time, while remaining elevated compared to baseline levels. This response was inhibited by blocking TRPV4 and ENaC. When UCs were exposed to a hypotonic stimulus, a sharp increase in ATP was exhibited followed by an immediate decrease to baseline levels. This increase in ATP was inhibited when blocking TRPV4, but was still present, albeit attenuated compared to the unblocked cells, when blocking ENaC. These results suggest that both ENaC and TRPV4 activation are necessary for ATP release during exposure to hydrostatic pressure. In addition, the osmotic shock results suggest that ENaC is upstream of the cell swelling response, while TRPV4 activation occurs between cell swelling and the ATP release.

In summary, the results of the present research provide evidence that UCs respond to hydrostatic pressure with an increase in cell volume, activation of multiple mechanosensitive ion channels, and elevated ATP release. We have identified a possible mechanism by which UCs detect pressure and are the first to show that UCs respond to hydrostatic pressure in the absence of tissue stretch, which provides a novel contribution to cell mechanobiology that hydrostatic pressure alone is an important parameter involved in bladder mechanotransduction. This knowledge, in turn, will help elucidate

the mechanism by which UCs, in normal and pathological cases, sense bladder fullness and ultimately aide in treatment of bladder disorders such as OAB.

-Acknowledgments-

I would first like to thank the Department of Bioengineering at Clemson University for giving me the opportunity to pursue my degree. In addition, I would like to thank Dr. Jiro Nagatomi for his support and guidance in both research and life over the past five years. I'd also like to thank my committee who have helped me shape my project goals and allowed me to delve deeper into my research than I ever thought possible. I wish to extend my deepest gratitude for those who have directly helped me with my research, including Joshua Stover, Stacy Steele, Lauren Eskew, Kevin Champaigne and all of the individuals at the Godley-Snell Research Center. Finally, I'd like to thank my friends and family, and specifically my wife, Kimberly, who have supported me and never stopped believing in me.

-Table of Contents-

	Page
Abstract	i
Acknowledgments	v
List of Figures	x
List of Tables	xiii
 Chapter 1: Introduction and Background	
1.1 Clinical Significance.....	1
1.2 Bladder Anatomy.....	1
1.3 Bladder Physiology.....	4
1.4 Cellular Mechanotransduction	7
1.5 Mechanosensitive Ion Channels.....	9
1.6 Ion Channel-Mediated Mechanotransduction in Mammalian Cells.....	17
1.7 Urothelial Mechanotransduction.....	21
1.8 Role of Ion Channels in Urothelial Mechanotransduction.....	23

Chapter 2: Rationale and Specific Aims

2.1 Rationale.....28

2.2 Research Hypothesis.....29

Chapter 3: To Examine the Role of Mechanosensitive Ion Channels in Pressure

Mechanotransduction in Rat Bladder Urothelial Cells

3.1 Introduction.....31

3.2 Materials and Methods.....34

3.3 Results.....42

3.4 Discussion.....49

Chapter 4: To Elucidate the Role of Cell Volume Change in Mechanotransduction of Hydrostatic Pressure in Urothelial Cells

4.1 Introduction.....56

4.2 Materials and Methods.....58

4.3 Results.....63

4.4 Discussion.....71

Chapter 5: To Characterize the ATP Release Kinetics by Urothelial Cells and to Determine the Potential Role of TRPV4 in Pressure Mechanotransduction

5.1 Introduction.....	78
5.2 Materials and Methods.....	80
5.3 Results.....	84
5.4 Discussion.....	92

Chapter 6: Conclusions

6.1 ATP Release by Urothelial Cells in Response to Hydrostatic Pressure.....	98
6.2 Specificity of Ion Channel Inhibition.....	99
6.3 Time-course Analysis of ATP Release.....	100
6.4 The Specific Pathway of ATP Release during Pressure Mechanotransduction.....	101
6.5 The Role of Ca ²⁺ in Pressure-Induced ATP Release	102
6.6 Cell Volume Increase due to Hydrostatic Pressure.....	103
6.7 Clinical Relevance- Overactive Bladder.....	104

6.8 Summary.....	105
6.9 Future Project Recommendations.....	106
Appendices:	
A: Primary Urothelial Cell Isolation Protocol.....	108
B: ATP Assay Analysis Protocol.....	111
C: Florescence and Confocal Imaging Analysis Protocol.....	113
D: Pressure Chambers Used in Experiments.....	118
References.....	122

-List of Figures-

	Page
Figure 3-1: Cell characterization images of urothelial cells.....	36
Figure 3-2: Custom-made pressure chamber.....	37
Figure 3-3: Gene expression of membrane-bound ion channels in urothelial cells.....	43
Figure 3-4: Time-course ATP release from urothelial cells exposed to hydrostatic pressure.....	44
Figure 3-5: ATP release from urothelial cells in response to hydrostatic pressure in the presence of a calcium chelator.....	45
Figure 3-6: ATP release from urothelial cells in response to hydrostatic pressure in the presence of ion channel blockers.....	48
Figure 4-1: Schematic diagram of custom-made pressure perfusion chamber.....	61
Figure 4-2: Pseudo-color fluorescence images of UROtsa cells under hydrostatic pressure.....	64
Figure 4-3: Change in cell volume of different cell types.....	65

Figure 4-4: Change in fluorescence intensity of primary urothelial cells undergoing osmotic shock.....	66
Figure 4-5: Confocal images of urothelial cells under hydrostatic pressure taken at $z = 1 \mu\text{m}$	68
Figure 4-6: Histogram of difference in total cell area between pressure and control groups.....	69
Figure 4-7: Relative change in fluorescence intensity of primary urothelial cells without Na^+ and in the presence of ENaC blocker.....	70
Figure 5-1: ATP release of primary urothelial cells when exposed to osmotic shock.....	85
Figure 5-2: ATP release of UROtsa cells when exposed to osmotic shock.....	86
Figure 5-3: ATP Release of primary urothelial cells when exposed to hydrostatic pressure	88
Figure 5-4: ATP release of UROtsa cells when exposed to hydrostatic Pressure.....	89
Figure 5-5: ATP Release of primary UCs when exposed to TRPV4 agonist.....	91
Figure A-1: Pressure chamber in cell culture incubator.....	118
Figure A-2: Assembled view of Warner RC-21 chamber.....	119

Figure A-3: Top-down view of custom perfusion chamber.....120

Figure A-4: 3-D CAD diagrams of the perfusion side and vacuum side of the
Vacu-Cell™ flow chamber.....121

-List of Tables-

	Page
Table 1.1: Properties of mechanosensitive ion channels possibly related to bladder sensory transduction.....	16
Table 3.1: Drugs used in ATP determination study.....	40
Table 4.1: Time constants calculated from osmotic shock experiments.....	67

-Chapter 1-

Introduction and Background

1.1 Clinical Significance

Overactive bladder (OAB) is a bladder disorder that, as of 2003, affected approximately 16.5% of adults in the United States and required an annual treatment cost of over \$65 billion [1]. OAB is characterized by the inability to control voiding, which leads to the involuntary leakage of urine. Typically, continence involves a state of balance in which the urethral pressure is higher than the bladder pressure, keeping the urine from exiting the bladder. However, in OAB, the patient is unable to keep the urethral pressure high, which causes urine to involuntarily leak from the bladder. There are several suggested causes of OAB, one of which involves the inability of the bladder to properly sense bladder pressure [2]. Whether it's the afferent nerves innervating the bladder wall, or the UCs lining the inside of the bladder, if the patient is unable to properly sense bladder filling, continence becomes very difficult. Therefore, research in the area of bladder mechanotransduction is critical for better understanding the possible causes of OAB at the cellular level.

1.2 Bladder Anatomy

The bladder is a hollow, muscular organ in the urinary system with the main function of storage and voiding of urine that is collected from the kidney through the

ureters. Its wall tissue is comprised of several layers of detrusor muscle, a submucosa, and a relatively thin urothelium [3].

Detrusor Layer

The detrusor muscle layer is composed of smooth muscle cells and the extracellular matrix (Type I and III collagen, elastic fibers, and glycosaminoglycans). These cells, in response to efferent nerve signals transmitted from the pelvic and hypogastric nerves originating in the spinal cord, contract to force urine out of the bladder through the urethra [4]. Detrusor contraction is similar to vascular smooth muscle contraction in that it depends on the interaction of contractile proteins actin and myosin as well as phosphorylation of myosin light chain by myosin light chain kinase [4].

Urothelium

The urothelium is the lining of the urinary tract between the renal pelvis and the bladder. The urothelium is comprised of at least three layers of cells: the basal cell layer attached to the basement membrane, an intermediate cell layer, and a superficial (apical) layer composed of large, hexagonally-shaped cells, also called umbrella cells [5]. Basal cells are the smallest cells (~10 μ m in diameter) that are in contact with the underlying connective tissue and capillaries. Intermediate cells (10-25 μ m in diameter) are pyriform in shape and sit on the basal layer to form a cross-section that can be anywhere from one

to several cell layers thick [6]. The large umbrella cells compose the superficial layer that normally range from 25-250 μm in diameter [6]. The umbrella cells contain tight junctions that prevent ions from passing from urine to the blood stream during the storage phase [5].

Neuroanatomy of Bladder

In addition to the transitional epithelial and smooth muscle layers that comprise the bladder, efferent and afferent nerve pathways of the peripheral nervous system are in contact with the basal layer of the urothelium. Retrograde studies in humans have determined that most of the nerves that receive sensation from the bladder are located in the thoracolumbar region of the spinal cord and transmits signals through the pelvic nerve [7]. In addition to the pelvic nerve, some afferent nerves are found to transmit bladder filling signals through the hypogastric nerve.

These nerve pathways are associated not only with normal bladder filling sensations, but also with bladder pain [8]. In a study of the distribution of bladder afferent nerves in rats [9], it was found that the axons were located in four different areas: (1) at the base of the epithelium, (2) inside junctions between epithelial cells, (3) on blood vessels, and (4) along muscle bundles. It is important to note that except for perivascular axons, all afferent axons lie either inside the urothelium or in a subepithelial plexus very close to the urothelium. These results suggest that the urothelium appears to play an important role in the physiology of the bladder.

1.3 Bladder Physiology

The bladder has two distinct functions for normal urological activity: urine storage and voiding. During storage, urine flows from the kidney passes through the ureters and is collected into the bladder; the urethra is closed and the bladder smooth muscle is relaxed, which allows for the bladder pressure to stay low ($< 10 \text{ cm H}_2\text{O}$) over a large range of bladder volumes [10]. When the bladder fills, the urothelium becomes thinner as the basal membrane begins to stretch. The underlying cells that were once multi-layered begin to be pushed laterally into a monolayer to make room for the increased urine volume. As a result, the umbrella cells express a large change in shape from cuboidal to a flat, squamous morphology [6]. The conventional view is that the afferent nerves of the parasympathetic nervous system are activated via mechano-sensitive A δ -fibers when the bladder is stretched due to filling [11]. These signals are interpreted by the central nervous system as fullness of the bladder and thus the desire to void.

The nerve afferents activated during bladder filling are myelinated A δ -fibers and unmyelinated C-fibers, which are located in the pelvic nerve and transmit signal from the bladder wall to both the pelvic nerve and hypogastric nerve in the spinal cord [8]. A δ -fibers send out information to the brain through afferent nerves regarding bladder filling by responding to active contraction and passive distention of the bladder wall [8]. The pressure threshold for these fibers is from 5cm to 15cm H $_2$ O, which is the normal pressure range at which humans report the sensation of bladder filling [8]. C-fibers are

activated mainly when chemical irritation occurs in the bladder. When the bladder is irritated the C-fiber afferents begin to spontaneously fire when the bladder is empty and increase firing during bladder filling [12].

During voiding the muscles of the urethra relax and the bladder smooth muscles contract. This contraction raises the intravesical pressure cause urine to expel from the urethra [6]. These actions are controlled by efferent sympathetic and parasympathetic nerves that emerge from the sacral and thoracolumbar sections of the spinal cord and lie near the basal layer of the bladder urothelium. When the bladder has finished voiding, the urethral contracts and the bladder wall relaxes to prepare for the next storage phase.

Until recently, it was considered that the storage and voiding functions of the bladder were controlled strictly by the nervous system with both sensing of bladder fullness and voiding of the bladder. Recent research, however, has shed light onto the urothelium as a possible component of bladder sensory function [13-16]. These findings that the urothelium releases signaling molecules in response to bladder filling and noxious stimuli such as pain and bladder impurities have replaced the previous perception of the urothelium as merely a passive barrier with the proposal of the urothelium being an important player in the sensing and mechanotransduction. Afferent nerve pathways that have been thought to aid in bladder mechanosensation run through and around urothelial cells (UCs) on the basal portion of the urothelium [11]. Recent evidence through multiple studies suggest that the urothelium may communicate bladder fullness by

transmitting signals via a paracrine signaling pathway in the underlying nervous system involving ATP release [3, 6].

ATP-Mediated Purinergic Signaling in the Bladder

Over three decades ago, Burnstock and colleagues proposed that the P2 receptor family, in sensory neurons, transmitted painful sensations in the presence of ATP [17]. It was originally hypothesized that the P2X receptor is an ATP-gated ion channel which likely consisted of three protein subunits [18]. Later, a total of seven mammalian P2X genes have been identified as P2X₁ – P2X₇. In the bladder, all seven P2X genes have been confirmed to be expressed [18]. It appears, however, that P2X₁ and P2X₃ play the most important role in normal bladder function. Specifically, P2X₁ has been found to be activated in the nerve efferents leading to the bladder, whereas P2X₃ is activated in the nerve afferents leading away from the bladder [19].

Purinergic P2X₃ receptors are abundant along the afferent pathways of the pelvic nerve that reside near the urothelium [16]. Patch-clamp studies on cell bodies of primary afferents have demonstrated two kinds of responses to ATP [20]. The first response is a rapidly rising inward current which desensitizes within 100 ms and the second is a slower rising inward current which decreases very little after 1-2 s [20]. This desensitizing and immediate non-desensitizing of the afferent pathways is what is believed to be responsible for the activation of neuronal pathways leading from the bladder to the spinal cord. The function of P2X₃ receptors in bladder mechanosensation has been further

confirmed in studies on mice lacking P2X₃ receptors [21]. Cockayne and colleagues demonstrated that P2X₃ knockout mice showed marked urinary bladder hyporeflexia with reduced voiding frequency and increased voiding volume. This suggested that P2X₃ plays an important role in the activation of afferent nerve fibers during bladder filling. This was further supported by a study by Vlaskovska and colleagues that demonstrated an increased bladder capacity in P2X₃ knockout mice compared to wild-type mice [22]. These findings suggest that P2X₃ is responsible for the sensing of bladder fullness in mice and that these receptors are most likely activated by ATP that is released through vesicle exocytosis from the urothelium in bladder mechanotransduction.

1.4 Cellular Mechanotransduction

Mechanotransduction is the mechanism by which cells sense external mechanical stimuli (i.e. pressure, temperature, etc.) and convert this signal into biological events. The ability of cells to sense changes in the environment and adapt is essential for physiology of many organ systems. In addition, mechanotransduction plays an important role in remodeling mechanosensitive tissues including bladder, bone [23], and cartilage [24]. Cellular mechanotransduction has multiple proposed mechanisms of action.

Cytoskeleton

The cytoskeleton has been thought to play a role in sensing changes in the mechanical environment around cells [25]. It has been suggested that the cytoskeleton

uses its load-bearing nature to distribute mechanical stresses across the cell and the extracellular matrix. Mechanical stress (i.e. stretch, shear flow) is dispersed among the cytoskeleton and transmitted to cell adhesion molecules, integrins, which in turn link intracellularly to the actin cytoskeleton. These integrins provide a suitable path for mechanical force to transfer across the plasma membrane [26]. While other types of mechanotransduction focus on intracellular cell signaling in response to mechanical stress on the cell surface (ex. ion channels and membrane protein changes), cytoskeletal mechanotransduction appears to be mediated by overall changes in cell shape [27].

Focal Adhesion

Focal adhesions are large protein complexes that connect the cytoskeleton of a cell to the ECM and also considered to play a role in mechanotransduction. The focal adhesion (FA) complex consists of structure proteins such as vinculin, α -actinin, and paxillin that anchor to the actin cytoskeleton of the adhering cell [28]. Sawada and Sheetz demonstrated that application of mechanical stretch to mouse fibroblastic cells using a Flexcell apparatus causes cytoskeletal proteins binding to focal adhesion points to send intracellular signals through activation of focal adhesion kinase (FAK) [29]. Activation of FAK has also been associated with an increase in cellular proliferation [30]. FA point mechanosensation is similar to cytoskeleton-mediated mechanosensation in that the application of mechanical stress (i.e. stretch) directly deforms the structure of the cell membrane proteins (vinculin, α -actinin), allowing the cell to sense mechanical stimuli.

Ion Channels

A number of studies have postulated that, in addition to the cytoskeleton and focal adhesion molecules, the activation of mechanosensing cells involves specific ion channels that are sensitive to mechanical stimuli. The influx of signaling ions (e.g. Ca^{2+} , Na^+) through mechanically-activated ion channels has been shown to be coupled with the release of secondary signaling molecules (e.g. ATP, NO) that trigger subsequent cellular events [31]. Thus, mechanosensitive ion channels (MSCs) have attracted much interest in the field of mechanotransduction. The following subsection will focus specifically on MSCs, as they have been the focus of extensive research in the field of bladder mechanotransduction over the past decade.

1.5 Mechanosensitive Ion Channels

Mechanotransduction involving MSCs typically involves a membrane-bound ion channel that becomes activated in response to a mechanical stimulus (fluid flow, membrane stretch, heat). As a result, extracellular ions, such as Na^+ , Ca^{2+} , and K^+ , flow into the cell and alter the intercellular concentration, which, in turn, triggers various cellular responses. Cellular responses as a result of an influx of ions include the release of regulating molecules [32] such as nitric oxide (NO) and ATP [15].

Stretch-activated Channels

It has been reported that in various types of cells, when exposed to a mechanical force that involves the membrane deformation of the cell, stretch-activated (SA) ion channels become activated [33]. The first family of SA channels was discovered in chick skeletal muscle and embryonic *Xenopus* muscle while applying pipette suction to form a seal [34]. Later, these channels have been shown to exist in human auditory cells, muscle spindles, vascular endothelium, and the bladder urothelium [35]. While cell swelling due to osmosis can dilute the concentration of impermeants that could act as volume sensors, a more reliable feedback system appears to be the function of SA cation channels [35]. SA channels are consistently cation selective, with a slight preference for K^+ over Na^+ . In the presence of a low concentration of gadolinium, SA channels are blocked and cease to function [36]. While they are almost exclusively activated by pressure-induced stretch of the cell membrane, studies on cultured endothelial cells from porcine aorta have shown that the vasomotion of blood vessels due to changes in blood pressure and shear stress due to blood flow are sufficient to activate these SA channels [37]. Stretch-activation of MSCs has been hypothesized to be a membrane phenomenon that does not involve soluble cytosolic messengers. This is supported by the observation that ion channels can be activated by stretch in environments absent of mediators such as Ca^{2+} and ATP [35].

Osmotic Swelling-Activated Channels

The maintenance of cell volume and intracellular solute concentration is an important regulatory function of the cell membrane. Cell volume is regulated by multiple cellular events such as alteration of the membrane potential, altered gene expression, and hormonal stimuli, all of which mediate the flow of water in and out of the cell [38]. Osmotic swelling occurs due to cellular efflux of KCl followed by a water gain through activation of K^+ and Cl^- channels. Because of this reaction, osmotic swelling has also been found to activate several different types of volume-sensitive K^+ channels including Ca^{2+} -activated K^+ channels, voltage-gated K^+ channels, and stretch-activated K^+ channels [39]. Fluctuation of the cell volume due to water movement across the cell membrane has also been shown to contribute to cellular functions including metabolism, cell proliferation, migration, and cell death [39]. It has been well documented that cell swelling creates membrane potential changes in both renal epithelial cells [40] and cardiac myocytes [41]. One example of membrane potential change due to cell swelling is the cardiac swell-activated Cl^- current ($I_{Cl,swell}$), which was discovered by performing experiments with rabbit ventricular myocytes in an iso-osmotic bathing solution designed to isolate Cl^- currents [41]. The current was recorded (after switching from an iso-osmotic media to a hypo-osmotic bathing media) while stepping up the clamped voltage from -100mV to +60mV. Because these osmotic swelling-activated channels are activated by changes in osmolality, which results in the outward stretching or inward shrinking of the cell membrane, they are considered to be modulators for

mechanotransduction through activation of other mechanosensitive ion channels (i.e. stretch-activated channels).

Pressure-Activated Channels

The existence of a pressure-activated cation channel (PAC) as a novel type of mechanosensitive channel was first reported by Köhler and colleagues in 2001 with research conducted using the aortic endothelium [42]. However, some controversy exists in the field of MSCs over whether PACs are a novel type of MSC or if they are merely a subtype of SACs [31]. This is due to the lack of a study exposing a cell to a pure pressure stimulus rather than pressure and stretch/shear. It is difficult to distinguish between pure pressure stress and distortional stress (shear stress) because the compressive loading on the tissues causes tissue deformation. It has been demonstrated at the cellular-level, that both direct stress from poking cells (involving membrane deformation) and indirect deformation of cells due to compression of the cell membrane inducing as much as 20% strain using a custom-designed compression rig [43], immediately increased the intracellular calcium concentration in chondrocytes [24]. To date, however, almost all studies have examined stresses that included cellular deformation, and not purely hydrostatic pressure. For this reason, to definitively confirm the existence of PACs, research must be performed on cells in which a pure pressure stimulus is applied to cells without the possibility of activating other mechanosensitive ion channels or deforming the cytoskeleton.

TRP Ion Channels

The transient receptor potential (TRP) channels are a family of membrane-bound ion channels with over 20 members prevalent in many mammalian tissues that have been demonstrated to respond to a variety of stimuli including pain, temperature changes, membrane stretch, and osmolality [44-47]. Two of the more researched TRP channels with respect to the bladder are the TRPV1 and TRPV4 channels, which are in the vanilloid subfamily of the TRP channels that are typically activated by heat, mechanical stimuli, and naturally occurring vanilloids [48].

TRPV1 channels are nonselective cation channels that are highly permeable to Ca^{2+} and allow for the influx of Ca^{2+} in response to the depletion of intracellular Ca^{2+} stores [49]. Capsaicin, the principal ingredient in chili peppers, has been discovered as a ligand that activates the TRPV1 channel as well [50]. In the bladder, TRPV1 is expressed in sensory nerve fibers, UCs, myofibroblasts, and probably smooth muscle cells [31]. Previous studies have shown that capsaicin-invoked desensitization affects neurons important for bladder mechanosensation. These studies suggest that these capsaicin-sensitive neurons participated in bladder physiology, specifically for bladder hyperreactivity [51].

TRPV4 is a nonselective cation channel that shares approximately 40% amino acid identity with TRPV1 [52]. TRPV4 has been found in epithelial cells in the renal tubule, trachea, and most recently in the bladder [53]. It was first discovered to be activated by hypotonicity-induced cell swelling and, thus, membrane stretch [54], but

more recently has been associated with mechanical stimuli such as shear stress and pressure in mice [31]. Ruthenium red, a staining dye, has been found to be an antagonist for TRPV4 in human embryonic kidney cells by blocking intake of signaling ions during activation of the channel by 4 α -phorbol 12,13-didecanoate (4 α PDD), a TRPV4 agonist [54]. Once activated in response to cell swelling and membrane stretch, TRPV4 mediates chain of events within mechanosensitive cells (e.g. vascular endothelium, bladder urothelium) that leads to a release of cellular signaling molecules (e.g. ATP, acetylcholine, NO).

In addition to TRPV1 and TRPV4, other less-studied, mechano-sensitive TRP ion channels have been demonstrated to be present in the urinary tract tissues. TRPM8, a channel sensitive to cold, is thought to be implicated in the bladder cooling reflex [55]. While TRPM8 is readily expressed in the bladder mucosa, it is not as prevalent in the urothelium as other mechanosensitive ion channels [56]. TRPA1 has recently been found to be expressed in rodent and human bladder urothelium and is potentially thought to respond to chemical or thermal stimuli [56]. Using an intravesical infusion on rat bladders, Du *et al* found that TRPA1 agonists cause bladder hyper-reflexia through C-fiber afferent pathways during continuous infusion cystometrograms. TRPV2, TRPC1, and TRPM3 have all been proposed to be mechanosensitive in mammals, but have yet to be found in the urinary tract [14].

Epithelial Sodium Channels

Epithelial sodium channels (ENaC) are highly selective cation channels that are considered mechanosensitive and known to be involved in the reabsorption of Na^+ ions into the epithelia of the colon, airways, distal nephron, and the bladder [57]. Using patch-clamp techniques, ENaCs have been demonstrated to transport Na^+ ions using a two-step process involving both ENaCs and a basolateral $\text{Na}^+\text{-K}^+$ pump [57]. ENaC is composed of three homologous α , β , and γ subunits. Canessa and colleagues demonstrated that while exposing the entire channel to amiloride, a diuretic compound, resulted in a detectable Na^+ current, the β and γ subunits alone did not exhibit a current in *Xenopus* oocytes [58]. These results suggested that the α subunit contains all of the biophysical and pharmacological properties of ENaC. While the functional roles of the β and γ subunits have not been completely characterized, it has been suggested that they aid in the formation of the channel pore [57].

ENaC has been studied extensively as a mechanosensory transducer in rats [59, 60], especially as baroreceptors and cutaneous sensory structures [14]. While the exact mechanism by which ENaCs function as mechanosensors is still partially understood, there are several hypotheses [61]. The first mechanism, and the most mechanically simple, is the bilayer tension model in which mechanical stress directly activates the membrane channel whether by possible thinning the membrane or changing the curvature. The second model is the extracellular ligand mechanism. In this model a ligand (e.g. ATP) is released possibly via membrane stretch and vesicle exocytosis from

an adjacent cell, attaches to the ion channel, and activates the channel to open. This proposal seems the least likely due to a contradiction between the time needed to bind the ligand and mechanotransduction being almost instantaneous. The final model is the tethered model in which the channel binds to the extracellular matrix and/or the intracellular cytoskeleton. This complex structure causes applied stresses to be amplified, thereby gating the channel for an influx of ions. While the bilayer tension model is the simplest, the tethered channel model appears to be the most likely due to data that suggests some subunits interact with type IV collagen of the ECM [61].

Table 1.1. Properties of mechano-sensitive Ion channels possibly related to bladder sensory transduction. Adapted from [31].

Ion Channel	Activator	Blocker	Location
ENaC	Mechanical (stretch), cold	Amiloride	Urothelium nerve endings dorsal root ganglia (DRG)
TRPV1	Heat ($\geq 43^{\circ}\text{C}$), low PH, voltage, anandamide vanilloids, capsaicin	Capsazepine	Urothelium nerve endings detrusor DRG
TRPV2	Noxious Heat ($>53^{\circ}\text{C}$), mechanical?	Ruthenium Red	Urothelium? nerve endings? myofibroblasts?
TRPV4	Moderate Heat ($>24^{\circ}\text{C}$), cell swelling, mechanical (shear stress), anandamide, 4α -PDD	Ruthenium Red	Urothelium DRG
TRPM8	Cold ($8\text{-}28^{\circ}\text{C}$), menthol, voltage		Urothelium Nerve Endings DRG
TRPA1	Mechanical, noxious cold?, marijuana, bradykinin		Urothelium Nerve Endings DRG

1.6 Ion Channel-Mediated Mechanotransduction in Mammalian Cells

Chondrocytes

Chondrocytes in articular cartilage respond to mechanical loading by modulating the rate of matrix synthesis and degradation, which, in turn, alters the composition of the tissue [62]. Chondrocytes under mechanical loading exhibit a change in membrane potential [63] largely due to the influx of Ca^{2+} ions into the cell. This increase in membrane potential due to ion exchange allows the capability of chondrocytes to be excellent sensors of ionic, biomechanical, and electrical signals.

Chondrocytes *in vivo* can be exposed to synovial and interstitial fluid pressure of near 10 MPa [24]. Even though it is postulated that some cells, including chondrocytes, are mechanically sensitive to hydrostatic pressure, the exact mechanisms by which they sense pressure is not well understood. To further understand pressure mechanotransduction, Mizuno and colleagues examined the effects of hydrostatic pressure on intracellular calcium concentration in bovine articular chondrocytes [24]. Using a custom-made pressure-proof chamber, Mizuno *et al.* exposed the chondrocytes to hydrostatic pressure (0.5 MPa) for five minutes and observed a significant increase in Ca^{2+} concentration under an inverted microscope. It was concluded that the observed pressure-induced calcium flux was initiated through a SAC because the increase in $[\text{Ca}^{2+}]$ was not inhibited in the presence of verapamil, an L-type voltage-gated calcium channel inhibitor, but with gadolinium, a SAC blocker [24]. This study, while it didn't provide

the direct evidence of membrane deformation, demonstrated that SACs do play a role in the calcium signaling cascade of chondrocytes during exposure to hydrostatic pressure.

Bone Cells

Because of their abundance and location within the bone, osteocytes are considered to translate loading on the skeleton into cellular signals that regulate bone remodeling [64]. Mechanical loading induces shear stress due to fluid flow in the lacuno-canalicular network and subjects osteocytes to shear stress. Like other mechanically sensitive cells, load-induced deformation of osteocytes and changes in the membrane potential lead to the opening of membrane ion channels [65]. These same mechanosensitive cation channels have also been found to be expressed in bone forming osteoblasts. Using patch-clamp techniques, it was demonstrated that the largest conductance channel (160pS) was K^+ -selective, and two others appeared to be non-selective for cations [66]. The α -subunit of ENaC was also found to be expressed in osteoblasts and the channel was shown to be activated after exposure to negative suction pressure by a patch pipette [67]. While the exact purpose of bone cell membrane ion channels has yet to be elucidated, they are believed to be associated with triggering bone remodeling by communication between osteocytes, osteoblasts and osteoclasts.

Vascular Cells

Vascular endothelial cells *in vivo* are constantly exposed to stretch, shear stress, and pressure due to blood flow [68] and respond to changes in these mechanical stimuli to moderate the constriction and dilation of blood vessels. Vascular endothelial cells have been shown to possess membrane ion channels sensitive to stretch and to shear stress. Both TRPC1 [69] and TRPV2 [70] have been found in human vascular endothelial cells and activated by the pulsatile stretch of the blood vessel wall, but it is still controversial if these channels are also stimulated by shear stress [32]. Once stimulated by a mechanical stress such as stretch or shear stress, vascular endothelial cells allow Ca^{2+} to enter the cell through membrane ion channels, possibly TRPC1 or TRPV2. In response to this increase in cytosolic $[\text{Ca}^{2+}]$, the endothelial cells release various vasoactive molecules such as NO, endothelium-derived hyperpolarizing factor (EDHF), and endothelins [32]. To date, however, very little conclusive evidence exists whether shear stress and membrane stretch activate distinct classes of ion channels on the endothelial cell membrane; only one study has reported that there may be stretch-activated Ca^{2+} -permeable channels that can be responsive to both shear stress and membrane stretch [71].

Epithelial Cells

Epithelial cells line the inside of visceral organs such as the lungs, kidney, and bladder, and glands throughout the body, and thus, encounter various forms of

mechanical stimuli. For example, the kidney tubular epithelial cells are constantly subjected to fluid flow-induced shear stress. Alenghat and colleagues reported that mechanical loading on the cell cytoskeleton played a significant role in calcium signaling of kidney epithelial cells in response to shear stress *in vitro*. [26]. Using a parallel flow chamber and microfluorimetric ratio imaging, murine kidney epithelial cells were exposed to a fluid shear stress of 0.75 dynes/cm², and the intracellular [Ca²⁺] was measured 10-15 s after flow stimulation. By chemically modulating the stability of microfilament (cytochalasins B & D, latrunculin B) or microtubules (colchicines, nocodazole), these authors demonstrated that the intake of calcium through polycystin-2 calcium channels was controlled by the overall status of the cytoskeleton. It was also determined that disruption of the cell tension resulted in an inhibited mechanotransduction response through a reduced calcium spike. These results provided evidence that it is not only membrane-bound ion channels, but also a complex that includes a cytoskeletal network directs how a cell detects mechanical stimuli.

In addition to calcium channels, the ENaCs have been shown to play a role in mechanotransduction by epithelia. Althaus *et al.* examined the response of ENaCs to laminar shear stress in rat colon epithelial cells and a *Xenopus* distal nephon cell line [72]. Using whole-cell recording with patch clamp techniques, these authors found that exposure of rat colon epithelial cells to shear stress of up to 20 dynes/cm² resulted in an inward current, which decreased in the presence of amiloride (10μM), suggesting that ENaCs were responsive to the shear stress. Moreover, the results of single-channel

recordings revealed that shear-induced ENaC activation was due to an increase in the ion channel open probability [72]. While little is known about the gating features of ENaCs on epithelial cells, this study has shown that shear stress is a plausible activator of ENaC activity.

Summary

In summary, mechanosensitive cells have shown to be prevalent in various organs throughout the body. From epithelial cells exposed to relatively low shear stress, to bone and cartilage cells under large levels of hydrostatic force, ion channels are crucial for the sensing of these mechanical stimuli and regulating cellular functions. While these ion channels have been well researched in many cell types including epithelial, vascular endothelial, and bone cells, they have just recently been suspected as crucial components in the urothelial mechanotransduction process. These findings lead many researchers to believe that the process of sensing mechanical pressure in the bladder relies more on ion channels embedded in UCs rather than purely bladder purinergic sensation.

1.7 Urothelial Mechanotransduction

The urothelium of the bladder has long been treated only as a passive barrier to retain urine and prevent unregulated movement of ions and salts from the bladder to the bloodstream. The barrier has been characterized as having a high transepithelial resistance (TER) and a relatively low permeability to water and urea [73]. The bladder

was considered to be controlled by the central nervous system along with parasympathetic, sympathetic, and somatic nerves innervating the detrusor muscle [73]. However, research conducted in the past decade has begun to piece together the potential mechanisms that contribute to the ability of the bladder urothelium to sense the fullness of the bladder via changes in hydrostatic pressure [15] and/or bladder stretch [14].

Currently Proposed Mechanism for Urothelial Mechanotransduction

Research on bladder mechanotransduction has typically focused on independent ion channels of UCs rather than analyzing macro-scale response to bladder filling. Therefore, in order to compile an accurate portrayal of the entire process of urothelial mechanotransduction, several studies analyzing urothelial cell mechanosensation must be examined. In the bladder, the pressure rises in a tri-phasic manner as the bladder fills with urine [6]. The first phase includes a pressure rise and then remains constant during the storage phase for typically 4-5 hours, but can extend as long as 12-15 hours. Following the storage phase is the voiding phase which is characterized by a rapid increase in pressure due to the smooth muscle contracting. Once the bladder voids, the pressure decreases with the UCs returning to their original transitional epithelial distribution and the cycle starts over [6]. In the storage phase, the urothelium becomes thinner as the urine accumulates and its volume increases. The thinning of the urothelium is the result of the intermediate and basal layers deforming laterally to accommodate more fluid. The deformation of these cells is suspected to activate

mechanosensitive ion channels (e.g. TRPV1, TRPV4, ENaC) embedded in the lipid bilayer of UCs, allowing for the transport of ions across the cell membrane [15, 50]. Most ion channels that are proposed to have a role in mechanotransduction (e.g. TRPV1, TRPV4) transport Ca^{2+} into the cell. This increase in intracellular $[\text{Ca}^{2+}]$ has been shown to produce an increase in ATP released from UCs. [15, 74]. Research conducted on ENaC channels have shown that blocking the channel leads to an inhibition of ATP release, suggesting that activation of ENaC channels also lead to ATP release from UCs [14]. ATP has been found to be abundant in the cytoplasm of all cells (3-5mM) [75]. ATP molecules can be released on the mucosal or serosal side of the cell into the extracellular space via connexin hemichannels [76], nucleoside transporters [77], or exocytosis of ATP containing vesicles [75]. It is speculated that once the ATP is released from the urothelial cell, it can bind to P2X_3 receptors on afferent nerve pathways lying on the basal side of the urothelium [18, 22]. The binding of ATP to the nerve pathways depolarize the nerve afferents and results in an electrical impulse sent via the central nervous system to the brain signaling that the bladder is full.

1.8 Role of Ion Channels in Urothelial Mechanotransduction

UCs have been found to express several types of ion channels that are considered mechanosensitive. These channels include ENaC (mechanical) [78], TRPM8 (cold) [55], TRPV1 (heat, stretch) [46], and TRPV4 (osmolality, pressure) [79, 80]. The following

section will focus on TRPV1, TRPV4, and ENaC as they have currently been shown to play a role in bladder mechanotransduction.

TRPV1

Birder and colleagues [50] investigated the role of TRPV1 on bladder function using TRPV1 knockout mice. By exposing the mucosal surface of the TRPV1 knockout mouse bladders to a fixed pressure (30cm H₂O) using a custom-designed pressure chamber *in vitro*, these authors demonstrated that bladders of these mice exhibited a diminished stretch-evoked ATP release from UCs in comparison to wild-type. In addition, the TRPV1^{-/-} mice exhibited a higher frequency of low-amplitude, non-voiding bladder contractions in a freely moving environment as compared to the TRPV1^{+/+} littermates. These results suggest that TRPV1 is essential for ATP release from UCs as well as regulating normal bladder contractions. One important area of notice, however, is that the pressure that the bladders were exposed to *in vitro* was higher than the normal sensing range for sensory nerve A δ -fibers in bladders (10-20 cmH₂O) [8].

In addition to the active role on the urothelium, TRPV1 has been found to be active in afferent nerves innervating the bladder. Using a spike processor to quantify afferent nerve activity of TRPV1 knockout and wild-type mice, Daly and colleagues [47] demonstrated that a TRPV1 antagonist, capsazepine (10 μ M), caused a significant attenuation of afferent discharge in TRPV1^{+/+} mice, while the response to bladder distention was significantly attenuated in the presence of capsazepine for TRPV1^{-/-} mice .

These authors concluded that, because TRPV1 contributed to the membrane excitability, its absence leads to reduced afferent nerve sensitivity and plays an indirect role in bladder mechanosensation. Taken together, it can be postulated that a decrease in ATP released from the urothelium of TRPV1^{-/-} mice can lower bladder afferent sensitivity. This reduction in sensitivity to bladder distention due to a lack of the TRPV1 ion channel can result in a reduced bladder response to filling in normal physiological conditions.

TRPV4

Recently, Birder and colleagues demonstrated the expression of TRPV4 channels in UCs and that *in vitro* exposure of these cells to synthetic phorbol ester 4 α -phorbol 12, 13-didecanoate (4 α -PDD), a known TRPV4 agonist led to a pronounced increase in Ca²⁺ influx and ATP release [45]. Moreover, a cystometry performed on anesthetized rats revealed that continuous intravesical infusion of 4 α -PDD (100 μ M) resulted in increased bladder voiding pressure [45]. These results suggest that activation of TRPV4 is associated with an increase in involuntary bladder contraction. When UCs are stimulated by a mechanical stimulus, TRPV4 is proposed to induce a cellular ATP release through vesicle exocytosis to signal the afferent input that the bladder is full via a purinergic pathway. This constant activation of purinergic receptors results in efferent nerve pathways sustaining bladder contraction even if the bladder is voided. The sensation felt when TRPV4 is artificially stimulated by 4 α -PDD is similar to human patients with urinary tract disorders (e.g. men with urethral outlet obstruction and women with multiple

sclerosis) when the feeling of incomplete bladder voiding can happen [45]. Due to the fact that ATP is released from the cell when TRPV4 is stimulated and that TRPV4 activation is correlated with an increase in bladder voiding pressure, it is hypothesized that TRPV4 plays an active role in urothelial mechanotransduction.

ENaC

Previous studies have shown that the degenerin/epithelial Na⁺ channel (ENaC) is present in the human urothelium [81] and that it has the ability to change its sodium transport properties after exposure to changes in hydrostatic pressure [78]. More recently Du and colleagues [14] examined the effects of amiloride, a diuretic compound and an ENaC blocker, on the micturition reflex of rat bladders *in vivo*, as well as stretch-evoked ATP release from bladder strips *in vitro*. By measuring the time interval between two consecutive bladder contractions, the authors found that UCs exposed to amiloride (1 mM) increased the pressure threshold for inducing micturition (i.e. the pressure at the point preceding a bladder contraction), but did not affect the micturition pressure. From these results it was concluded that the voiding efficacy did not change, but the sensitivity to bladder fullness decreased due to ENaC inhibition. In other words, only the bladder afferent pathways, not efferent, were inhibited by the infusion of amiloride. Du *et al.* also found that amiloride (1 mM) blocked ATP release by a full-thickness rat bladder in response to stretch (up to 50%) *in vitro*, but did not affect basal ATP release. Since more than 90% of the ATP was released from the bladder mucosal layer, they concluded that

stretch-evoked ENaC channel activation triggered the ATP release from the bladder mucosa. These results concur with an earlier study reported by Birder and colleagues that pretreatment with amiloride (10 μ M) suppressed ATP release by feline UCs in response to a hypo-osmotic solution *in vitro* [82].

While several studies have successfully examined specific ion channels that appear to be activated during bladder filling, the precise role that these ion channels play in urothelial mechanotransduction has not yet been elucidated. With that being said, much research must still be done to better understand these previously studied ion channels as well as examining the possibility of undiscovered mechanosensitive ion channels in the urothelium.

-Chapter 2-

Rationale and Specific Aims

2.1 Rationale

Recent research has suggested that the bladder urothelium is not just a passive barrier, but is also sensitive to various mechanical stimuli (stretch, pressure) and responds by releasing neurotransmitters (NO, ATP) that signal bladder fullness. Thus, it has been suggested that overactive bladder, which affects approximately 17% of adults [83], is caused, at least in part, by altered sensitivity to bladder fullness by urothelial cells (UCs). This is supported by evidence that several types of mechanosensitive ion channels (e.g., TRPV1, TRPV4, TRPA1, TRPM8, ENaC) are present in the bladder urothelium and are activated by multiple types of stimuli including pH [84], temperature [55], and stretch [85, 86]. Previous *in vitro* studies that examined the effects of pressure on the urothelium mounted on a modified Ussing chamber [15, 50] demonstrated that urothelial tissue responds to the mechanical stimulus by altering the current across the cell membrane, presumably due to ion channel opening, and also with a release of ATP [15, 85]. However, these studies did not separate the effects of hydrostatic pressure from pressure-induced tissue stretch on UCs. In the field of mechanobiology, it is generally accepted that cells are sensitive to membrane deformation. In contrast, it is considered by some that hydrostatic pressure, which would not deform the cell membrane under the assumption that cells are incompressible, is not a stimulus that is capable of eliciting a

response in mechanosensitive cells. However, previous work on vascular endothelial cells, chondrocytes, and bone cells has provided evidence that hydrostatic pressure triggers various cell signaling responses [24, 42, 87]. Since the bladder wall exhibits non-linear mechanical behavior between pressure and stretch, it is necessary to examine the effects of pressure on the bladder without the added stimulus of tissue stretch to better understand the mechanism of sensing bladder fullness. We, therefore, focused our research on examining the role of mechanosensitive ion channels in hydrostatic pressure mechanotransduction in UCs.

2.2 Research Hypothesis

The objective of the present research is to test our hypothesis that bladder UCs respond to hydrostatic pressure, specifically with ATP release, and that this response is triggered by mechanosensitive ion channel activation. To test this hypothesis, using custom experimental setups, rat primary UCs and immortalized human bladder UROtsa cells were exposed to controlled hydrostatic pressure in the presence of various pharmacological agents while quantifying extracellular ATP release and cell volume change. The specific aims of the present research were as follows.

- **Aim 1** – To examine the role of mechanosensitive ion channels in pressure mechanotransduction in rat bladder urothelial cells

- ❑ **Aim 2** – To elucidate the role of cell volume change in mechanotransduction of hydrostatic pressure in urothelial cells
- ❑ **Aim 3** – To characterize the ATP release kinetics by urothelial cells and to determine the potential role of TRPV4 in pressure mechanotransduction

-Chapter 3-

Aim 1: To Examine the Role of Mechanosensitive Ion Channels in Pressure

Mechanotransduction in Rat Bladder Urothelial Cells

3.1 Introduction

Mechanotransduction, the process by which cells sense external mechanical stimuli and convert these signals into biological events, is essential for cells to perform normal functions in many organ systems. Epithelial cells lining the inner walls of organs are constantly subjected to mechanical force stimuli and play critical roles in both physiological and pathological events. The epithelium of the bladder, urothelial cells (UCs), are exposed to both stretch and hydrostatic pressure during filling and are considered to play a role in sensing fullness [33, 88]. Deficient or heightened sensitivity of bladder fullness may lead to urinary incontinence or frequent urges to urinate. To date, however, the exact mechanisms by which UCs sense these mechanical stimuli are not fully understood.

The bladder urothelium is a transitional epithelium, consisting of multiple layers of epithelial cells, that was previously thought to only function as a lining for urine storage and a solid barrier that prevents urine and blood from coming into contact [6]. Recent studies, however, have shown that the urothelium is capable of sensing thermal [89], chemical [90], and mechanical stimuli [22, 50]. Using a feline model, it was found that exposing the bladder to cold temperatures through intravesical infusion with a saline

solution induced the micturition reflex suggesting that the bladder wall, including the urothelium, is capable of detecting temperature change [91]. Recent data over the past several years also indicate that the urothelium plays a role in chemical signaling through bradykinin receptors [92], purinergic receptors [93], and ion channels [13, 55]. A number of *in vitro* studies have demonstrated that the urothelium is sensitive to mechanical stimuli and releases ATP in response to tissue stretch [15, 85, 94]. The physiological importance of ATP released from the urothelium is based on the proposal that it binds to the purinergic receptors present on the bladder afferent nerves and triggers the sensation of bladder fullness [18]. In these experiments, either a mouse or rabbit urothelium, separated from the bladder, was mounted on a modified Ussing chamber while hydrostatic pressure (ranging between 5 and 45 cmH₂O) was applied to the serosal side of the tissue while ATP release was quantified on the mucosal side. These studies, however, exposed multilayers of UCs to not only pressure, but also to tissue stretch, which compounded the effect of applied mechanical stimuli. A more recent study by Yu *et al.* [22, 50] attempted to separate the effects of pressure and stretch using a modified Ussing chamber and applying equal pressure (up to 64 cmH₂O) to both sides of the urothelial tissue (serosal and mucosal). The authors reported that exposing urothelial tissue to elevated pressure without distention through this approach did not induce any changes in electrophysiological properties of the tissue and concluded that it was stretch, not pressure, that was the critical stimuli for urothelial mechanotransduction [22, 50]. Clearly, this was an important first attempt to examine the effects of hydrostatic pressure

on the urothelium. However, since UCs are highly polarized cells with distinct apical and basolateral domains [22, 50], application of pressure only on the apical side may be more appropriate for examining the urothelial cell responses to hydrostatic pressure. As such, the exact nature of bladder mechanotransduction remains unclear and a different approach is necessary for deeper understanding.

Several classes of membrane-bound mechanosensitive ion channels (MSCs) have been implicated in the urothelium response to distention. For example, by using knockout mice for transient receptor potential V1 (TRPV1) [50, 82], Birder *et al.* demonstrated that these channels mediate ATP release from UCs in response to elevated pressure and mechanical stretch applied to the bladder *in vivo* using a cystometry apparatus. Moreover, by applying stretch (~3%) to primary murine UCs harvested from *Trpv4* knockout and normal animals on an elastic silicone membrane, Mochizuki *et al.* demonstrated that TRPV4 activation plays a role in stretch-induced ATP release by UCs [86]. In addition to these TRP channels, the degenerin/epithelial Na⁺ channel (ENaC) has been implicated in bladder mechanotransduction. The potential involvement of ENaC has been determined through measuring stretch-evoked ATP release from bladder strips *in vitro* in the presence or absence of amiloride, a diuretic ENaC blocker [14]. Together, these studies strongly suggest that mechanosensitive ion channels located in the urothelium play a role in bladder mechanotransduction

The goal of the present study was to test the hypothesis that UCs detect physiological-level hydrostatic pressure without the added variable of stretch, and that

this response is mediated by activation of specific ion channels. To test this hypothesis, the present study quantified ATP release from monolayer cultures of primary UCs on rigid substrates following exposure of the apical side of the cells to hydrostatic pressure using a custom experimental setup. The ATP release by UCs under hydrostatic pressure was further examined by blocking the ENaC, TRP, stretch-activated channels and L-type voltage gated channels.

3.2 Materials and Methods

Urothelial Cell Culture

Primary UCs were harvested from bladders of female Sprague-Dawley rats according to methods reported in the literature [95]. The animals were cared for and euthanized in accordance with an animal use protocol approved by the Clemson University IACUC. Briefly, under sterile conditions, the bladders were excised from animals immediately after sacrifice and trimmed of any excess fat and connective tissue. The bladder was then inverted using a blunt 18 ½ gauge needle and filled with 2-3 ml of sterile phosphate buffered saline (PBS) solution. The inflated bladder was tied off with a sterile suture and incubated in 0.05% trypsin (Invitrogen, Carlsbad, CA) with gentle stirring under standard cell culture conditions (37 °C, 95% air/5% CO₂, humidified environment) for 25 minutes. The trypsin solution that contained UCs was combined with equal volume of fresh fibroblast medium (FM: DMEM/F12 (Invitrogen) medium supplemented with 10% fetal bovine serum (FBS) (Hyclone, Logan, UT), penicillin

(10,000 units/mL), and streptomycin (10,000 µg/mL)), and centrifuged at 1000 RPM for five minutes. The cell pellet was then resuspended in the UC growth medium [95], a 1:1 mixture of 3T3 fibroblast-conditioned FM and keratinocyte growth medium (KGM: keratinocyte medium (Invitrogen) supplemented with 2% FBS, bovine pituitary extract (12.5 mg/ml, Invitrogen), insulin-transferrin-selenium (1 mg/mL), hydrocortisone (50 µg/mL), epidermal growth factor (35 ng/µL, Invitrogen), amphotericin (250 µg/mL), and gentamicin (50 mg/mL)). The primary UCs were cultured for up to 7 days until they reached confluence and used in experiments. The urothelial cell phenotype of these primary cells was confirmed by the cell morphology and immunostaining using commercially available primary antibodies for CK 17 (positive) and desmin (negative), and the fluorescently (Alexa Flour 488) tagged secondary antibody (Figure 3-1, Frames A-C).

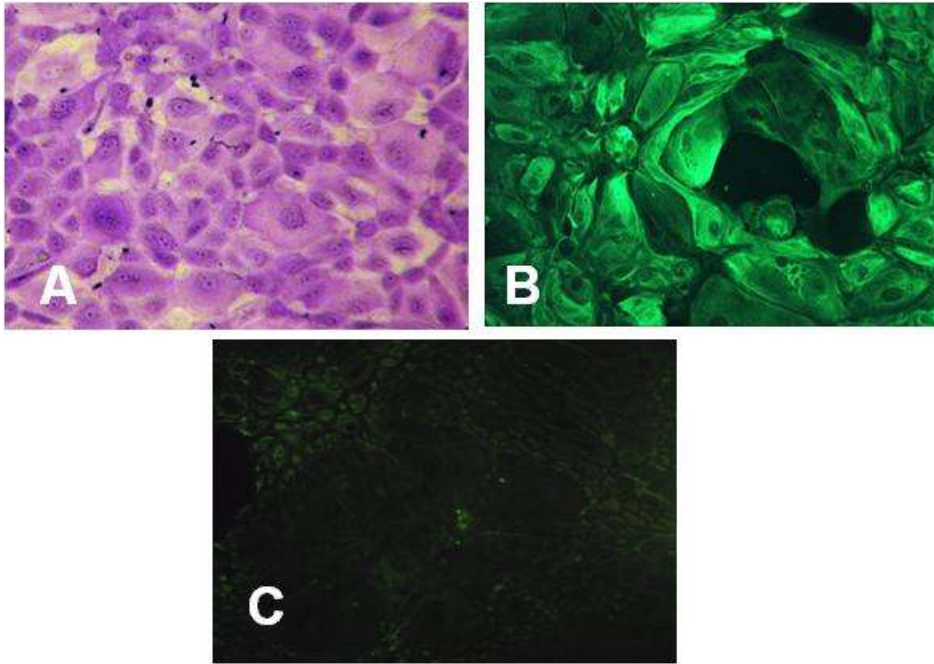


Figure 3-1: Cell characterization images of urothelial cells. Primary rat bladder UCs stained with Coomassie Blue exhibited characteristic cuboidal morphology (Frame A) (100x). The positive staining for CK17 (Frame B) (100x), and epithelial cell marker, and negative staining for desmin (Frame C) (100x), an intermediate filament found in smooth muscle cells, further confirmed the urothelial phenotype of these cells.

Hydrostatic Pressure Experiments

A custom-made pressure system [96] was used to expose UCs to sustained hydrostatic pressure (Figure 3-2). Briefly, the system consisted of a computer with a custom Lab View code (National Instruments, Corporation, Austin, TX) and electronics that controlled a pressurized environment inside a sealed chamber where cell culture dishes were placed. The pressure was monitored with a pressure transducer and regulated

by opening and closing inlet and outlet valves that controlled the flow of 95% air/ 5% CO₂ through the pressure system. During the experiments, the pressure chamber was maintained in an incubator under standard cell culture conditions. As was previously reported [96], the pH, pO₂, and pCO₂ of the culture media were not affected by application of the hydrostatic pressure at the levels tested in the present study.

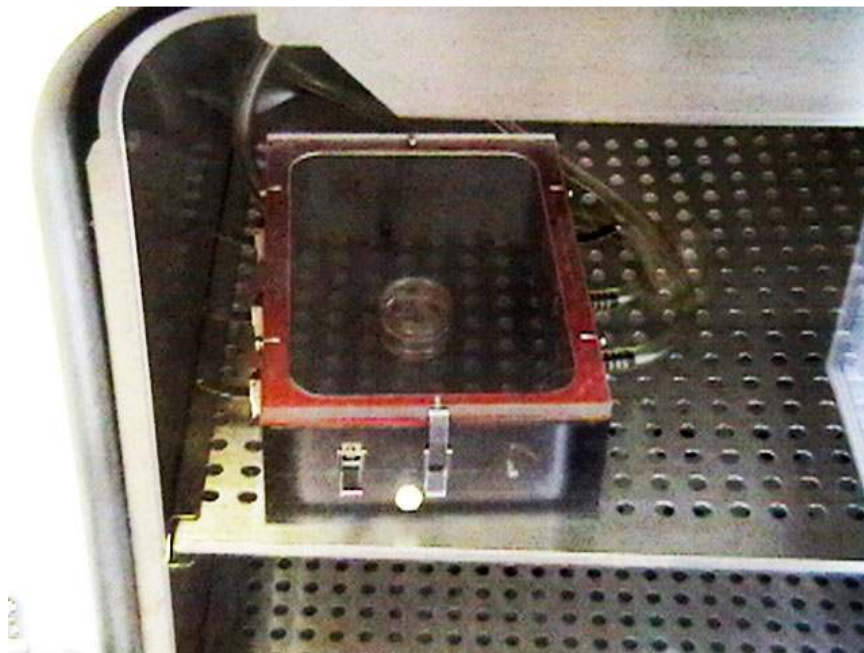


Figure 3-2: Custom-made pressure chamber. Cell culture dishes were placed in the pressure chamber and exposed to hydrostatic pressure (5-20 cmH₂O) for 5, 10, and 15 minutes. Control group was placed in a similar chamber with no pressure.

In preparations for experiments, UCs were cultured (approximately 40,000 cells/cm²) in the growth media (a 1:1 mixture of KGM and 3T3 fibroblast-conditioned

FM) under standard cell culture conditions. The cells were grown to confluence before application of pressure in order to best mimic the umbrella cell lining in vivo during bladder filling. One hour prior to exposure of these cells to pressure, the culture media were switched to phenol red-free DMEM/F12 medium (Invitrogen) supplemented with 2% FBS to minimize interference by the color of media with measurements in the luciferin-luciferase ATP assay (see *ATP Quantification*). Both the control and experimental groups had a volume of media (1.0 ml), which supplied an additional 0.33 cmH₂O. Therefore, it must be noted that the pressure values listed are differential, and not absolute. Under normal physiological conditions, in both human and rats, the storage pressure for the bladder is relatively low (<10 cmH₂O) during filling [97, 98]. Once this pressure reaches the threshold for inducing voiding, the sense of fullness is felt and the bladder can be voided voluntarily (in adults) or reflex voiding takes places (in infants) [11]. In case of rats, this threshold pressure is approximately 16 cmH₂O [99], and voiding pressure (generated by bladder contraction) can reach up to 40 cmH₂O [50]. Therefore, in order to expose UCs to physiologically relevant levels of pressure, UCs were prepared in separate dishes for each parameter group and subjected to hydrostatic pressure at 5, 10, 15, and 20 cmH₂O, each for 5, 15, and 30 minutes. For the time-course experiments, the UC baseline ATP concentration was quantified before pressure exposure at time point 0. During the drug blocking experiments, the no-pressure, no-drug groups were maintained in a similar culture medium under static conditions for the duration of the experiments. Cells were not exposed to multiple stimuli and were discarded after

each experiment. At the conclusion of each trial, the supernatant media were collected for ATP quantification

ATP Quantification

Supernatant media were collected before and after exposure of UC's to pressure. ATP concentration was determined using a commercially available luciferin-luciferase assay kit (Invitrogen) and following the manufacturer's instructions. The luminescence values of the media were measured using a Tecan Genios microplate reader (Tecan US, Inc., Durham, NC) and converted to ATP concentration (nM) using a standard curve that was prepared before each assay with serial ATP concentrations diluted from the ATP stock solution supplied in the kit. The ATP concentration was normalized to the ATP values of the UCs maintained under control conditions. The data for the time-course ATP release experiments and the drug treatment experiments were normalized to the control group and presented as fold-changes compared to control.

Drug Treatments

In some experiments, UCs were pretreated with specific drugs to either block or activate ion channels of interest prior to exposure to hydrostatic pressure. All drugs used in the present study (concentration and exposure time) are listed in Table 3.1. BAPTA was purchased from Invitrogen. All other drugs were purchased from Sigma-Aldrich (St. Louis, Missouri).

Table 3.1. Drugs used in ATP determination study.

Drug	Concentration	Exposure Time	Action
BAPTA	1 mM	10 min	Extracellular Ca ²⁺ chelator
GdCl ₃	50 μM	30 min	SAC blocker
Nifedipine	10 μM	30 min	L-type voltage-gated channel blocker
Ruthenium Red	1 μM	10 min	Non-specific TRP channel blocker
Amiloride	1 mM	20 min	ENaC blocker
Capsaicin	10 μM	2 min	TRPV1 channel agonist
4α-PDD	10 μM	2 min	TRPV4 channel agonist

Key- BAPTA- 1,2-bis(o-aminophenoxy)ethane-N,N,N',N'-tetraacetic acid; GdCl₃- gadolinium chloride; 4α-PDD- 4α-Phorbol 12,13-didecanoate.

Reverse Transcription (RT)- PCR of Ion Channels

Purified mRNA (1 μg) from primary cultures of UCs was reverse transcribed with RETROscript first strand synthesis kit (Ambion, Austin, TX). The cDNA strands were amplified using the Rotor Gene thermal cycler (Qiagen, Valencia, CA)) and SYBR green real-time quantitative PCR kit (Qiagen) with primers specific for TRPV1, TRPV4, ENaC (α, β, and γ subunits) and L-type voltage-gated channels. For TRPV1 the primers were 5'-AGTAACTGCCAGGAGCTGGA-3' (sense) and 5'-GTGTCATTCTGCCATTGTG-3' (antisense). For TRPV4 the primers were 5'-CCCCATCCTCAAAGTCTTCA-3' (sense) and 5'-ATCAGTCAGGCGCTTCTTGT-3' (antisense). For L-type voltage-gated channels the primers were 5'-CGACAAGCAGAGGAGTGCAG-3' (sense) and 5'-TGGTTAGGTCACAGGCATCG-3' (antisense). For ENaC-alpha the primers were 5'-TGTGAAGTCCCAGGATTGGAT-3' (sense) and 5'-AGGCTGACCATCGTGACAGAA-3' (antisense). For ENaC-beta the

primers were 5'-TCTAGCTCTTGCCCACCCTA-3' (sense) and 5'-CTGCACACCCCCAAGTCTAT-3' (antisense). For ENaC-gamma the primers were 5'-CCCAGCCAACAGTATTGAGA-3' (sense) and 5'-CGGGCGATGATAGAGAAGAA-3' (antisense). Beta-glucuronidase (β -GUS) was the housekeeping gene, with the primers being 5'-GCCTTCATTTTGCGAGAGAG-3' (sense) and 5'-ACGGTCTGCTTCCCATACAC-3' (antisense). PCR amplification was carried out for 35 cycles at 94° C (15 s), 60° C (30 s), and 72° C (30 s). After confirming that amplification for all genes of interest occurred within appropriate threshold cycles (30-35), the PCR products were electrophorated on a 2% agarose gel at 100V for 1 hour 15 minutes using a 500 bp ladder for visual confirmation of the base pair size of amplicons.

Statistical Analysis

Each experiment was performed in duplicates with a minimum of 3 repetitions (n=3). The mean values of data from three experiments were calculated and compared using single-factor analysis of variance (ANOVA). When a statistically significant difference was detected, a *post-hoc* pairwise analysis was conducted using the Tukey test. Statistical analyses of numerical data were performed using Sigma Stat software (Systat Software Inc., Richmond, CA). *P*-values less than 0.05 were considered statistically significant.

3.3 Results

Cell Characterization and mRNA Expression of Select Ion Channels

Primary rat UCs exhibited characteristic cuboidal morphology, which was confirmed with a Coomassie blue stain (Figure 3-1A). The cells stained positive for CK17 (Figure 3-1B), an epithelial cell marker, and stained negative (no green fluorescence) for desmin (Figure 3-1C), an intermediate filament in smooth muscle cells and fibroblasts, further confirming the urothelial phenotype of these cells. To confirm mRNA expression of the ion channels of interest (TRPV1, TRPV4, L-type voltage gated, ENaC), real-time quantitative PCR was performed and amplicons were visualized on an ethidium bromide-stained agarose gel. When referenced with a 500-bp ladder loaded on the gel, the bands of the amplicons were located at the target size. In addition, the absence of bands in negative-RT control samples indicated that the visual bands were not a result of genomic DNA amplification and mRNA expression of all ion channels of interest were confirmed (Figures 3-2A, 3-2B).

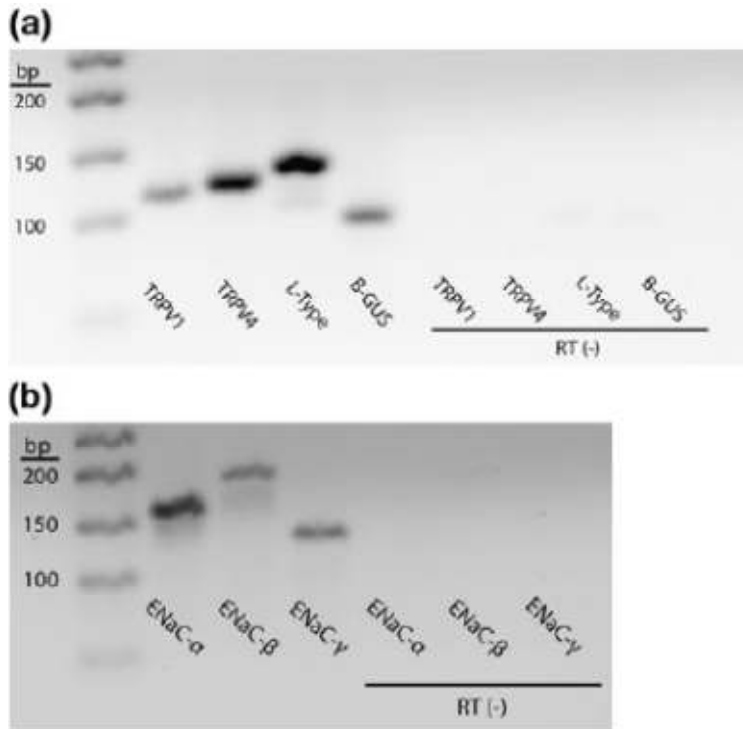


Figure 3-3. Gene expression of membrane-bound ion channels in urothelial cells.

The results of RT-PCR confirmed mRNA expression for TRPV1, TRPV4, and L-type voltage gated ion channels (Frame A), and the α -, β -, and γ - subunits of ENaC (Frame B). β -D-glucuronidase (β -GUS) expression served as a house-keeping gene.

ATP Release from UCs Exposed to Hydrostatic Pressure is Dependent on Duration and Magnitude

When primary rat UCs were exposed to hydrostatic pressure at either 5 or 20 cmH₂O for 5, 15, and 30 minutes, the level of ATP in the supernatant was not significantly different from the baseline (measured immediately prior to exposure to pressure). However, when UCs were exposed to hydrostatic pressure at 10 and 15

cmH₂O for 5 minutes, as well as at 15 cmH₂O for 15 minutes, the supernatant contained significantly ($p < 0.05$) higher concentrations of ATP. These increases in ATP concentrations diminished to the baseline level at subsequent time points (Figure 3-4).

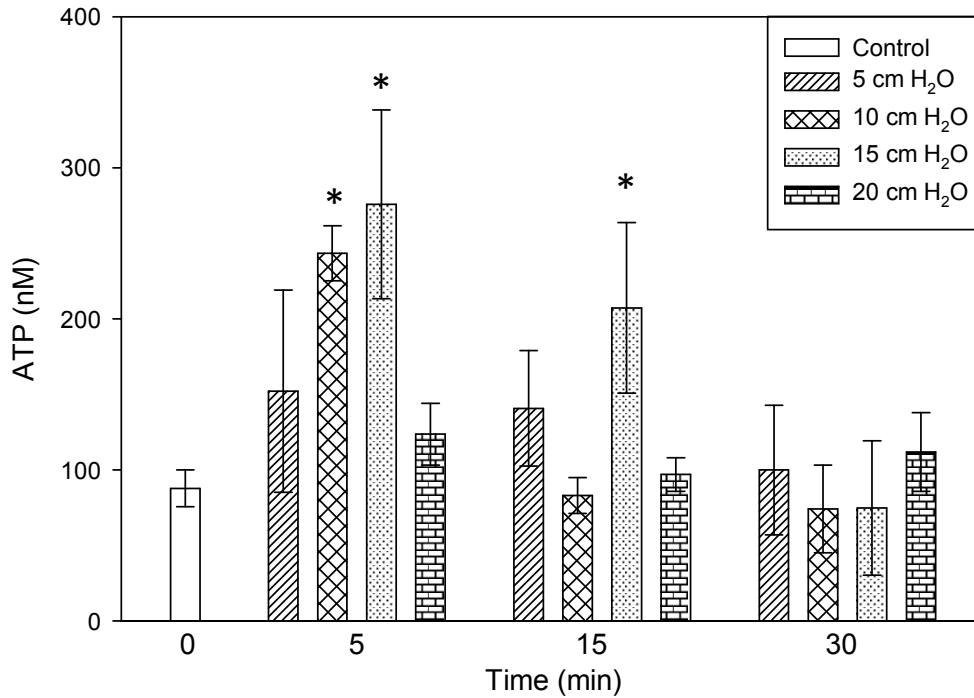


Figure 3-4. Time-course ATP release from urothelial cells exposed to hydrostatic pressure. Supernatant media were collected and analyzed following exposure to hydrostatic pressure (5-20 cmH₂O) for 5, 15, and 30 minutes. Cells exposed to hydrostatic pressure for 5 minutes (10 and 15 cmH₂O) and for 15 minutes (15 cmH₂O) exhibited an increase in ATP concentration compared to the control group. ATP is expressed as a fold-change relative to the baseline concentration. Results shown were

collected previously by Joshua Stover. Data are mean \pm SEM; * $p < 0.05$, analyzed by ANOVA and tukey-test; n=3 experiments.

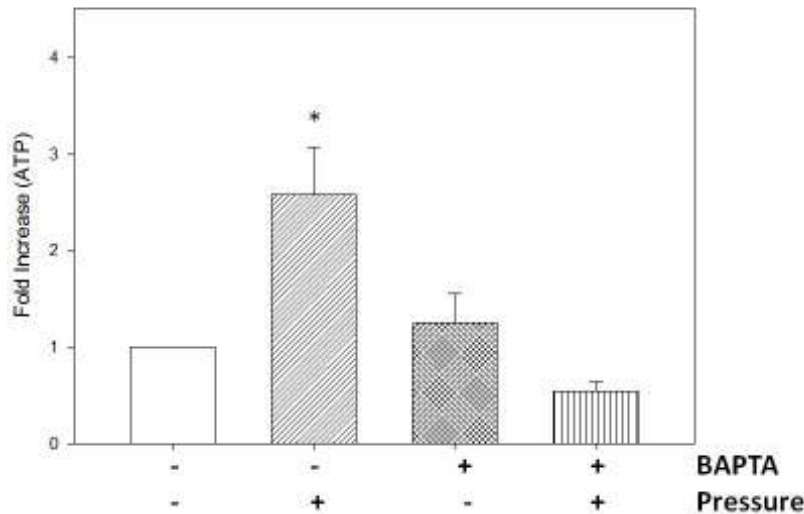


Figure 3-5. ATP release from urothelial cells in response to hydrostatic pressure in the presence of a calcium chelator. Rat UCs were exposed to hydrostatic pressure of 10 cmH₂O for 5 minutes with or without pretreatment with BAPTA (1 mM). Cells exposed to pressure exhibited an increase in ATP concentration compared to the control, while BAPTA-treated cells exhibited no change in ATP concentration in the presence of hydrostatic pressure. Data collected previously by Joshua Stover. Data are mean \pm SEM; * $p < 0.05$, analyzed by ANOVA and tukey-test; n=3 experiments.

Extracellular $[Ca^{2+}]$ Plays a Role in the UC ATP Response to Hydrostatic Pressure

The pressure experiments were repeated under a single set of parameters (10 cmH₂O, 5 minutes) following pretreatment of UCs with either calcium chelator BAPTA (1 mM) or the vehicle (1X PBS) alone. Compared to the control (no pressure, no drug), the cells exposed to pressure alone exhibited a significant ($p < 0.05$) increase in supernatant ATP concentration (Figure 3-5). However, when the cells were exposed to hydrostatic pressure following the pretreatment with BAPTA, levels of ATP were similar to the control indicating that extracellular calcium ions are important for UC response to hydrostatic pressure.

Hydrostatic Pressure-induced ATP Release by UCs is Inhibited in the Presence of Select Ion Channel Antagonists

The involvement of select ion channels in pressure transduction by UCs was examined by pharmacologically blocking these channels. When exposed to nifedipine (10 μ M), a blocker of L-type voltage-gated calcium channel (LVCC), ATP release under hydrostatic pressure was unchanged compared to cells exposed to pressure without nifedipine (Figure 3-6B). However, pretreatment of cells with gadolinium chloride (50 μ M), an inhibitor of gadolinium-sensitive stretch-activated channels (SAC), ruthenium red (1 μ M), a non-specific TRP inhibitor, and amiloride (1 mM), a degenerin/ENaC channel blocker, all resulted in a significant reduction of pressure-induced ATP release (Figures 3-6A, C, D). These results suggest that, not LVCC, but SAC, TRP, and ENaC

channels may be involved in mechanotransduction of hydrostatic pressure by UCs. To confirm that TRP channels in the primary UCs are functional and induce ATP release when activated, separate experiments were performed; different batches of primary UCs that have been exposed to neither pressure nor any ruthenium red were subjected to TRPV1 and TRPV4 agonists, capsaicin (10 μ M) and 4 α -phorbol 12,13-didecanoate (4 α -PDD; 10 μ M), respectively. After 2 minutes, both cultures exposed to capsaicin and 4 α -PDD exhibited near a 4-fold increase in supernatant ATP concentration (Figure 3-6C) compared to baseline.

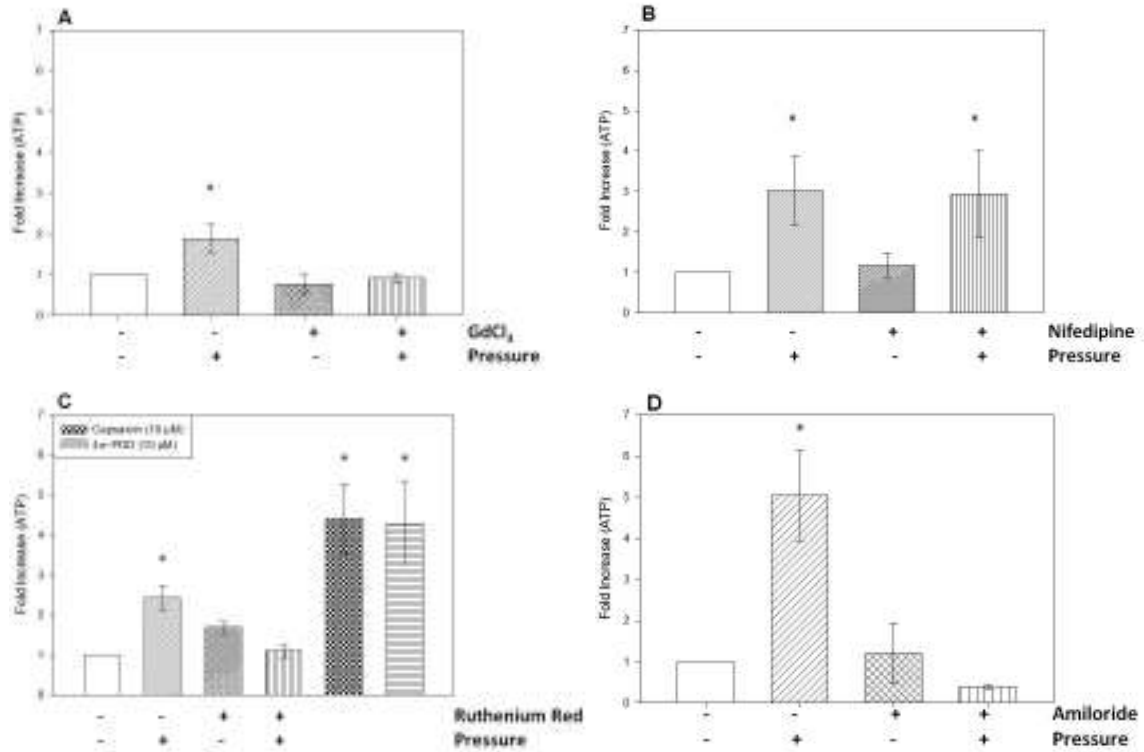


Figure 3-6. ATP release from urothelial cells in response to hydrostatic pressure in the presence of ion channel blockers. Rat UCs were exposed to hydrostatic pressure at 10 cmH₂O for 5 minutes with or without pretreatment with GdCl₃ (Frame A; 50 μM), nifedipine (Frame B; 10 μM), ruthenium red (Frame C; 1 μM), or amiloride (Frame D; 1 mM). Cells exposed to gadolinium chloride, ruthenium red, and amiloride, in the presence of hydrostatic pressure, exhibited a reduction in ATP release compared to cells exposed to only pressure. Nifedipine did not exhibit an inhibitory effect on hydrostatic pressure-induced ATP release by UCs. In separate experiments, UCs were exposed to TRPV1 and TRPV4 agonists capsaicin (10 μM) and 4α-PDD (10 μM), respectively without exposure to hydrostatic pressure (Frame C). Exposure of the cells to both

capsaicin and to 4 α -PDD resulted in a significant increase in ATP release. Data are mean \pm SEM; * $p < 0.05$, analyzed by ANOVA and tukey-test; n=3 experiments.

3.4 Discussion

The present *in vitro* study sought to explore the role of select ion channels in UC hydrostatic pressure mechanotransduction. Using a custom-made pressure system previously reported [96], a monolayer culture of primary UCs were exposed to hydrostatic pressure at various levels (5, 10, 15, and 20 cmH₂O) for durations up to 30 minutes, and the ATP concentration of supernatant culture media was quantified (Figure 3-4). This experimental model was used since, *in vivo*, the apical side of the umbrella cells is subjected to the sustained hydrostatic pressure from containment of urine within the bladder. By exposing a monolayer of UCs to sustained pressure, the present model allowed the ability to mimic this physical relationship between the cells and fluids. While the lowest (5 cmH₂O) and the highest (20 cmH₂O) pressure levels tested in the present study did not elicit a notable ATP response by UCs at any time point, a significant ($p < 0.05$) increase in ATP release was observed at 10 cmH₂O (5 mins) and 15 cmH₂O (5 and 15 mins). These results provide evidence that UCs are sensitive to pure hydrostatic pressure, assuming that there was no cell deformation since cells are considered incompressible [100, 101]. In contrast to the present study, previous studies have typically examined UC response to mechanical stimuli by exposing the serosal side of urothelium tissue to a column of buffer solution with the mucosal side unsupported via a

modified Ussing chamber [15, 50, 85, 94]. It should be noted that this method of pressure application also causes tissue deformation (bowing), introducing another variable, namely stretch, to the model. That was not the case in the present study, since UCs were exposed to hydrostatic pressure on a rigid substrate.

The time-dependent ATP response in the present study showed an increase at 5 and 15 minutes and a decrease to the baseline at 30 minutes, which may be explained by the following. First, studies have shown that ion channels in UCs can desensitize after continuous exposure to stimuli [102], suggesting that constant pressure application eventually may attenuate the ion channel-mediated ATP response to pressure. Second, a recent *in vitro* study by Matsumoto-Miyai *et al* has demonstrated that ATP released by the urothelium is degraded to nearly 50% of the original concentration within 60 minutes due to the action of native ecto-ATPases [94]. While their model systems are different (using a whole urothelium tissue, rather than a monolayer culture) than the present setup, it is possible that the UC's response to pressure is a rapid and transient event and the ATP level returned to the baseline due to ATP degradation. To verify this, however, further studies are necessary to determine the dynamic ATP response of UCs to pressure.

The pressure levels tested in the present study were selected based on a report in the literature that the threshold to trigger micturition in rats was in this range (16.3 ± 2.2 cmH₂O) [99]. The observation that a significant ATP release by UCs occurred in a specific range (10-15 cmH₂O), but not above or below these magnitudes (Figure 3-4), suggests that UC's response to hydrostatic pressure may be part of the mechanism for

sensing bladder fullness. We speculate that certain ion channels play a role in this physiological function. Because it has been shown that a number of ion channels are only activated by temperature within specific ranges (TRPM8 8-28°C; TRPV4 35-42°C, TRPV3 40-50°C) [31, 103], it is possible that certain ion channels may only be activated by pressure near the micturition threshold and not above or below this range.

In order to determine the role of various ion channels in pressure mechanotransduction, pressure experiments were repeated in the presence and absence of select agents. Since calcium has been shown to play a role in cellular mechanotransduction in various organ systems including the bladder [45, 104, 105], the UCs were pretreated with BAPTA, an extracellular calcium chelator, and quantified the ATP concentration following exposure to pressure. The results of these experiments (Figure 3-5) were in agreement with previous reports that removal of extracellular calcium inhibits mechanically-triggered ATP release by UCs [82]. To further investigate how Ca^{2+} is involved in pressure mechanotransduction of ATP release in UCs, L-type calcium channel was examined because of its high affinity with Ca^{2+} and its suggested role in secondary messenger release (NO) in rat bladder UCs [106]. Blocking these channels with nifedipine (10 μM), however, did not affect pressure-evoked ATP release (Figure 3-6B), suggesting that the L-type calcium channel does not play a role in bladder pressure mechanotransduction.

As discussed previously, the TRP channels have been studied extensively in UCs for their role in temperature, chemical, and stretch sensing in the bladder [50, 86]. In the

present study, the expression and functionality of TRPV1 and TRPV4 in the UC cultures with RT-PCR (Figure 3-3A) was confirmed, and activation of the ion channels using capsaicin and 4 α -PDD, respectively; the UCs exhibited a 4-fold increase in ATP release when exposed to these specific TRP channel agonists (Figure 3-6C). Following pretreatment with ruthenium red, a non-specific TRP channel antagonist, the UCs exposed to hydrostatic pressure exhibited similar levels of ATP to the no pressure control group, indicating that at least one or both TRP channels are involved in mechanotransduction of hydrostatic pressure. A study by Caterina *et al.* demonstrated that *Trpv1* knockout mice were still able to detect harmful pressure applied to the hindlimb paws, while a different study by Suzuki *et al.* provided evidence that *Trpv4* knockout mice have impaired sensation for harmful pressure to the tail [80, 107]. Since these studies have suggested that TRPV4, and not TRPV1, functionality is required to sense pressure on the body surface, it is possible that TRPV4 is necessary for the bladder response to hydrostatic pressure as well.

Although at a lesser degree, inhibition of pressure-induced ATP release from UCs was also observed following pretreatment with GdCl₃, a blocker of stretch-activated channels (SACs) (Figure 3-6A) suggesting that SACs possibly play a role in the UC detection of hydrostatic pressure. In the field of continuum mechanics, cells are generally considered to be incompressible, and thus, cells are not expected to deform under hydrostatic pressure, especially at physiologically relevant levels [100, 101]. These results, however, suggest that UCs may undergo deformation to cause membrane

stretch when exposed to hydrostatic pressure. A more plausible explanation, however, is the off-target effects of the GdCl_3 used in these experiments. In addition to being a primary inhibitor of SACs, gadolinium ($50 \mu\text{M}$) has been shown to inhibit multiple TRP channels including TRPC1, TRPC4, TRPC5, and TRPV1 [108]. Therefore, it remains possible that the attenuated ATP response to pressure in the presence of GdCl_3 was due to inhibition of TRPV1 or TRPV4, rather than SACs.

The involvement of ENaCs in urothelial cell mechanosensory function was demonstrated previously by Ferguson and others [15]. However, because the experimental setups used in these studies allowed tissue stretch under the applied pressure, it was not definitively distinguished whether pressure, stretch, or a combination of both, triggered ATP release by UCs. In addition, because these previous studies were conducted with urothelial tissue rather than a monolayer of cells, it was not clear whether UCs or underlying myofibroblasts responded to the stimuli. These results showed a significant inhibition of pressure-induced ATP release when cells were pretreated with amiloride (Figure 3-6D), a blocker of ENaCs, which is not only in agreement with previous reports that ENaCs play a role in urothelial mechanotransduction [14, 15], but also demonstrated for the first time that pressure transduction may be mediated by ENaCs. While it has been reported that amiloride ($\text{IC}_{50} = 129 \mu\text{M}$) can block activation of TRPC-6 channels in arterial smooth muscle cells [109], its cross reactivity with other TRP channels present in the urothelium has not been demonstrated to the best of the authors' knowledge. Since neither ruthenium red nor gadolinium is known to effectively

inhibit ENaCs, the authors have postulated two possible explanations for a mechanism that requires both TRP channels and ENaCs to be activated in the UC response to pressure. First, it is possible that co-activation of TRPV channels and ENaCs is necessary for subsequent ATP release by UCs under hydrostatic pressure. It has been reported that co-activation of K^+ and Cl^- channels occurs during cell swelling of vascular endothelial cells, which leads to modulation of Ca^{2+} ion current into the cell [110, 111]. Similar mechanisms may be at work for UCs with co-activation of TRPV channels and ENaCs in Ca^{2+} -dependent ATP response to hydrostatic pressure. Second, TRPV channels and ENaCs could be activated in series, rather than in parallel. It is possible that hydrostatic pressure activates one of these channels, which could lead to a signaling cascade that activates the other ion channel, ultimately resulting in ATP release. However, using only end-point analysis without performing real-time electrophysiological measurements or Ca^{2+} imaging, this conclusion cannot definitively be made.

While this study focused on the possible activation of ion channels directly by hydrostatic pressure, there remain other indirect mechanisms by which UCs may detect hydrostatic pressure via activation of these channels. As mentioned earlier, it is unlikely that physiologically relevant levels of hydrostatic pressure in the bladder could directly cause cell deformation. However, due to the increase in entropy associated with pressure change, exposure to hydrostatic pressure may cause depolymerization of the microtubules making up the cellular cytoskeleton [112]. The subsequent change in cell membrane

stability could allow for water to either leave or enter the cell, resulting in cell volume change and, consequently, membrane deformation. Therefore, it remains possible that UC ion channels are indirectly activated by membrane deformation rather than by hydrostatic pressure.

In the present study, it was demonstrated for the first time that cultured UCs release ATP when exposed to sustained hydrostatic pressure in the physiological threshold range that would trigger micturition (10-15 cmH₂O). This release of ATP also appeared to be dependent on the exposure time, as cells exposed to pressure for thirty minutes did not elicit a significant ATP release. The results of the present study provided evidence that at least one or multiple types of ion channels that are considered mechanosensitive play a role in mechanotransduction of hydrostatic pressure. These results support a view that not only tissue stretch or tension, but also pressure is an important parameter for mechanosensing of bladder fullness. However, further study with different experimental approaches is necessary to determine the exact mechanism by which these channels are activated under hydrostatic pressure and to advance the current understanding of mechanotransduction.

-Chapter 4-

Aim 2: To Elucidate the Role of Cell Volume Change in Mechanotransduction of
Hydrostatic Pressure in Urothelial Cells

4.1 Introduction

Conventionally, the bladder-lining urothelial cells (UCs) were thought to only serve as a barrier between urine and the underlying tissue. However, recent research has indicated that UCs play a role in sensing mechanical and chemical stimuli to the bladder [33, 88]. More specifically, the afferent nerves innervating the bladder have been found to be activated by molecules such as nitric oxide (NO) [46], adenosine triphosphate (ATP) [15, 85, 94], and acetylcholine [113] released by UCs, with the claim that the majority (50-75%) of afferent activity in the bladder is due to ATP [114]. These results suggest that problems with the sensory function of UCs can result in altered bladder sensitivity and various forms of voiding dysfunction [21]. To date, however, the exact mechanisms for how UCs sense mechanical stimuli are yet to be elucidated. Moreover, a debate exists as to whether tissue stretch [85, 94] or hydrostatic pressure [15, 33, 115] is the mechanical signal by which the bladder senses fullness.

Several groups have examined the mechanosensitivity of the urothelium by exposing one side of a mouse or rabbit tissue to pressure (up to 45 cmH₂O) on a modified Ussing chamber and quantifying the ATP released in response [15, 85, 94]. The results to date indicated that the mechanically-induced ATP release was potentially through

membrane-bound gating mechanisms [15] and dependent on extracellular Ca^{2+} concentration [86] as well as on ion transport across the apical membrane [85]. While these studies provided important information about the urothelial response to pressure, the inherent limitations of the experimental setup design prevented from decoupling pressure and the associated tissue stretch, making it difficult to determine the sole effect of hydrostatic pressure on UCs.

Previously, we reported that rat bladder UCs cultured on a rigid substrate released an increased amount of ATP in response to physiological-level (10-15 cmH_2O) hydrostatic pressure when compared to baseline (0 cmH_2O) levels [115]. These results provided the first evidence that UCs are indeed responsive to hydrostatic pressure. In addition, we observed that this ATP release was attenuated by chelating extracellular Ca^{2+} , or blocking transient receptor potential (TRP) and epithelial sodium channels (ENaC) with BAPTA, ruthenium red, and amiloride, respectively. Although these ion channels are known to be activated by membrane stretch due to distention of bladder tissue [15, 50, 86, 94] or hypotonic cell swelling of cells [116, 117], they have not been shown to be involved in mechanotransduction of hydrostatic pressure. Cells are generally considered incompressible, and thus, are not expected to deform under physiologically relevant levels of hydrostatic pressure [100]. Therefore, we have postulated that either these ion channels are also sensitive to hydrostatic pressure or UCs undergo cell swelling during exposure to hydrostatic pressure.

In the present study, the latter case was examined to describe part of a novel mechanism for urothelial cell mechanotransduction of hydrostatic pressure. More specifically, in order to quantify urothelial cell volume changes during exposure to hydrostatic pressure, real-time cell imaging was conducted using fluorescence microscopy and a custom-made pressure perfusion chamber. Furthermore, the present study examined the roles of both Na⁺ ions and ENaC in the urothelial cell volume response to hydrostatic pressure.

4.2 Materials and Methods

Cell Culture

Primary UCs were harvested from bladders of Sprague-Dawley rats according to methods described previously [95, 115]. Briefly, under sterile conditions, the bladders were excised from animals immediately after sacrifice and trimmed of any excess fat and connective tissue. The bladder was then inverted using a blunt 18 ½ gauge needle and filled with 2-3 ml of sterile phosphate buffered saline (PBS) solution. The inflated bladder was tied off with a sterile suture and incubated in 0.05% trypsin (Invitrogen, Carlsbad, CA) with gentle stirring under standard cell culture conditions (37 °C, 95% air/5% CO₂, humidified environment) for 25 minutes. The trypsin solution that contained UCs was combined with equal volume of fresh fibroblast medium (FM: DMEM/F12 (Invitrogen) medium supplemented with 10% fetal bovine serum (FBS) (Hyclone, Logan, UT), penicillin (10,000 units/mL), and streptomycin (10,000 µg/mL)), and centrifuged at

1000 RPM for five minutes. The cell pellet was then resuspended in the UC growth medium [95], a 1:1 mixture of 3T3 fibroblast-conditioned FM and keratinocyte growth medium (KGM: keratinocyte medium (Invitrogen) supplemented with 2% FBS, bovine pituitary extract (12.5 mg/ml, Invitrogen), insulin-transferrin-selenium (1 mg/mL), hydrocortisone (50 µg/mL), epidermal growth factor (35 ng/µL, Invitrogen), amphotericin (250 µg/mL), and gentamicin (50 mg/mL)). UCs were cultured for up to 7 days until they reached confluence prior to use in experiments. Urothelial phenotype was confirmed by the characteristic, cobble-stone cell morphology and immunostaining with CK17 and the fluorescently (Alexa Fluor 488) tagged secondary antibody [115]. UROtsa cells were kindly provided by Dr. Naoki Yoshimura, Department of Urology, University of Pittsburgh. UROtsa cells were cultured in Dulbecco's modified Eagle's medium (DMEM) supplemented with 5% fetal bovine serum (FBS) and 1% antibiotic-antimycotic. UROtsa cells used in experiments were passage number ten through fifteen. 3T3-Swiss albino mouse fibroblast cells (ATCC #CCL-92) were cultured in fibroblast medium (FM) according to the vendor's instructions. 3T3 fibroblasts used in experiments were passage number three through five.

Application of Hydrostatic Pressure to Urothelial Cell Culture

Cells were seeded on collagen-coated coverslips at a density of 5.0×10^5 cells/coverslip and cultured under standard cell culture conditions (at 37°C in humidified 5% CO₂ 95% air) for 24 hours. Thirty minutes prior to experiments, cells were loaded

with calcein-AM (5 μ M; Invitrogen, CA). Coverslips were then placed in a custom-made perfusion chamber adapted from a study by Mandal et al [118] and perfused with Hanks Balanced Salt Solution (HBSS containing (137.0 mM NaCl, 5.4 mM KCl, 0.25 mM Na₂HPO₄, 0.44 mM KH₂PO₄, 1.3 mM CaCl₂, 1.0 mM MgSO₄ pH=7.4, 37°C). In separate experiments to test the role of Na⁺ ions in cell volume change, a Na⁺-free HBSS solution was made by replacing NaCl and Na₂HPO₄ with N-methyl-D-glucamine (NMDG; 140mM). In these same experiments to test the role of epithelial sodium channels (ENaC), amiloride (1 μ M) was added to the standard HBSS. All compounds used in the HBSS solution were obtained from Sigma-Aldrich (St. Louis, MO). In order to minimize dye leakage, probenecid (1 mM; Invitrogen) was added to the perfusion solution. Perfusion of heated HBSS solution (35-40°C) was achieved by using a peristaltic pump (MINIPULS 2, Gilson Inc., Middleton, WI) at a flow rate of 1.0 ml/min. The HBSS solution flowed through a custom-made inline heater and a pulse dampener before entering the flow chamber. Hydrostatic pressure experienced by the cells was controlled by raising the height of the perfusion outlet to the desired pressure level (cm) using a custom-made, computer-controlled vertical actuator. (Figure 4-1)

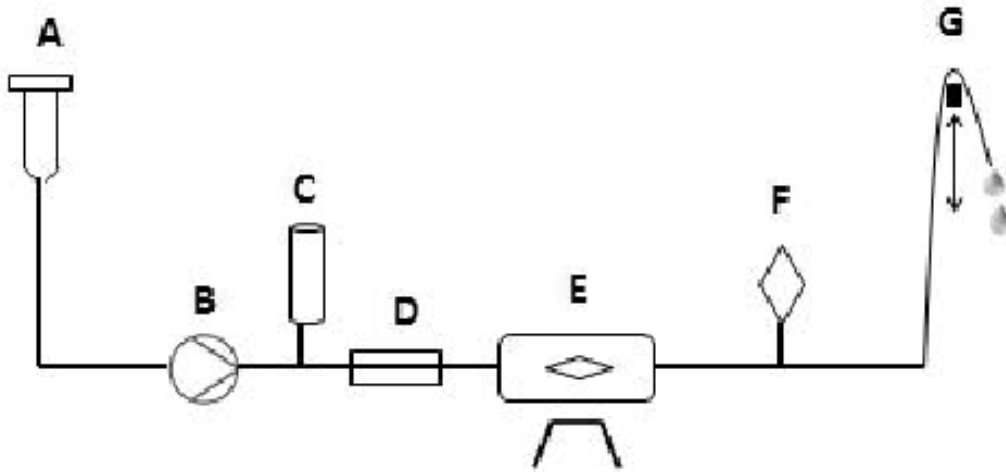


Figure 4-1. Schematic diagram of custom-made pressure perfusion chamber. Perfusate solution from a reservoir (A) was driven by a peristaltic pump (B) at a rate of 1 ml/min through a flow dampener (C) and a custom-made inline heater (D) into the chamber (E) where the cells were imaged by an inverted fluorescence microscope. Pressure levels experienced by the cells were constantly monitored by a pressure transducer (F) and controlled by an automated vertical actuator (G).

Image-based Quantification of Cell Volume Changes

Using real-time imaging with an Olympus IX-81 fluorescence microscope (Olympus America, Center Valley, PA) and a CCD camera (Hamamatsu Corporation, Sweden), changes in the fluorescence intensity of the calcein dye inside cells during exposure to the pressure stimulus were captured. The data were plotted as relative fluorescence intensity with initial equilibrium conditions serving as 1.0 using MetaMorph

software (Molecular Devices, Silicon Valley, CA). A decrease in the fluorescence intensity, ΔFI , was calculated as FI normalized to baseline values obtained under equilibrium (0 cmH₂O) conditions. In trials where constant dye leaching was apparent, resulting in an overall decrease in FI over time, data were adjusted by re-calibrating FI values under equilibrium conditions to 1.0. The time constants (τ), the time each cell took to reach 63% of its final steady-state fluorescence intensity value, were calculated with the following equation.

$$F(t) = F_0 e^{-\frac{t}{\tau}}, \text{ where} \quad (1)$$

F (t) = Fluorescence intensity at time (t),
F₀ = Ending fluorescence intensity,
t = Time (sec),
 τ = Time constant (sec).

Confocal Imaging and Cell Volume Measurement

Cells pre-loaded with Calcein-AM were imaged using the spinning disk confocal function of the Olympus IX-81 fluorescence microscope at 0 cmH₂O (ambient) and 10 cmH₂O pressure levels. Multiple images were taken in the z-plane at 0.2 μm intervals to cover the entire height of all cells in the field of view. Using the MetaMorph software, the area of the cells in each plane was determined by layering the image with a fluorescence intensity threshold. Total cell area was computed by MetaMorph and the cell volume was then estimated by multiplying the area of each plane by the height (z-axis) of each cell.

Statistical Analysis

Each volume change experiment was performed with a minimum number of 20 cells per field of view. The mean values of data from three experiments were calculated and compared using single-factor analysis of variance (ANOVA). The mean values of data from the Na⁺ experiments were calculated and compared using ANOVA and Tukey-test. When a statistically significant difference was detected, a post hoc pairwise analysis was conducted using the Tukey-test. Statistical analyses of numerical data were performed using Sigma Stat software (Systat Software Inc., Richmond, CA, USA). P-values less than 0.05 were considered statistically significant.

4.3 Results

Exposure of Urothelial Cells to Hydrostatic Pressure Results in Fluorescence Intensity Decrease

The experiments were conducted by exposing calcein-loaded primary UCs, UROtsa cells, and 3T3 fibroblasts to varying levels of pressure while measuring changes in fluorescence intensity. Comparison of pseudo-color fluorescence images of UROtsa cells before and during exposure to hydrostatic pressure (Figure 4-2) revealed a decrease in fluorescence intensity exhibited by cells exposed to 20 cmH₂O of pressure compared to the control. The time-plot of fluorescence intensity indicated that both UCs (Figure 4-3A) and UROtsa cells (Figure 4-3B) exhibited a sharp drop in fluorescence intensity when exposed to hydrostatic pressures of up to 20 cmH₂O. When 3T3 fibroblasts were

exposed to hydrostatic pressure of similar levels (0-15 cmH₂O), (Figure 4-3C) these cells exhibited no detectable change in fluorescence intensity.

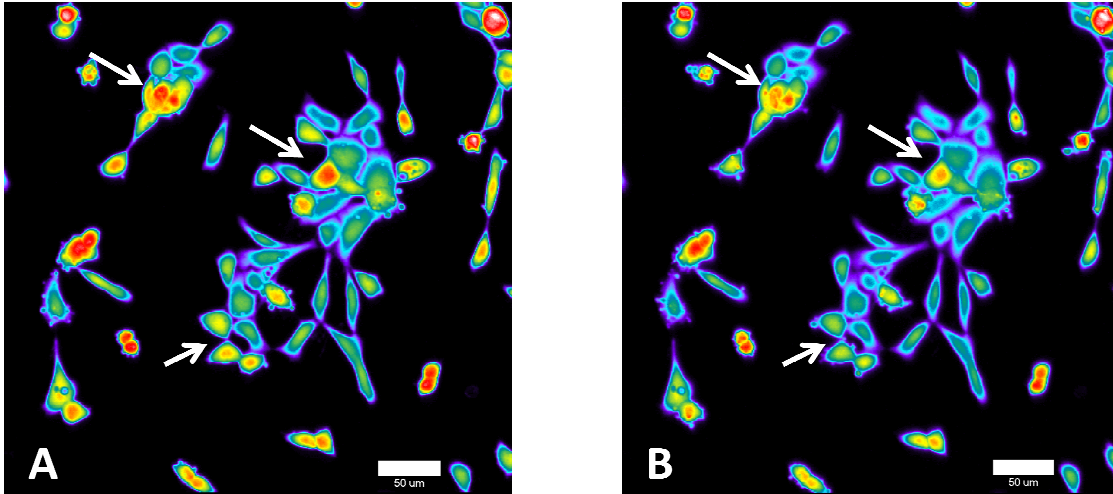


Figure 4-2. Pseudo-color fluorescence images of UROtsa cells under hydrostatic pressure. UROtsa cells loaded with calcein-AM were imaged at 0 cmH₂O (Frame A) and 20 cmH₂O (Frame B) (20x; NA=0.45). Higher F.I. values are denoted by the “hotter” colors. Arrows denote representative cells that exhibit a Δ FI. Scale bar = 50 μ m.

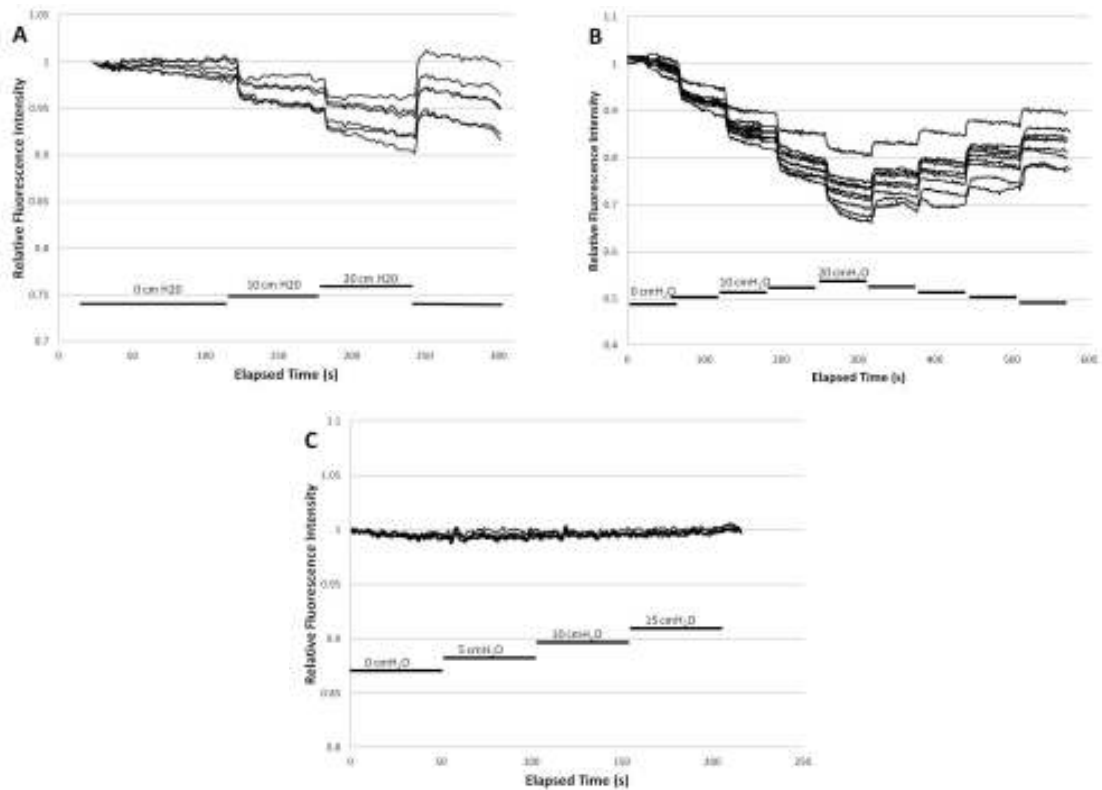


Figure 4-3. Change in cell volume of different cell types. Primary UCs, UROtsa and 3T3 fibroblasts were all exposed to hydrostatic pressure varying from 0 to 20 cmH₂O using a custom perfusion chamber. Both primary UCs (Frame A) and UROtsa (Frame B) exhibited sharp Δ FI values when exposed to hydrostatic pressure. Fibroblasts (Frame C) did not show any noticeable Δ FI when exposed to hydrostatic pressure up to 15 cmH₂O. The observed gradual change in fluorescence intensity over time in some trials was attributed to minor dye leaching

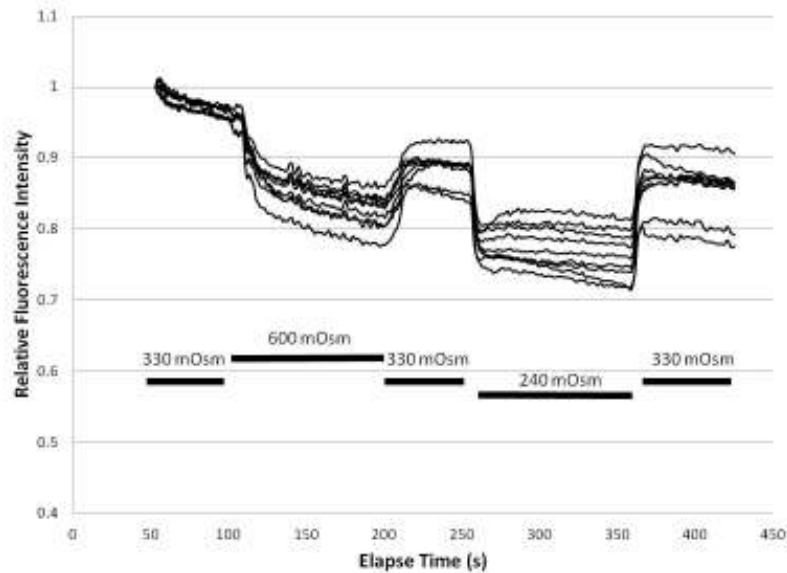


Figure 4-4. Change in fluorescence intensity of primary UCs undergoing osmotic shock. Primary UCs loaded with calcein-AM were exposed to HBSS with various tonicities and F.I. was measured. Both hypertonic (600 mOsm) and hypotonic (240 mOsm) solutions caused a decrease in F.I., however the hypotonic stimulus resulted in a much sharper Δ FI.

Osmotic Shock Elicits a Measurable Change in Fluorescence Intensity

To calibrate the imaging setup to measure the real-time fluorescence intensity of UCs during changes in cell volume, UCs were exposed to hypotonic (240 mOsm) and hypertonic (600 mOsm) solutions compared to the standard isotonic solution (330 mOsm). Both the hypotonic and hypertonic solutions caused a decrease (10-15%) in fluorescence intensity (Figure 4-4). The response plots for these solutions exhibited different shapes. In order to differentiate between cell swelling and shrinkage, the time

constant (τ) of the fluorescence intensity drop was calculated for both the hypotonic and hypertonic solutions. The time constant for the cell response to the hypertonic solution was found to be significantly higher ($p < 0.05$) than to the hypotonic solution (Table 4.1). These values were then used as a reference to determine whether exposure to hydrostatic pressure results in cell volume increase or decrease. By comparing the behavior of the fluorescence intensity decrease due to hydrostatic pressure ($\tau=2.720 \pm 1.836$) to that found in cells exposed to a hypotonic stimulus it was determined that UCs increase in cell volume during exposure to hydrostatic pressure.

Table 4.1. Time constants calculated from osmotic shock experiments

Stimulus	Time Constant (τ; sec)	n (Cells)
Hypertonic (600 mOsm)	7.56 ± 3.70	28
Hypotonic (240 mOsm)	$2.95 \pm 0.95^*$	27
Hydrostatic Pressure	$2.72 \pm 1.84^*$	17

Data are mean \pm SEM; * $p < 0.05$ analyzed by ANOVA and Tukey-kramer test.

Confocal Imagery Suggests Increase in Cell Volume Involves Spreading at the Base

Confocal images of UCs were taken before and during exposure to hydrostatic pressure at 10 cmH₂O to quantify the layer-by-layer changes in cell area. Qualitatively, it appeared that cells exposed to hydrostatic pressure exhibited an increase in volume near the bottom third of the cell. The interstitial space between cells appeared to decrease when exposed to pressure in images taken at 1 μ m from the base of the cells (Figure 4-5).

These observations were confirmed when examining a histogram of total cell area vs. z-position (measured from the coverslip level) (Figure 4-6). Overall, the estimated total cell volume of 15 cells was 7.7% greater in cells exposed to 10 cmH₂O compared to control.

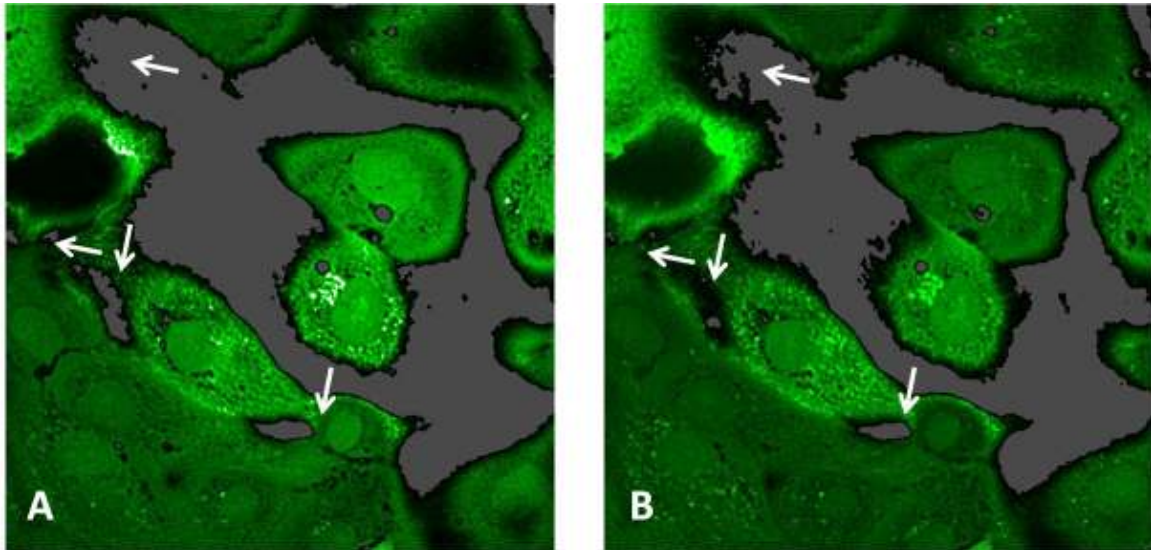


Figure 4-5. Confocal images of urothelial cells under hydrostatic pressure taken at $z = 1.0 \mu\text{m}$. Primary UCs were loaded with calcein-AM and exposed to 0 and 10 cmH₂O while imaged using spinning-disk confocal microscopy (40x; NA=0.60). Cells exposed to 10 cmH₂O of pressure (Frame B) appear to have a decreased interstitial space, denoted by white arrows, than the control group (Frame A).

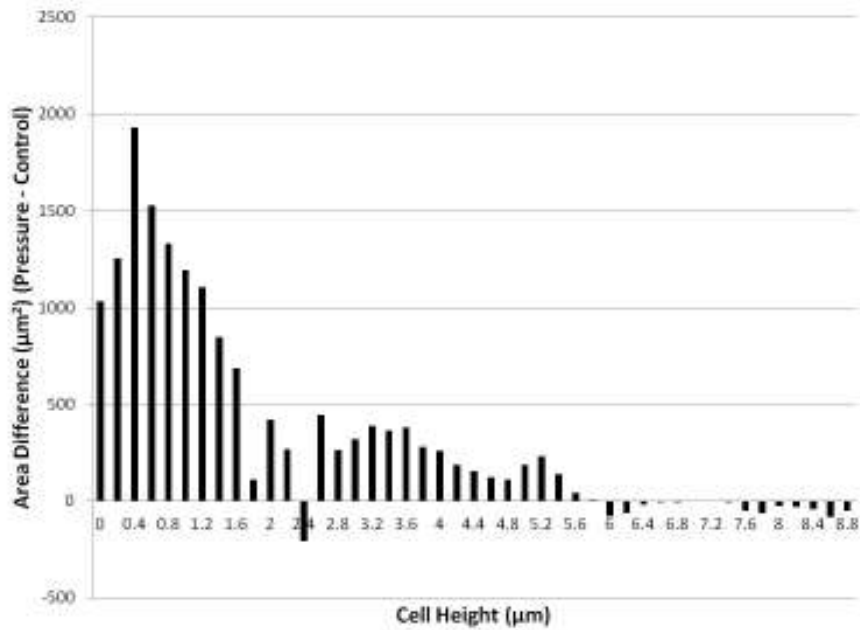


Figure 4-6. Histogram of difference in total cell area between pressure and control groups. Primary UCs were imaged using spinning-disk confocal microscopy. Total area of cells in the field-of-view (n=15 cells) at each step in the z-direction (0.2μm) was calculated. UCs exposed to 10 cmH₂O exhibited a larger total area in the bottom 1/3 of the cell height compared to the control group, suggesting that UCs spread near the base of the cell when exposed to hydrostatic pressure.

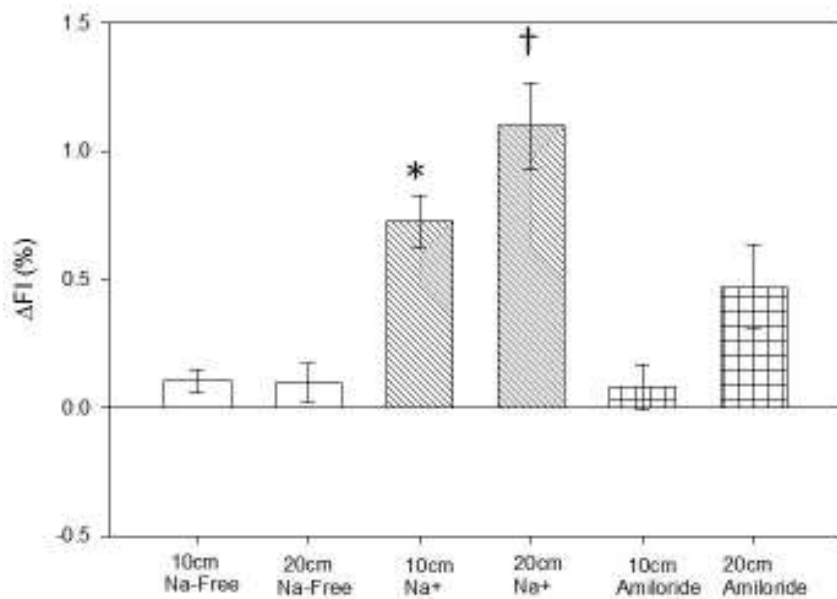


Figure 4-7. Relative change in fluorescence intensity of primary urothelial cells without Na⁺ and using ENaC blocker. Primary UCs were exposed to hydrostatic pressure with and without Na⁺ present in the perfusion solution. The ΔFI was significantly higher in the presence of Na⁺ both at 10 and 20 cmH₂O than the Na-free group. When blocking ENaC with amiloride (1 μM) while in the presence of Na⁺, the ΔFI was attenuated at both pressure levels. However, the relative ΔFI was significantly higher at 20 cmH₂O in the amiloride group. Data are mean ±SEM; *† p <0.05 analyzed by ANOVA and Tukey-test; n = 26 cells.

Na⁺-dependent Cell swelling Response of Urothelial Cells to Hydrostatic Pressure

To elucidate the mechanism by which UCs increase in cell volume under hydrostatic pressure, the experiments were repeated with a Na-free solution. Cells perfused with the Na-free solution exhibited negligible increase in cell volume (ΔFI) when exposed to both 10 and 20 cmH₂O hydrostatic pressure, which were significantly ($p < 0.05$) lower when compared to the ΔFI of cell exposed to pressure in the presence of Na⁺ (Figure 4-7). Moreover, under both 10 and 20 cmH₂O of pressure, UCs perfused in the presence of amiloride (1 μ M) exhibited significantly ($p < 0.05$) smaller ΔFI values than the cells exposed to pressure in the absence of amiloride. However, cells perfused in the presence of amiloride at 20 cmH₂O pressure did display a noticeable ΔFI , which was significantly higher than the ΔFI of cells exposed to a similar pressure in the Na-free solution.

4.4 Discussion

The present *in vitro* study sought to examine the role of cell volume change in urothelial cell mechanotransduction of hydrostatic pressure. Previously, we observed that hydrostatic pressure elicited a release of ATP from UCs which was attenuated when certain ion channels (TRP, ENaC) were blocked [115]. Others have demonstrated that these ion channels are sensitive to membrane stretch [15, 50, 86, 94], but not necessarily to hydrostatic pressure. Thus, we speculated that UCs might exhibit membrane deformation through either cell swelling or cell-shrinking under hydrostatic pressure.

Due to the fact that a number of in vitro studies have shown that hypotonic shock, a model mechanical stimulus that causes rapid cell swelling, induces ATP release in epithelial cells of the lung [119], liver [120], and bladder [82, 121-123], we hypothesized that exposure of UCs to hydrostatic pressure may lead to cell swelling, which subsequently causes ATP release. Using a custom-made perfusion chamber (Figure 4-1), primary UCs, UROtsa cells, and 3T3 fibroblasts pre-loaded with calcein-AM were exposed to hydrostatic pressure up to 20 cmH₂O while being imaged using fluorescence microscopy. Both UCs and UROtsa cells exhibited a sharp decrease in fluorescence intensity, but not the fibroblasts (Figure 4-3). These results were compared with our experiments that exposed primary UCs to both hypertonic (600 mOsm) and hypotonic (240 mOsm) solutions (Figure 4-4). Qualitatively, the hypotonic stimulus elicited a sharp decrease in fluorescence intensity due to a dilution of dye, while exposure of cells to the hypertonic stimulus resulted in a gradual decrease due, most likely, to self-quenching of calcein fluorophores [124]. In order to quantitatively compare the responses, the time constant (τ) of the response to both stimuli was calculated (Table 4.1). Since the response of urothelial and UROtsa cells to pressure was similar to the response to a hypotonic stimulus, it was concluded that these cells undergo a rapid increase in cell volume during exposure to hydrostatic pressure. Although mechanical deformation of the coverslip due to application of pressure could possibly affect measurements, we confirmed that the changes in fluorescence intensity were cell volume response when

fibroblasts exposed to similar pressures up to 15 cmH₂O did not exhibit any changes in fluorescence measurements.

The cell-volume increases observed using the real-time fluorescence imaging were further confirmed using spinning-disk confocal microscopy. From images taken before and during exposure to 10 cmH₂O hydrostatic pressure at the identical z-position (1 μm from the base of the cells; Figure 4-5), it was apparent that cells exposed to hydrostatic pressure were greater in area. The increase in cell-volume under pressure was confirmed by calculating and comparing the total area of the cells in each image (Figure 4-6) between control and pressure groups from all z-positions. While there was no detectable change in cell height between the two groups, there were large increases in total areas of cells in the pressure group compared to the control. These results also provided evidence that cell volume increase under hydrostatic pressure occurred in the bottom third of the cell, whereas the upper portion of the cells remained relatively unchanged. This localized change indicates that cell cytoplasm is not a simple continuum as often modeled [100], but rather a compartmentalized structure. However, further investigation with more sophisticated imaging approaches will be necessary to quantify the dynamic changes in local deformation to confirm this.

The results of the present study contrast previous work by Tschumperlin *et al.*, which demonstrated that the lateral interstitial space (LIS) between normal human bronchial epithelial (NHBE) cells decreased, but no change in cell volume was detected when exposed to pressure (20 cmH₂O) for 30 minutes [125]. More specifically, a

confluent layer of NHBE cells on cell culture inserts subjected to transmural pressure (20 cmH₂O) exhibited an approximately 10% decrease in height, but an increase in width in the middle portion of the cell, resulting in a zero net change in cell volume. The different results in these studies may be due to the difference in setups and/or time scales of experiments in addition to the differences in the species (human vs. rat) or cell origin (lung vs. bladder). In the present study, thick glass coverslips were used to minimize deformation of substrates under pressure in order to isolate the effect of pressure from combined effects of pressure and stretch. In contrast, the cell culture inserts used in the Tschumperlin study may have allowed for bowing of the substrates under pressure, which could lead to lateral stretching of cells. Moreover, the present study focused on the immediate volume response of UCs to hydrostatic pressure within seconds rather than investigating the pressure effects on a growth-factor signaling pathway over a period of 30 minutes. Therefore, it is possible that the volume increase by UCs under pressure observed in the present study may be a transient response, which over a period of time equilibrates to allow recovery of their original volume. While the observed responses to pressure by urothelial and NHBE cells are different, together these studies illustrate promising progress in the field of cellular mechanotransduction of pressure.

In order to elucidate possible mechanisms for pressure-evoked cell swelling, the present study examined the roles of sodium, and ENaC in urothelial cell volume response to hydrostatic pressure. It had previously been shown that blocking ENaC with amiloride in human vascular endothelial cells [126] or removal of extracellular Na⁺ from cultures of

glial cells [127] prevented cell swelling in response to hypotonic challenge. Furthermore, without active transport by membrane-bound Na^+ -pumps, the accumulation of intracellular Na^+ ions results in cell swelling [128]. Thus, we hypothesized that altered Na^+ transport via ENaC might be part of the cell swelling mechanism in UCs under hydrostatic pressure. The results of the present study provided evidence that for UCs to respond to hydrostatic pressure (at both 10 and 20 cmH_2O), the presence of extracellular Na^+ was necessary (Figure 4-7). Although cells blocked with amiloride (1 μM) expressed a significantly ($p < 0.05$) smaller ΔFI than the experimental group exposed to similar pressures without amiloride, at 20 cmH_2O the value was significantly higher than those in the Na-free group. Together, we can speculate that the activation of ENaC may play a role in cell swelling due to a Na^+ -influx through these channels under hydrostatic pressure. However, a second mechanism (e.g. a different cation channel or sodium transporter) for pressure-induced Na^+ -influx and cell swelling may be turned on at higher pressures.

The Na^+ -, and possibly, ENaC-dependent cell swelling provides some explanation for our previous study which found that blocking extracellular Ca^{2+} , as well as either TRP channels or ENaC, prevented ATP from being released under exposure to pressure. It was originally hypothesized that ENaC and TRP channels could be co-activated, requiring both channels to be activated during transduction of hydrostatic pressure. The amiloride-sensitive volume increase of UCs under pressure, however, suggests that activation of ENaC may precede TRP channel activation in urothelial pressure

mechanotransduction. The cell membrane stretch due to swelling may activate TRP channels [79, 86, 129] and lead to intracellular calcium increase and subsequent ATP release by UCs [86]. While understanding this pathway will require further experimentation, the results of our present and previous studies together suggest that swelling-induced activation of membrane-bound ion channels is part of the pressure mechanotransduction by UCs.

At this point, several possible scenarios exist for the mechanism by which UCs increase cell volume under hydrostatic pressure. First, hydrostatic pressure may directly activate ENaC on the cell membrane and a subsequent influx of Na^+ ions could lead to water influx and cell swelling. To date, however, neither the existence of pressure-sensitive ion channels nor a theoretical understanding for activation of ion channels by pressure alone has been confirmed. Second, it has been suggested that, due to an increase in entropy associated with increased hydrostatic pressure, depolymerization of the cytoskeleton may occur when cells are under elevated pressure [130]. This sudden loss of support for cell membrane stability may allow water to enter the cell, leading to cell swelling, although the involvement of Na^+ in this process is unclear at this point. Finally, as proposed by Rauch et al., hydrostatic pressure may alter the homeostatic cycle of membrane recycling for endocytosis and exocytosis [131]. An increase in exocytosis under elevated pressure and the resultant increase in membrane surface area may be part of the cell-volume increase in UCs under hydrostatic pressure observed in the present study. However, to better understand the mechanisms by which UCs increase cell

volume under hydrostatic pressure, further studies involving various real-time recording approaches will be necessary.

The present study demonstrated for the first time that UCs increase in cell volume when exposed to hydrostatic pressure of up to 20 cmH₂O and that this process may be partially controlled by activation of ENaC and the presence of extracellular Na⁺. These results provided part of a novel mechanism for urothelial mechanotransduction of hydrostatic pressure and an explanation for the ENaC-dependent, pressure-evoked ATP release by UCs [14, 15, 81]. In addition, these findings support a view that hydrostatic pressure is as important a parameter as tissue stretch in the mechanosensory function of the bladder. Overall, the present study has revealed a new possible mechanism by which bladder UCs sense hydrostatic pressure. Better understanding of the mechanisms that initiate urothelial cell volume increase during exposure to pressure and the signaling events that trigger this response will advance our understanding of pressure mechanotransduction in UCs as well as other mechanosensitive cells.

-Chapter 5-

- **Aim 3-** To Characterize the ATP Release Kinetics by Urothelial Cells and to Determine the Potential Role of TRPV4 in Pressure Mechanotransduction

5.1 Introduction

Previously, we demonstrated that rat bladder urothelial cells (UCs) released elevated levels of ATP in response to physiologically relevant hydrostatic pressure (10-15 cmH₂O) and that this ATP release was inhibited when the cells were pretreated with ruthenium red, amiloride, and gadolinium chloride, known blockers of mechanosensitive ion channels [132]. In addition, using real-time fluorescence imaging we demonstrated that both rat primary urothelial and UROtsa cells exhibited an increase in cell volume when exposed to hydrostatic pressure (5-20 cmH₂O). Together, we hypothesized that the UC response to hydrostatic pressure is mediated by an increase in cell volume and subsequent activation of ion channels.

ATP release in response to mechanical stimuli (e.g. stretch, pressure, cell swelling) *in vitro* has been well documented in many cell types, including, but not limited to, human fibroblasts, murine glial cells, rat liver epithelial cells, and rabbit UCs [15, 74-76, 120, 133]. Extracellular ATP is known to interact with purinergic receptors present on cells, and afferent nerves, to trigger physiological responses such as vascular tone, muscular contraction, and cellular proliferation [134, 135]. In the bladder, ATP released by UCs in response to bladder filling is thought to bind to P2X₃ receptors on afferent

nerves innervating the bladder wall triggering the sensation of fullness [18, 21, 22]. Patients with interstitial cystitis, a pathological bladder condition characterized by extreme bladder urgency and pain, has been found to exhibit increased ATP release both *in vivo* and *in vitro* [136, 137]. Previously, Birder *et al.* examined the ATP release by UCs harvested from normal and interstitial cystitis (FIC) cats and found that osmotic shock due to a hypotonic stimulus elicits a robust increase in extracellular ATP and that this response was inhibited when blocking epithelial sodium channel (ENaC) activity with amiloride in normal cells, but not FIC cells [82]. They concluded that ATP release occurs, in part, by vesicle exocytosis, which may be altered in FIC. This work provided an important step in investigating the mechanisms by which ATP is released from UCs, as well as establishing a link between ENaC activation and ATP release. Taken together these previous studies suggest that ATP signaling in the bladder is an important component in normal, and pathological, bladder mechanosensation.

Previous research by our group has provided evidence that blocking ENaCs with amiloride inhibits ATP release in cultured UCs exposed to hydrostatic pressure (10-15 cmH₂O) [132]. Other studies have also found that rat bladder strips exposed to hydrostatic pressure [15] and membrane stretch (30-50%) exhibited decreased ATP release when blocked with amiloride [14]. Additionally, bladder strips taken from patients suffering from bladder outlet obstruction exhibited an overexpression of ENaC subunits, which led to the authors' conclusion that increased ENaC expression might change afferent activity, which is involved in detrusor instability found in bladder outlet

obstruction [81]. Transient receptor potential vanilloid-4 (TRPV4) is another channel that has been implicated in bladder urothelial cell's mechanosensory function [13, 86, 132, 138]. Deletion of the TRPV4 gene in knockout mice resulted in a lower frequency of voiding, as well as a decrease in ATP release from bladders *in vivo* [138]. In addition, UCs from TRPV4 knockout mice exhibited a lower intracellular $[Ca^{2+}]$ increase than wild-type cells when subjected to stretch (100-150%) *in vitro* [86]. Together with our previous studies, these results suggest that both TRPV4 and ENaC play an important role in UC pressure mechanotransduction. Specifically, we hypothesize that pressure activates ENaC, triggering an influx of Na^+ ions into the cell. The resulting cell swelling then activates TRPV4 due to membrane deformation, which signals an increase in intracellular $[Ca^{2+}]$, followed by a release of extracellular ATP. To test this hypothesis, we compared the time-course ATP release of UCs to both osmotic shock and hydrostatic pressure and determined the ATP release kinetics of UCs during an increase in cell volume. In addition, the role of the TRPV4 channel and ENaC during pressure exposure was investigated to improve understanding of the mechanism of ion channel activation in urothelial pressure mechanotransduction.

5.2 Materials and Methods

Cell Culture

Primary UCs were harvested from bladders of Sprague-Dawley rats according to methods described previously [95, 115]. Briefly, under sterile conditions, the bladders

were excised from rats immediately after sacrifice and trimmed of any excess fat and connective tissue. A blunt 18 ½ gauge needle was then inserted into the neck of the bladder, which was filled with 1 ml of 0.05% trypsin (Invitrogen, Carlsbad, CA). The inflated bladder was tied off with a sterile suture and incubated in phosphate buffered saline (PBS) solution under standard cell culture conditions (37 °C, 95% air/5% CO₂, humidified environment) for 25 minutes. After incubation, the bladder was cut open and the trypsin solution that contained UCs was combined with equal volume of fresh fibroblast medium (FM: DMEM/F12 (Invitrogen) supplemented with 10% fetal bovine serum (FBS) (Hyclone, Logan, UT), penicillin (10,000 units/mL), and streptomycin (10,000 µg/mL)), and centrifuged at 1000 RPM for five minutes. The cell pellet was then resuspended in the UC growth medium [95], a 1:1 mixture of 3T3 fibroblast-conditioned FM and keratinocyte growth medium (KGM: keratinocyte medium (Invitrogen) supplemented with 2% FBS, bovine pituitary extract (12.5 mg/ml, Invitrogen), insulin-transferrin-selenium (1 mg/mL), hydrocortisone (50 µg/mL), epidermal growth factor (35 ng/µL, Invitrogen), amphotericin (250 µg/mL), and gentamicin (50 mg/mL)). UCs were cultured for up to 7 days until they reached confluence prior to use in experiments. Urothelial phenotype was confirmed by the characteristic, cobble-stone cell morphology and immunostaining with CK17 and the fluorescently (Alexa Fluor 488) tagged secondary antibody [115]. UCs used in the experiments were passage number one through three. UROtsa cells were kindly provided by Dr. Naoki Yoshimura, Department of Urology, University of Pittsburgh. UROtsa cells were cultured in Dulbecco's

modified Eagle's medium (DMEM) supplemented with 5% fetal bovine serum (FBS) and 1% antibiotic-antimycotic. UROtsa cells used in experiments were passage number ten through fifteen.

Urothelial Cell Perfusion Experimental Setup

UCs were exposed to hypotonic stimulus and elevated hydrostatic pressure using a custom setup, which was adapted from published methods [118, 139]. Briefly, cells were seeded on collagen-coated coverslips at a density of 5.0×10^4 cells/coverslip and cultured under standard cell culture conditions (at 37°C in humidified 5% CO₂ 95% air) for 24 hours. Cells seeded on coverslips were then placed in a Vacu-Cell™ chamber (C&L Instruments, Hershey, PA) and perfused with standard Hanks Balanced Salt Solution (HBSS) (Invitrogen) (137.0 mM NaCl, 5.33 mM KCl, 0.34 mM Na₂HPO₄, 0.44 mM KH₂PO₄, 1.26 mM CaCl₂, 0.41 mM MgSO₄, 0.49 mM MgCl₂, 4.17 mM NaHCO₃, 5.56 mM D-Glucose, pH=7.4, 330 mOsm, 37°C). Hypotonic (240 mOsm) HBSS was prepared by diluting standard HBSS with dH₂O to adjust the osmolarity. Heated HBSS solution (35-40°C) was perfused using a peristaltic pump (MINIPULS 2, Gilson Inc., Middleton, WI), through a pulse dampener and the chamber at a flow rate of 0.5 ml/min. Hydrostatic pressure was applied to the cells by raising the height of the perfusion outlet to the desired pressure level (cm) using a custom-made, computer-controlled vertical actuator. The area exposed to flow in the Vacu-Cell™ chamber measured (LxWxH) 7mm x 10 mm x 0.25mm.

Drugs Used in Cell Perfusion

All drugs used in the current study were purchased from Sigma-Aldrich (St. Louis, MO). In order to block ENaC and TRPV4, cells were first pretreated with amiloride (1 μ M) and HC-067047 (1 μ M), respectively, for 30 minutes prior to experiments. During experiments under hydrostatic pressure and osmotic shock, cells were continuously exposed to the blocking drugs in the perfusion solutions at the same concentrations as pretreatment. As a positive control experiment, primary UCs were perfused with 4 α -phorbol 12, 13-didecanoate (4 α -PDD) (10 μ M), a TRPV4 agonist.

Measurement of ATP Release

ATP released from urothelial and UROtsa cells was measured using a commercially available luciferin-luciferase bioluminescence ATP kit and following the manufacturer's instructions (Sigma). Perfusate was collected from the outlet every minute for the duration of the experiment (10-15 minutes) and the luciferin-luciferase reagent was added to each sample before the luminescence measured with a Tecan Genios microplate reader (Tecan US, Inc., Durham, NC). Luminescence values were converted to ATP concentration (pM) using a standard curve that was prepared before each experiment using serial dilutions (100-5000 pM) from the stock ATP solution supplied in the kit. Data were reported as mean ATP concentration (pM) \pm SEM.

Statistical Analysis

Each experiment was performed at least three separate times (n=3). The mean values of data from three experiments were calculated and compared using single-factor analysis of variance (ANOVA). When a statistically significant difference was detected, a *post-hoc* pairwise analysis was conducted using the Tukey test. Statistical analyses of numerical data were performed using Sigma Stat software (Systat Software Inc., Richmond, CA). *P*-values less than 0.05 were considered statistically significant.

5.3 Results

Urothelial Cells Release ATP in Response to Osmotic Cell Swelling

Primary UCs were exposed to a hypotonic stimulus (240 mOsm) in order to cause osmotic cell swelling. UCs exhibited a significant ($p < 0.05$) increase in ATP release within the first minute of exposure ($523 \text{ pM} \pm 180 @ t = 0 \text{ min}$; $5788 \text{ pM} \pm 1411 @ t = 1 \text{ min}$; $n = 3$), which returned to baseline values in the second minute (Figure 5-1). In the presence of HC-067047 ($1 \text{ } \mu\text{M}$), a specific inhibitor of TRPV4, elevated ATP release due to hypotonic cell swelling was virtually abolished ($230 \text{ pM} \pm 91 @ t = 0 \text{ min}$; $277 \text{ pM} \pm 130 @ t = 1 \text{ min}$; $n = 3$). When UCs were perfused in the presence of amiloride ($1 \text{ } \mu\text{M}$), an inhibitor of ENaC, an increase in ATP release during hypotonic stimuli was present, but at a lesser magnitude compared to the unblocked group ($577 \text{ pM} \pm 197 @ t = 0 \text{ min}$; $1776 \text{ pM} \pm 1252 @ t = 1 \text{ min}$; $n = 5$). UROtsa cells also showed a significant increase in ATP release when exposed to the hypotonic stimulus ($260 \text{ pM} \pm 54 @ t = 0 \text{ min}$; 1908

pM \pm 441 @ t = 1 min; n = 4) (Figure 5-2). However, compared to the UC response to osmotic shock, the UROtsa response was less drastic and remained elevated for the duration of the experiment rather than immediately returning to baseline levels.

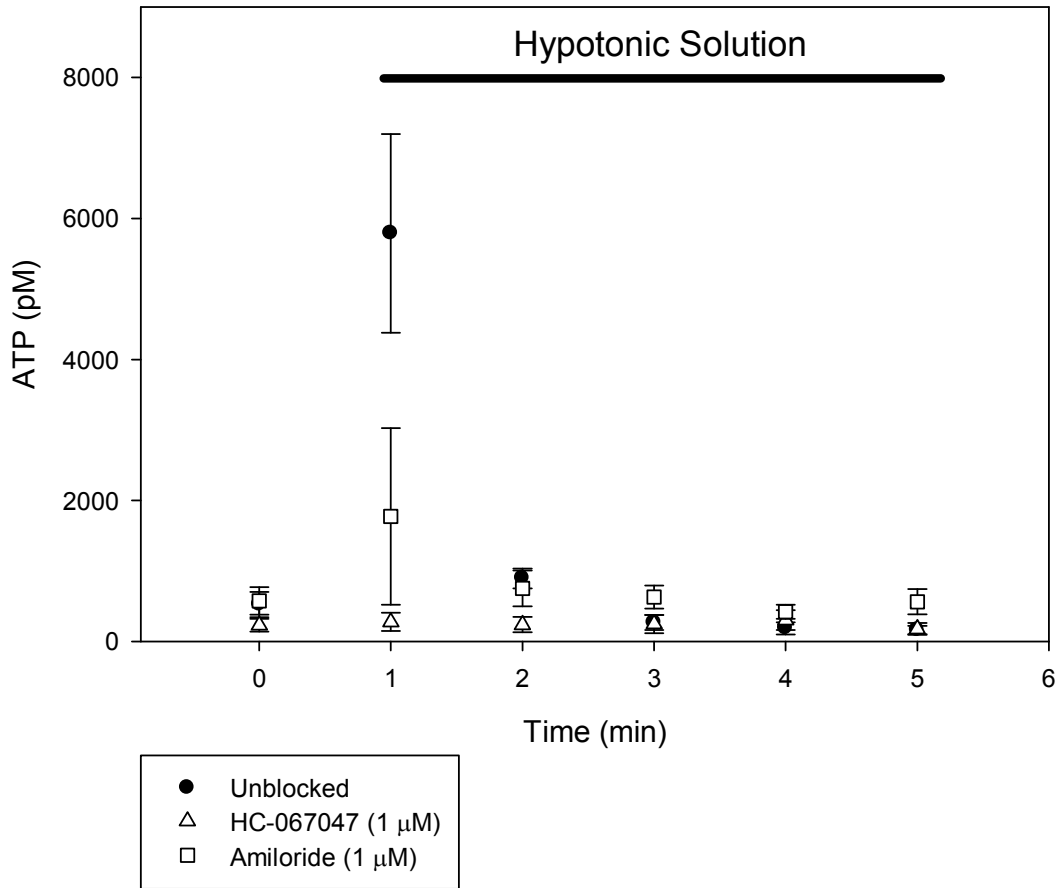


Figure 5-1. ATP release of primary urothelial cells when exposed to osmotic shock.

Primary UCs were exposed to osmotic shock (240 mOsm), unblocked, as well as in the presence of a TRPV4 inhibitor, HC-067047, and ENaC inhibitor, amiloride. Unblocked cells exhibited a sharp increase in ATP release before returning to baseline values, while

cells blocked with HC-067047 showed no change in ATP release. UCs blocked with amiloride showed an increase in ATP, however attenuated compared to the unblocked cells.

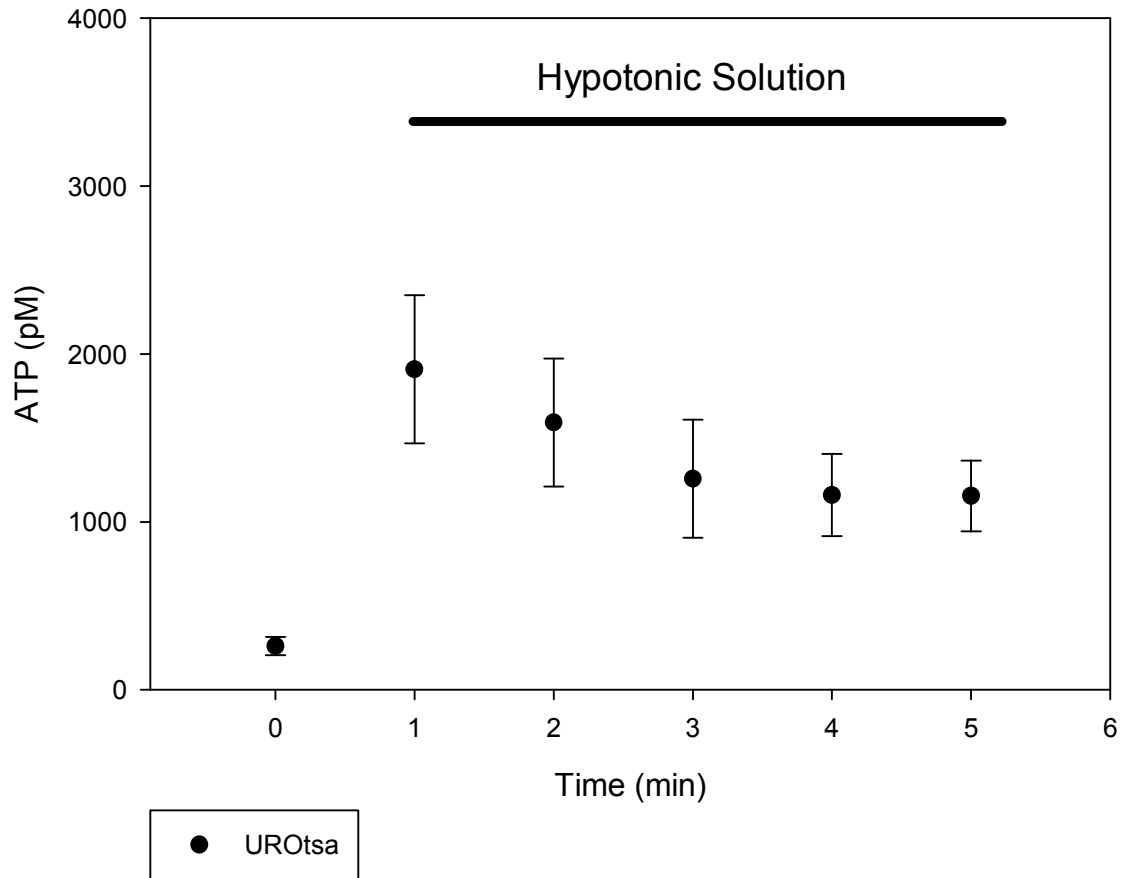


Figure 5-2. ATP release of UROtsa cells when exposed to osmotic shock. Human bladder UROtsa cells showed a significant increase in ATP when exposed to a hypotonic stimulus. The ATP release remained elevated above baseline levels for the remainder of the experiment.

ATP Release due to Hydrostatic Pressure is Inhibited When Blocking Certain Ion Channels

When exposed to hydrostatic pressure (10 cmH₂O), UCs exhibited an increase in ATP release which reached a peak within two minutes (273 pM ± 114 @ t = 0; 2623 pM ± 518 @ t = 2 min; n = 3), and remained elevated for a few minutes before decreasing steadily toward the baseline levels (Figure 5-3). When the cells were perfused in the presence of HC-067047 (1 μM) during exposure to pressure, ATP release remained at the baseline level (424 pM ± 117 @ t = 0 min; 345 pM ± 117 @ t = 2 min; n = 4) over the course of 9 minutes exposure to pressure. Similarly, when cells were perfused in the presence of amiloride (1 μM) during pressure exposure, ATP remained at baseline levels (328 pM ± 69 @ t = 0 min; 314 pM ± 27 @ t = 2 min; n = 3).

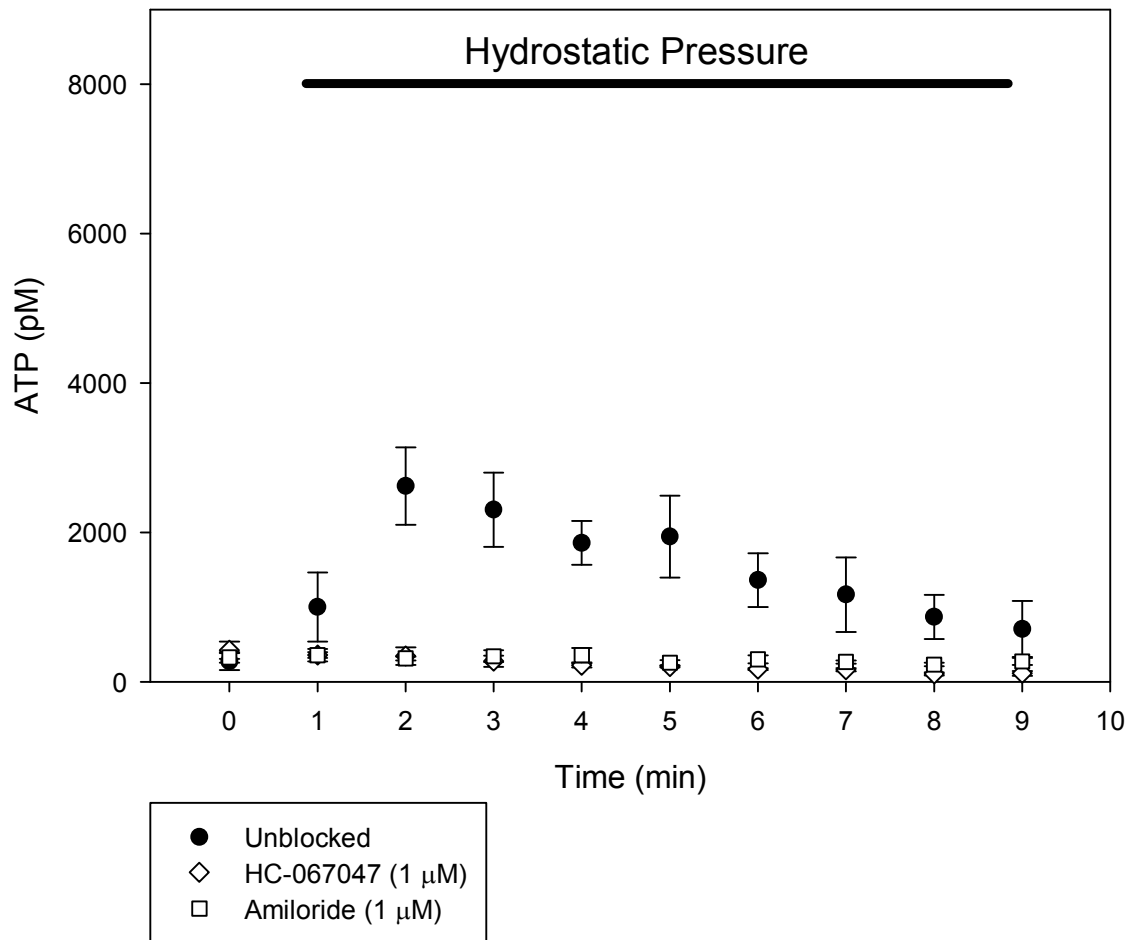


Figure 5-3. ATP Release of primary urothelial cells when exposed to hydrostatic pressure. Primary rat UCs were exposed to hydrostatic pressure (10 cmH₂O) for 9 minutes. Unblocked cells exhibited an increase in ATP release when exposed to pressure. UCs blocked either with HC-067047 or amiloride showed no change in ATP release under pressure.

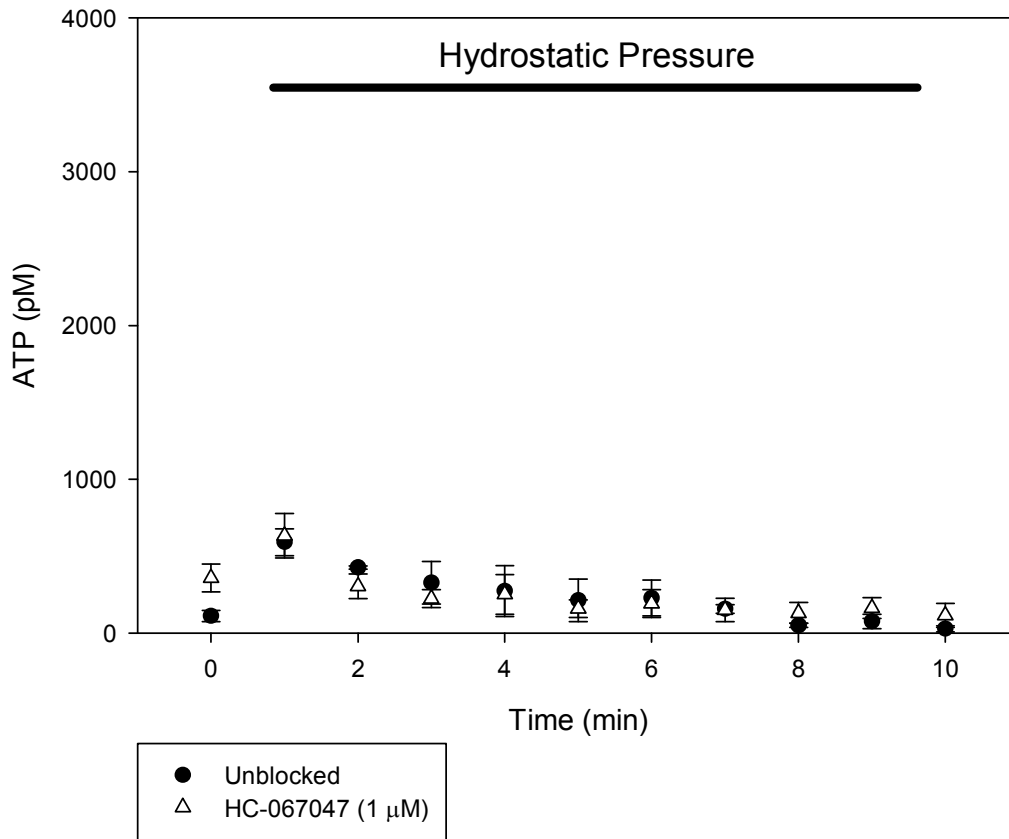


Figure 5-4. ATP release of UROtsa cells when exposed to hydrostatic pressure. Human UROtsa cells were exposed to hydrostatic pressure (10 cmH₂O) for 10 minutes. Unblocked cells exhibited an increase in ATP release under pressure, however not to the extent of primary rat UCs. UROtsa cells blocked with HC-067047 also showed an increase in ATP release under pressure.

UROtsa ATP Release During Hydrostatic Pressure Exposure is not Affected by TRPV4 Inhibition

UROtsa cells exhibited a significant ($p < 0.05$) increase in ATP when exposed to hydrostatic pressure (10 cmH₂O) (111 pM \pm 36 @ t = 0 min; 591 pM \pm 88 @ t = 1 min; n = 3), which then decreased steadily to baseline values over the next 7 minutes (Figure 5-4). When blocked with HC-067047 (1 μ M), ATP release again was elevated under pressure and was not significantly different from the unblocked group (358 pM \pm 91 @ t = 0 min; 632 pM \pm 145 @ t = 1 min; n=3).

Blocking with HC-067047 Prevents TRPV4 Activation

In order to confirm that HC-067047 was blocking the activation of TRPV4, primary UCs were perfused with 4 α -PDD (10 μ M), a TRPV4 agonist, with and without HC-067047 (1 μ M). When unblocked UCs were perfused with 4 α -PDD, they exhibited a significant ($p < 0.05$) increase in ATP release (1110 pM \pm 499 @ t = 0 min; 4433 pM \pm 1005 @ t = 1 min; n = 3) which remained elevated for the remainder of the experiment (10 minutes) (Figure 5-5). When UCs were pretreated with HC-067047 for 30 minutes and perfused with both HC-067047 and 4 α -PDD, the cells showed no change in ATP release (411 pM \pm 54 @ t = 0 min; 408 pM \pm 120 @ t = 1 min; n=3).

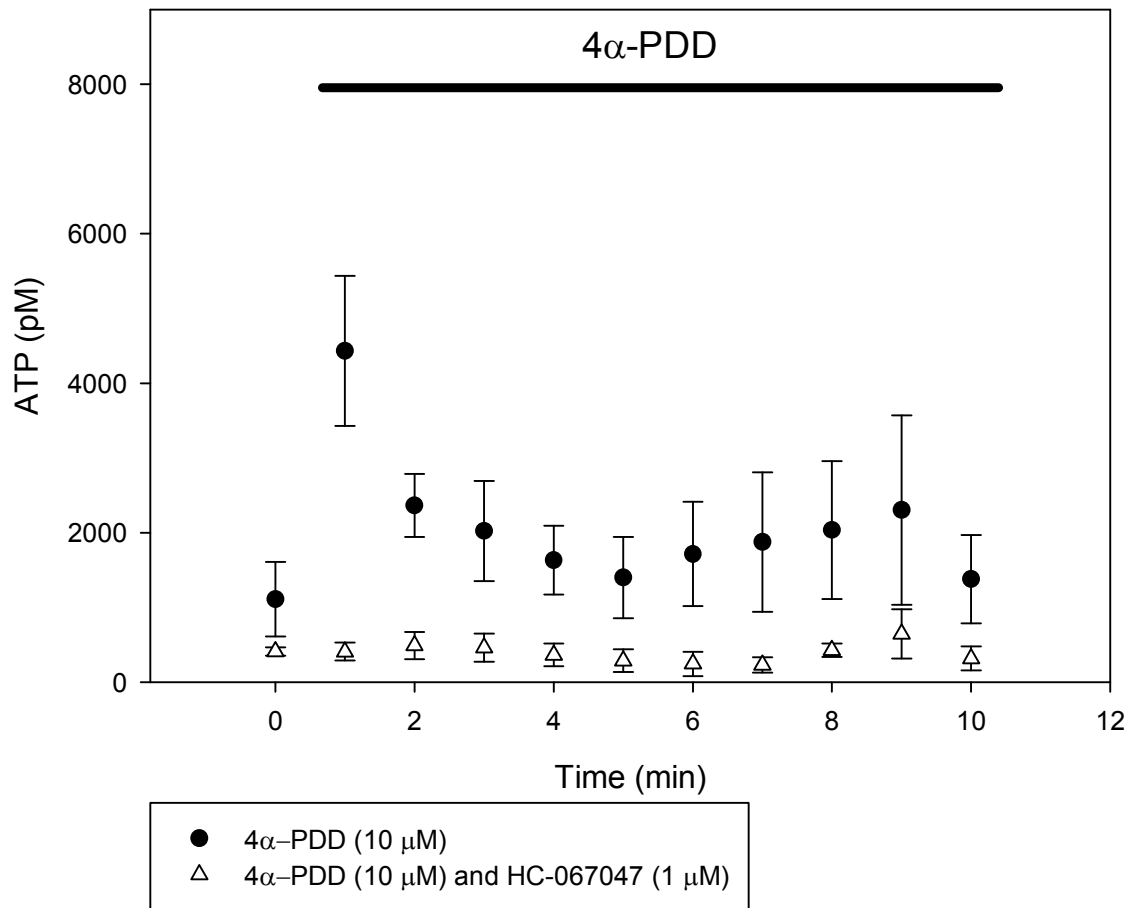


Figure 5-5. ATP Release of primary UCs when exposed to TRPV4 agonist. Primary rat UCs were exposed to a TRPV4 agonist, 4α-PDD, for 10 minutes. UCs exhibited a significant ($p < 0.05$) increase in ATP release when perfused with 4α-PDD, which remained elevated for the duration of the experiment. When blocked with TRPV4 antagonist, HC-067047, while being perfused with 4α-PDD, UCs showed no change in ATP release compared to baseline levels.

5.4 Discussion

The aim for the present study was to analyze the time-course ATP release of UCs during exposure to hydrostatic pressure, and to elucidate the mechanism by which cells respond to hydrostatic pressure. In our previous study (Chapter 3), we demonstrated that blocking either TRP channels, with ruthenium red, or ENaC, with amiloride, prevented an ATP release by rat primary UCs under hydrostatic pressure (10 cmH₂O for 5 minutes), suggesting that both classes of ion channels may be involved through a yet unknown mechanism. In addition, we used real-time fluorescence imaging and demonstrated that when UCs were exposed to hydrostatic pressure (5-15 cmH₂O) they exhibited an increase in cell volume with a matter of 10-15 seconds (Chapter 4). Since the removal of extracellular Na⁺ and blocking of ENaC with amiloride could both prevent this pressure-evoked cell volume increase, it was hypothesized that ENaC activation and cell swelling are followed by TRP activation and ATP release in the urothelial response to pressure.

In order to better understand the mechanism behind ATP release by cells in response to pressure-induced cell swelling, UCs were exposed to hypotonic osmotic shock in a perfusion chamber. By removing hydrostatic pressure from the system and only exposing UCs to an increase in cell volume, we aimed to gain insight into the order of events that occur between pressure exposure and ATP release. In addition, using the same setup to apply hydrostatic pressure, we compared effects of the two stimuli on UCs. Because an introduction of perfusion (flow-induced shear stress) can trigger cells to release ATP, UCs were first perfused for at least five minutes to achieve a stable,

baseline ATP level before data were collected. Following this equilibration period, when primary UCs were exposed to the hypotonic stimulus (240 mOsm), the cells exhibited a significant increase in ATP release and then returned to baseline values within 1 minute (Figure 5-1). This increase in ATP release by rat UCs under hypotonic stimulus is in agreement with previous studies which demonstrated that feline UCs and rabbit urothelial tissue exhibit a significant increase in ATP release (500-1000%) in response to hypotonic stimuli (25-50%) *in vitro* [74, 82]. However, the present study is the first to our knowledge to characterize the time-course ATP release by UCs in response to osmotic shock. In contrast to the transient, more robust UC ATP release response to the hypotonic stimulus, UCs exposed to hydrostatic pressure (10 cmH₂O) exhibited a 10-fold increase in ATP, which then stayed elevated above baseline values for the remainder of the pressure exposure period (9 minutes) (Figure 5-3). Moreover, when total ATP released by UCs was compared, the pressure exposure resulted in twice as much as osmotic shock (5.7 pmol ± 1.4 vs. 2.8 pmol ± 0.60). This may be due to a regulatory volume decrease that cells undergo during osmotic shock that doesn't occur during exposure to pressure. Thus, the sustained increase in cell volume during pressure would result in a longer period of elevated ATP release and a higher overall ATP release. In order to confirm this hypothesis, longer experiments to monitor cell volume changes under hydrostatic pressure would need to be conducted.

The present study provided first evidence that cells blocked with HC-067047 showed no increase in ATP release from baseline levels when exposed to osmotic shock.

In contrast, cells blocked with amiloride exhibited an increase in ATP release, albeit attenuated compared to the unblocked group. In pressure experiments, UCs blocked with either HC-067047 or amiloride showed no change in ATP release when exposed to 10 cmH₂O compared to baseline values, indicating that pressure-mediated ATP release requires both TRPV4 and ENaC activation. The lack of cell swelling-induced ATP release by UCs in the presence of a TRPV4 blocker supports the view that it is a mechanically activated channel, specifically due to osmotic swelling. This observation corroborates a previous report that hypotonic cell swelling elicits an increase in intracellular [Ca²⁺], presumably due to influx through activated TRPV4, in murine CHO cells transfected with TRPV4, compared with untransfected cells [129].

The partial inhibition of UC ATP release in the presence of amiloride under a hypotonic stimulus suggests that ENaC activation is not the sole mechanism by which ATP release occurs due to osmotic cell swelling. However, it is also possible that osmotic cell swelling leads to ENaC activation, which is why an attenuated ATP release under osmotic shock was observed when blocking with amiloride. The reduction in ATP release by amiloride-treated primary UCs under osmotic shock is similar to a previous observation by Birder *et al.* that feline UCs exposed to a 25% hypotonic stimulus in the presence of amiloride (10 μM) elicited a 50-60% decrease in ATP release [82]. Their results showed that calcium signaling inhibition completely eliminated ATP release while blocking with amiloride only partially inhibited the ATP release. This suggests that intracellular Ca²⁺ increase, possibly triggered by activation of TRPV4 and/or other

calcium permeable channels, plays a dominant role in ATP release over activation of ENaC. In contrast, the complete inhibition of UC ATP release by amiloride under hydrostatic pressure suggests that ENaC activation precedes pressure-induced cell swelling and subsequent ATP release. These results lend credence to our hypothesis that TRPV4 activation occurs due to membrane deformation during cell swelling, which results from ENaC activation and subsequent Na⁺ influx under hydrostatic pressure.

While rats are frequently used as an animal model for bladder research, human cells can provide basic scientific findings with greater clinical impacts. Therefore, UROtsa cells, an immortalized normal human urothelial cell line [140], were used in experiments to determine whether the pressure mechanotransduction events were dependent on species. As observed in rat primary UCs, UROtsa cells exhibited a sharp increase from baseline levels in ATP release when exposed to a hypotonic stimulus in the first minute (Figure 5-2). However, instead of immediately returning to baseline values, ATP release remained elevated for the remainder of the exposure period (9 minutes) and the peak ATP release was significantly ($p < 0.05$) lower than that achieved by the primary UCs (UC = $5788 \text{ pM} \pm 1411$; UROtsa = $1908 \text{ pM} \pm 441$). This difference in response to the hypotonic stimulus might suggest that UROtsa cells do not exhibit a regulatory volume decrease response in the presence of osmotic cell swelling. Moreover, when UROtsa cells were exposed to hydrostatic pressure (10 cmH₂O), ATP release by these cells was significantly greater than baseline levels, but blocking with HC-067047 did not inhibit this elevated ATP release (Figure 5-4). This overall lower response to pressure

(compared to primary UCs) as well as the lack of inhibition by HC-067047 may be due to low expression or a complete lack of functional TRPV4 in UROtsa cells that can be activated by cell swelling. We previously demonstrated that UROtsa cells exhibited an increase in cell volume when exposed to hypotonic stimulus as well as hydrostatic pressure (5-20 cmH₂O), similar to the response found in primary rat UCs (Chapter 4). Thus, it can be speculated that the hydrostatic pressure-evoked ATP release by UROtsa cells may be mediated by activation of mechanosensitive ion channels other than TRPV4 (i.e. TRPV1, TRPV2, TRPA1, TRPM8, or non-TRP family stretch-activated channels) [47, 55, 84, 89]. Although human UCs have been shown to express TRPV1 [141], and TRPV2 [142] ion channels as rat UCs do, to our knowledge, no work regarding the functionality of the TRPV4 ion channel in either primary urothelial or UROtsa cells has been published. While care must be taken when interpreting results from an immortalized cell line, as there may be unknown changes with the ion channel properties, further investigation of TRPV4 functionality in UROtsa and human bladder cells would be a necessary step to develop a link between our observations in rat and human UC mechanotransduction.

In summary, the results of the present study confirm our initial hypothesis that the mechanism for UC pressure mechanotransduction requires activation of both ENaC and TRPV4 to signal ATP release. In addition, by examining the UC response to cell swelling without the added stimuli of pressure, we determined that ENaC is activated by hydrostatic pressure prior to cell swelling, whereas TRPV4 activation occurs due to

osmotic cell swelling Finally, with human UROtsa cells displaying a different mechanism for triggering ATP release under pressure, the present study demonstrated needs for further investigation of additional mechanosensitive ion channels in order to gain insight into the mechanisms of human bladder cell mechanotransduction.

-Chapter 6-

Conclusions

6.1 ATP Release by Urothelial Cells in Response to Hydrostatic Pressure

This doctoral thesis research investigated the response of bladder urothelial cells (UCs) to physiological level hydrostatic pressure in vitro specifically by quantifying ATP released by these cells and examining the role of mechanosensitive ion channels (MSCs) in pressure mechanotransduction. In addition to being an energy molecule, ATP is considered to be an important neurotransmitter involved in a number of physiological events including bladder mechanotransduction [15, 45, 74, 94, 143]. This follows the main concept that ATP released from the bladder urothelium binds to purinergic P2X₃ receptors present on afferent nerves innervating the organ to signal bladder fullness [8, 16, 20, 22, 93]. Therefore, ATP release from UCs is an important parameter for investigating bladder mechanotransduction. Although a number of previous studies by other groups had examined the effect of pressure (and concomitant stretch) on ATP release from the urothelium tissue [15, 85, 94], the present study was the first to examine the effects of applied hydrostatic pressure on UCs without the added stimulus of tissue stretch. For the first time, our results provided evidence that UCs release elevated amounts of ATP in response to hydrostatic pressure (10-15 cmH₂O) alone and that this ATP release could be inhibited by blocking select ion channels or chelating extracellular Ca²⁺. While our initial study (Chapter 3) was an important step in the right direction for

evaluating the urothelial response to pressure, there were inherent limitations in the experimental methods that needed to be addressed in the follow-on studies to best examine urothelial mechanotransduction.

6.2 Specificity of Ion Channel Inhibition

The potential cross reactivity and side effects of some drugs used in our first set of experiments to block ion channels (ruthenium red, gadolinium chloride) left some questions as to which specific ion channels are responsible for the inhibition of ATP release under hydrostatic pressure. For example, ruthenium red is an ion channel antagonist that non-specifically blocks members of the TRP ion channel family. Likewise, while gadolinium chloride is considered to be an antagonist for “so-called” stretch-activated ion channels, it has also been shown to inhibit multiple classes of ion channels including TRPV1 [108] and ENaC [144]. Therefore, it remains possible that our results with gadolinium were in part due to inhibition of those ion channels, but did not provide a specific candidate that mediated pressure mechanotransduction. Part of the problem with non-specific blocking effects of these drugs was addressed by using HC-067047, a selective antagonist for TRPV4 (Chapter 5). By specifically blocking TRPV4, we were able to isolate the TRP ion channel that we believe is partially responsible for ATP release during exposure to hydrostatic pressure. These results can be further confirmed using bladder UCs obtained from transgenic mice that do not express the

genes for ion channels of interest (e.g. TRPV4 knockout) or by selectively silencing those ion channels using siRNA technology.

6.3 Time-course Analysis of ATP Release

The experimental setup used for the application of hydrostatic pressure in early studies only allowed us to measure ATP in supernatant culture media at the end of prescribed time periods (5, 15, and 30 minutes). Therefore, the results gathered from these experiments did not provide precise characterization of ATP release kinetics under pressure. Originally, we postulated that ATP release at later time points (at 15 and 30 min) that was similar to the baseline level (Figure 3-4, Chapter 3) could be due to ATP degradation by ecto-ATPases or due to desensitization of UCs to pressure over time. Using a perfusion chamber to expose UCs to pressure (Chapter 5) allowed for collection of media sample and quantification of ATP at finer time points than our earlier work, which provided evidence that the peak ATP release by UCs during pressure exposure occurred much sooner than we originally thought (< 2 minutes). Although we haven't ruled out the effect of ecto-ATPases, it is likely that the lower ATP concentration in the supernatant media at 30 minutes may have been simply due to hydrolysis of the ATP released in the first few minutes of pressure exposure. However, in humans under normal physiological conditions bladder fullness can be felt continuously for much longer than 30 minutes. Therefore, it remains necessary to investigate ATP release by UCs for longer

durations (> 30 minutes) in the presence or absence of ATPase inhibitors to determine the cause of lower ATP release at later timepoints.

6.4 The Specific Pathway of ATP Release during Pressure Mechanotransduction

While we have a better understanding of ATP kinetics of urothelial pressure mechanotransduction than before, the path by which ATP release occurs is still not completely understood. Previous work by Birder *et al.* provided evidence that ATP is released by vesicle exocytosis in UCs exposed to osmotic shock [82]. This was demonstrated by the absence of osmotic shock-evoked ATP release from UCs that had been treated with either monensin or brefeldin A, which disrupt intracellular vesicle formation and vesicle trafficking to the cell surface, respectively. In other cell types, ATP is also released through connexin hemichannels in astrocytes [76], or through anion channels in kidney macula densa cells [145]. Vesicle exocytosis is a potential mechanism for ATP release by UCs in the response to hydrostatic pressure as our results indicate that exposure to pressure leads to cell swelling similar to that induced by osmotic stimuli. However, this must be examined experimentally along with connexin hemichannels, which have been implicated in the urothelial response to pressure [16], and anion channels, which have been found to be expressed in UCs, but not yet demonstrated to be sensitive to pressure [146]. By isolating the exact pathway of ATP release under hydrostatic pressure, we could provide insight into the etiology and potential targets for therapies for elevated ATP release found in patients with various voiding dysfunctions.

6.5 The Role of Ca^{2+} in Pressure-Induced ATP Release

The results of the present study also suggest that extracellular Ca^{2+} is necessary for UCs to release ATP in response to hydrostatic pressure. Numerous studies have demonstrated that mechanical stimuli (fluid flow, membrane stretch) can activate ion channels [14, 37, 41, 69, 70, 80, 86, 103, 116, 129] to increase the intracellular concentration of Ca^{2+} , which, in turn, triggers a release of ATP [22]. Conversely, other studies have demonstrated that the release of ATP from UCs did not depend on extracellular Ca^{2+} [14, 82], but was due to a release of Ca^{2+} from the endoplasmic reticulum [94]. Therefore, in order to resolve the controversy between the results of the present and previous studies regarding the role of extracellular Ca^{2+} in UC mechanotransduction, it is necessary to determine the source of intracellular Ca^{2+} increase, whether by Ca^{2+} influx due to ion channel activation or by release of Ca^{2+} from intracellular stores. Understanding the mechanism by which intracellular Ca^{2+} increases would link TRPV4 activation and ATP release in UCs during exposure to pressure. This may be accomplished by exposing cells, prior to application of hydrostatic pressure, to either BAPTA (an extracellular Ca^{2+} chelator) to prevent the influx of Ca^{2+} through ion channels, or to caffeine (to release Ca^{2+} from intracellular stores) to inhibit internal intracellular Ca^{2+} increase.

6.6 Cell Volume Increase due to Hydrostatic Pressure

The results of the present study also provided first evidence that UCs exhibit cell swelling when exposed to hydrostatic pressure, and that this cell swelling can be inhibited by removing extracellular Na^+ as well as blocking ENaC with amiloride (Chapter 4). These results exhibited the first indication that UCs may detect bladder fullness with a change in cell volume. In addition, these results may open the door to investigating cell volume responses to hydrostatic pressure in other organ systems (lung, eye, heart) which contain mechanosensitive cells that are exposed to changes in hydrostatic pressure. Although the evidence of urothelial swelling under hydrostatic pressure is highly convincing, there are several ways we can improve the methods to quantify changes in cell volume. For example, in the present study we differentiated cell swelling and shrinkage by the speed in which the cells decreased in fluorescence intensity (Table 4.1, Chapter 4). By developing a protocol which allows for cell shrinkage and cell swelling to exhibit opposite changes in fluorescence intensity we can strengthen our conclusions that UCs do swell in response to pressure. In addition, by using a higher resolution microscope and more sophisticated image analysis software, cell volume calculation from confocal images could be automated, allowing for more precise values of cell volume change as opposed to comparing the differences in total cell area.

6.7 Clinical Relevance- Overactive Bladder

The results of the present study suggest that pressure mechanotransduction is an important function of UCs in normal physiological sensing of bladder fullness. In addition, it can be speculated that UCs of the bladder with pathological conditions (OAB, interstitial cystitis) may exhibit dysfunction in responses to pressure (i.e. ATP release, ion channel activation, Ca^{2+} signaling, cell volume changes). Therefore, understanding UC pressure mechanotransduction could help design treatment approaches for bladder diseases such as OAB and interstitial cystitis [136, 143].

As discussed in Chapter 5, the eventual shift from an *in vitro* rat cell model to a higher order species and ultimately to clinical investigation is necessary to best translate our scientific findings into impactful clinical benefits. The use of UROtsa cells, human immortalized UCs, is an important step towards investigating human bladder mechanotransduction. However, the results to date demonstrated that UROtsa cells and primary rat UCs do not share identical characteristics in their respective responses to hydrostatic pressure. This does not preclude our findings from being translated to human UCs, but it does require further investigation of the mechanisms by which UROtsa cells respond to hydrostatic pressure to provide a more conclusive comparison between the findings in rat and human cells. One option for future projects would be a shift to human primary cells. This would provide a more physiologically accurate *in vitro* model for urothelial pressure mechanotransduction. Another approach would involve the use of animal models to characterize the response of the bladder to hydrostatic pressure *in vivo*

using cystometry. This would require starting with a mouse or rat model and scaling up to higher order animals (e.g. cats) before examining bladder mechanotransduction in clinical studies.

6.8 Summary

In summary, the results of the present research provide evidence for the first time that UCs respond to hydrostatic pressure in the absence of tissue stretch with an increase in cell volume, activation of multiple mechanosensitive ion channels, and elevated ATP release. With these results, we have identified a possible mechanism by which UCs detect changes in pressure to signal the fullness of the bladder. In addition, we are the first to show that cells swell under hydrostatic pressure, a rather counterintuitive event, which is completely novel in itself and makes a significant contribution to the field of cell mechanobiology as a potentially common mechanism of detecting hydrostatic pressure in multiple cells types. The results of the present study also imply that intravesical pressure, not bladder wall tissue stretch, may be an important parameter in clinical assessment of bladder function. However, further research, as outlined below, is necessary to advance our understanding of bladder urothelial cell mechanotransduction to ultimately aide in treatment of bladder disorders such as OAB.

6.9 Future Project Recommendations

- ❑ Investigate the pathways by which ATP is released from UCs in response to pressure.
- ❑ Characterize the ATP release by UCs under hydrostatic pressure in longer periods of time (hours vs. minutes)
- ❑ Examine the role of Ca^{2+} in UC pressure mechanotransduction and determine the source of intracellular Ca^{2+} increase
- ❑ Improve methods of cell volume measurements with protocols that allow for more conclusive fluorescence imaging results and more precise confocal imaging analysis
- ❑ Characterize the response of human UROtsa and primary urothelial cells to hydrostatic pressure
- ❑ Develop an animal model using bladder cystometry to examine the effects of pressure on voiding behaviors *in vivo*

-Appendices-

-Appendix A-

Primary Urothelial Cell Isolation Protocol

Materials Needed

1. Collagen coated 60mm dishes (as per protocol)
2. 3T3 fibroblast cells growing in T25 flasks
3. 50 cc tube filled with ~ 25ml of sterile 1X PBS
4. Bucket of ice
5. 0.05% Trypsin-EDTA
6. Blunt needle, syringe, black thread
7. Black isolation petri dish
8. 10 ml glass beaker (sterile)
9. Isolation tools for lab (forceps, scissors, blade holder)

Animal Sacrifice

1. Sprague-Dawley rat, female, 250-350g, Harlan
2. Sacrifice via CO₂ asphyxiation. You must be trained by the Godley-Snell staff in order to perform CO₂ asphyxiation. Otherwise, you must have a lab technician do it.
3. Wet abdomen with ethanol and shave hair of lower abdominal region with electric hair clipper
4. Cut open the abdominal wall and remove bladder. **NOTE:** Bladder will be a slight pinkish color surrounded by the white and gray-colored intestines.

5. Place bladder in sterile PBS on ice to transport to lab for cell isolation

Cell Isolation

(Modified from Kurzrock, et al, 2005. Original protocol called for inversion of bladder and placing in a trypsin-filled beaker. By filling the bladder with trypsin, you can obtain a higher amount of cells with better cell purity)

1. Under the cell culture hood, use forceps to place the bladder neck over the blunt needle/syringe. Blunt needle is reusable. If it is lost, simply cut a syringe needle, and file to a blunt edge.
2. Use black thread to tie a knot, securing the bladder neck over the blunt needle.
3. Fill the inside of the bladder with ~0.5 ml trypsin, or until bladder is adequately taut.
4. Remove bladder from needle and tied off again with another knot.
5. Place bladder in sterile 10 ml glass beaker filled with sterile 1X PBS. Cover beaker with aluminum foil and place in incubator for 30 minutes.
6. Remove bladder from beaker and place on a 35 mm petri dish.
7. Cut open bladder with blade, and combine liquid contents with 2-3 ml of FM (DMEM/F12)
8. Centrifuge at 1000 rpm for 5 min
9. Remove supernatant and resuspend in a 1:1 mixture (4 ml) of 3T3-conditioned FM and KGM (keratinocyte media supplemented with 2% FBS and antibiotics).
10. Place the suspension on the collagen coated 60 mm petri dish.

Collagen Coating of Dishes

1. Collagen Type I (MP Biomedical # 0215002680) is dissolved in 0.2% acetic acid at a concentration of 2 mg/ml. This takes approximately 2 hours.
2. The collagen solution is filtered through a 5 μm syringe filter, then filtered again through a 0.45 μm cellulose acetate filter. This second step may require multiple filters.
3. This stock solution can be stored at 4°C until needed in a 50 cc tube
4. Dilute the stock solution 1:4 with collagen:dH₂O. Only dilute as much as needed, as this cannot be stored for later use.
5. Dispense the following amounts into the tissue culture dish and allow to sit overnight in the hood under UV exposure
 - a. 2 ml/ 35 mm dish
 - b. 3 ml/ 60 mm dish
 - c. 4 ml/ T-25 flask
 - d. 12 ml/ T-75 flask
6. The following day, aspirate the diluted collagen solution from the dish and allow to air dry in the hood.
7. When dry, rinse thoroughly 3x with sterile PBS.
8. Air dry the dishes inside the hood, seal edges with parafilm and store at 4 °C until needed.

-Appendix B-

ATP Assay Analysis Protocol

Materials Needed

1. ATP Determination Kit (Sigma # FLAA)
2. White/white 96-well plate (VWR # 82050-726)

ATP Assay (Prepare stock solutions no more than 24 hours prior to experiments)

1. Add 5.0 ml of dH₂O to ATP assay mix (good for 2-3 weeks in 0C)
2. Add 50.0 ml of dH₂O to dilution buffer
3. Dilute stock ATP to several 10 μ M aliquots (good for 2-3 weeks in -20C)
4. Before experiment, make standard ATP concentrations and store in ice bucket (good for a few hours)
 - a. 100 pM, 500 pM, 1000 pM, 5000 pM
 - b. Change if needed
5. Make ATP reaction buffer by diluting the assay mix with the dilution buffer (keep shielded from light)
 - a. With a fresh kit, typical range is 10:1 – 20:1. Stronger dilutions needed for lower ATP levels.
 - b. As kit ages, dilutions will need to be stronger
6. Gently invert tube to mix. **DO NOT VORTEX.**

7. Using the white 96-well plate, place 100 μL of reaction buffer with 100 μL of sample.
 - a. Make sure to fill 1 well with 100 μL of the reaction buffer with 100 μL of HBSS/dH₂O to take the background luminescence. Subtract this value from all measured values.
 - b. When setting up luminometer, make sure to choose “Luminescence” instead of “Absorbance” as the parameter
 - c. In the plate parameters, find the correct type of plate (For these experiments it was “white flat-bottom 96-well Costar”)
8. To create a standard curve, combine 100 μL of each standard with 100 μL of the reaction buffer.
9. Generate a standard curve. Plot ATP concentration (x-axis) vs luminescence (y-axis). Use a linear regression line to calculate sample concentration.

-Appendix C-

Fluorescence and Confocal Imaging Analysis Protocol

Cell Preparation

1. For calcein-AM imaging, cells must be loaded with dye for 30 minutes at 37°C. Concentration of the loading dye should be no higher than 5 μM .
2. To load dye, combine 10 μL of pluronic F-127 (Invitrogen # P3000MP) with the calcein-AM (Invitrogen # C3100MP). Mix the solution and add to 10 mL of your loading solution (typically HBSS). This will create a stock dye concentration of 7.6 μM . Dilute accordingly.
3. Wash cells 3x with HBSS after loading before starting experiments.
4. Mount coverslip onto chamber and begin perfusion with HBSS at a flow rate of 0.5 ml/min (set speed to 300 on peristaltic pump).

Imaging During Real-time Volume Experiments

1. For fluorescence experiments, 20x objective is typically used for a larger sample area. Slide the objective focuser ring to 0.17 if using a glass coverslip.
2. Turn on the components in the order of: microscope, camera, shutter, filter. Turn off in opposite order when done.
3. In order to find your specimen, use the “Illumination” drop-down box and click “Eyes-FITC”. Make sure that the shutter is in the “Open” state.
4. Once the cells are found, change the Illumination to “Camera-FITC cube”, make sure the shutter is open, then click the “Live” quicktab.

5. Before starting the real-time acquisition, click the “Configure acquisition” quicktab. Auto-expose if necessary, and change the “Frames to avg” to 2 or less. The higher the “Frames to avg”, the clearer the picture, but the cells will exhibit more photobleaching.
6. To start a real-time acquisition, click “Acquire” >>> “Acquire timelapse”. Select your time interval (typically 2 seconds or less), and duration. Select your destination folder and press “OK”.
7. Once your timelapse starts, you can pause or stop at any time with the appropriate buttons. In order to monitor the fluorescence intensity during the experiment, simply pause the experiment after the first image. Click on the “Ellipse region” quicktab and draw regions around the cells. Then click “Measure” >>> “Region measurements”. The graph will come up showing the intensity values. Make sure that the X-axis is the elapsed time. Resume the experiments until it ends.
8. Once the experiment ends, save the time series. You can then draw more accurate regions with the “multi-line” region tool to get more accurate fluorescence intensity data.
9. In the region measurements box, click the “Measurements” tab, make sure that you have charted both “Elapsed time” and “Average Intensity”, then click “Open Log”. Press “OK with the “Text File” box checked. Save the .LOG file in the desired folder, then press F9 to log the data. When you are done with the

experiment, click the “Log” tab in the menu, then “Close data log”. This must be done in order to create separate logs for each experiment.

10. These .LOG files can be opened in Excel and then converted to graphs with the desired axes.

Confocal Imaging

1. Repeat steps 1-4 as for the volume imaging with the only difference being that you will use a higher objective magnification (preferably 40x or 60x oil).
2. The confocal microscope must be turned on by pressing the “Select DISK-IN.JNL” quicktab.
3. To allow for maximum light, click “Device” >>> “Device control” >>> “Component control”. The component should be set to “Olympus ND” and the position should be set to “100%”. For normal fluorescence imaging, this should be set to no higher than “6%” in order to prevent photobleaching.
4. Click the “Multi-dimensional acquisition” quicktab. The settings in this box are very important so ensure that all settings are what you desire for your experiment.
 - a. Main- select “Z-series”.
 - b. Saving- select the directory in which you will save the files, as well as the base name for your files.
 - c. Wavelength- choose FITC Cube. Experiment with the EM gain and exposure beforehand using the “Configure acquisition” tab as explained in Step 5 under “Volume Experiments” to determine the best settings. For

scientific accuracy, the EM gain should be kept the same for all experiments; however the exposure time can be adjusted.

- d. Z-series- Manually adjust the focus using the “Step focus up” and “Step focus down” quick tabs to determine the bottom and top limits for your z-stack. It is always better to overshoot the cell, as you can always trim the stack later. The recommended step size should be 0.2 μm if you are using an oil objective, but do not set the step size any smaller than the recommended size. The number of steps will be automated.
- e. Check your summary to make sure everything is where you want it, then click “Acquire” to start the experiment.

Confocal Post-Imaging Analysis

1. Open the image stack using Metamorph Premier Offline.
2. Deconvolve the image by selecting “Process” >>> “3D Deconvolution” >>> “AutoQuant Deconvolution”.
 - a. This will sharpen your image and remove out-of-focus intensities that could interfere with area measurements
 - b. Default settings are appropriate at 40 iterations. Click “Apply”
3. Find the plane that you will consider as the bottom of the cell. This plane will have the largest area of cells.
4. On the left side of the image window, Click “Threshold” >>> “Inclusive Threshold”. Then Click “Threshold Image” in the same drop down menu.

- a. Play with the low end slider bar until you find an appropriate intensity that accurately includes the entirety of the cell without picking up intensity measurements outside of the cells.
5. Click on “Measure” >>> “Integrated Morphometry Analysis”
 - a. Under “Area”, check “Display” and “Filter”. Under “Comparison” change to “>=”, and change “Limit 1” to “100” (This prevents random individual pixels from being counted by the program”
 - b. Click “Measure”. This will convert your region to a green color, which is now an Object.
6. Click the quicktab “Create Regions Around Objects”
7. Click “Measure” >>> “Region Measurements”
 - a. This will provide the area (in pixels) of each object. Since each pixel is $0.4 \mu\text{m} \times 0.4 \mu\text{m}$, multiply the area by 0.16 to get the area (μm^2).
8. Insert the areas into an Excel spreadsheet to keep track of each cell’s area per image plane.
9. Click the quicktab “Clear Overlay” >>> “Clear Object Overlay”. Click the quicktab “Clear All Regions”
 - a. This will reset your image planes to the original setting.
10. Move on to the next image plane and repeat from Step 5.

-Appendix D-

Pressure Chambers Used in Experiments

Original Custom-made Pressure Chamber



Figure A-1: Pressure chamber in cell culture incubator

- Original pressure chamber used in ATP experiments in Aim 1
- Measures 12" x 8" x 3"
- Pressure is applied to cultured cells via 5% CO₂/air mixture regulated by custom Labview program
- **Pros**
 - Application of pressure via gas allows for higher pressures (>40 cmH₂O)
 - Experiments can be conducted at 37°C in 5% CO₂/95% air environment
 - Labview programming provides high accuracy of pressure application (tolerance of ~0.1 cmH₂O).
- **Cons**
 - Inherent design limitations prevent multiple ATP samples taken from same experimental group during pressure application
 - Handling of petri dishes can cause elevated levels of extracellular ATP

Warner RC-21 Large Closed Bath Imaging Chamber



Figure A-2: Assembled view of Warner RC-21 chamber

- Chamber used in first cell volume imaging experiments
- Total bath volume = 358 μ l
- Vacuum grease was used to adhere coverslip to chamber
- **Pros**
 - Laminar flow
 - Stage adapter allows for stable chamber during experiments
 - Large window allows for higher sample size
- **Cons**
 - Hard to achieve a good seal under elevated pressures
 - Pressure causes bowing of coverslip due to large window

Custom-fabricated Perfusion Chamber

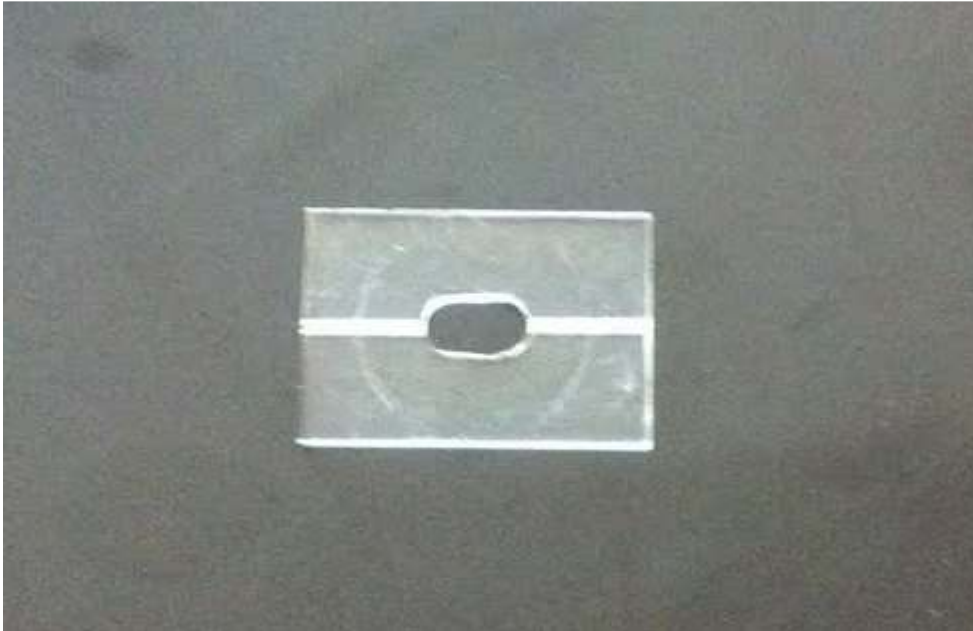


Figure A-3: Top-down view of custom perfusion chamber

- Chamber used for majority of fluorescence imaging and confocal imaging
- Designed by Kevin Champaigne to have similar dimensions as Warner chamber with a smaller window
- Double sided tape was used to adhere coverslip to chamber
- **Pros**
 - Smaller window mitigated effects of pressure on coverslip deformation
 - Double-sided tape achieved better seal under pressure than vacuum grease
- **Cons**
 - Design of chamber did not ensure uniform laminar flow
 - Double-sided tape application required longer set-up times between experiments

Vacu-cell™ Laminar Flow Chamber

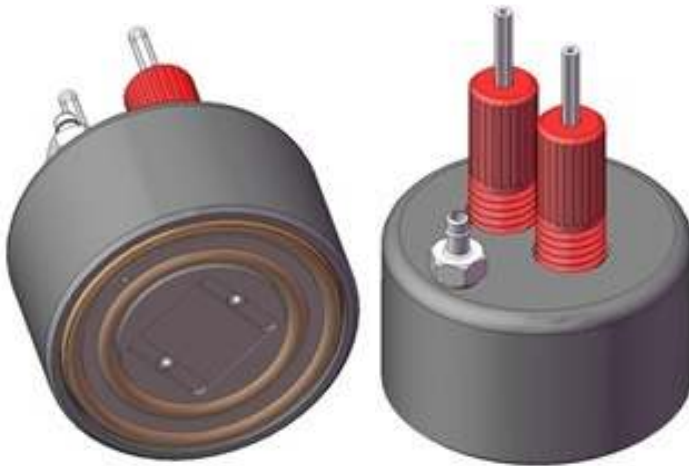


Figure A-4: 3-D CAD diagrams of the perfusion side (left) and vacuum side (right) of the Vacu-cell™ flow chamber.

- Chamber used during ATP perfusion experiments
- Vacuum applied to coverslip seals the chamber
- Total bath volume = 17.4 μ l
- **Pros**
 - Vacuum seal eliminates leakage and vastly improves set-up times
 - Small bath volume requires less solution per experiment
- **Cons**
 - Small viewing window limits sample size during imaging experiments
 - Small bath volume requires much lower flow rate to lessen shear stress

-References-

1. Ganz, M.L., et al., *Economic Costs of Overactive Bladder in the United States*. Urology, 2010. **75**(3): p. 526-532.e18.
2. Li, M., et al., *Augmented bladder urothelial polyamine signaling and block of BK channel in the pathophysiology of overactive bladder syndrome*. Am J Physiol Cell Physiol, 2009. **297**(6): p. C1445-51.
3. de Groat, W.C., *The urothelium in overactive bladder: Passive bystander or active participant?* Urology, 2004. **64**(Supplement 1): p. 7-11.
4. Levin, R.M., et al., *Update on bladder smooth-muscle physiology*. World J Urol, 1994. **12**(5): p. 226-32.
5. Birder, L.A. and W.C. de Groat, *Mechanisms of disease: involvement of the urothelium in bladder dysfunction*. Nat Clin Pract Urol, 2007. **4**(1): p. 46-54.
6. Apodaca, G., *The Uroepithelium: Not Just a Passive Barrier*. Traffic, 2004. **5**(3): p. 117-128.
7. Lincoln, J., et al., *Innervation of normal human sural and optic nerves by noradrenaline- and peptide-containing nervi vasorum and nervorum: effect of diabetes and alcoholism*. Brain Res, 1993. **632**(1-2): p. 48-56.
8. Andersson, K.-E., *Bladder activation: afferent mechanisms*. Urology, 2002. **59**(5, Supplement 1): p. 43-50.
9. Gabella, G. and C. Davis, *Distribution of afferent axons in the bladder of rats*. J Neurocytol, 1998. **27**(3): p. 141-55.

10. de Groat, W.C. and N. Yoshimura, *Pharmacology of the lower urinary tract*. Annu Rev Pharmacol Toxicol, 2001. **41**: p. 691-721.
11. de Groat, W.C., *A neurologic basis for the overactive bladder*. Urology, 1997. **50**(6A Suppl): p. 36-52; discussion 53-6.
12. Habler, H.J., W. Janig, and M. Koltzenburg, *Activation of unmyelinated afferent fibres by mechanical stimuli and inflammation of the urinary bladder in the cat*. J Physiol, 1990. **425**: p. 545-62.
13. Barrick, S., et al., *Receptors and channels: TRPV4 receptors in urinary bladder urothelium: involvement in urinary bladder function*. The Journal of Pain, 2004. **5**(3, Supplement 1): p. S10-S10.
14. Du, S., et al., *Amiloride-Sensitive Ion Channels in Urinary Bladder Epithelium Involved in Mechanosensory Transduction by Modulating Stretch-Evoked Adenosine Triphosphate Release*. Urology, 2007. **69**(3): p. 590-595.
15. Ferguson, D., et al, *ATP is released from rabbit urinary bladder epithelial cells by hydrostatic pressure changes -- a possible sensory mechanism?* Journal of Physiology, 1997. **505**(2): p. 503-11.
16. Wang, E.C., et al., *ATP and purinergic receptor-dependent membrane traffic in bladder umbrella cells*. J Clin Invest, 2005. **115**(9): p. 2412-22.
17. Burnstock, G., *P2X receptors in sensory neurones*. Br. J. Anaesth., 2000. **84**(4): p. 476-488.

18. Rapp, D.E., et al., *A Role for the P2X Receptor in Urinary Tract Physiology and in the Pathophysiology of Urinary Dysfunction*. *European Urology*, 2005. **48**(2): p. 303-308.
19. O'Reilly, B.A., et al., *P2X Receptors and their Role in Female Idiopathic Detrusor Instability*. *The Journal of Urology*, 2002. **167**(1): p. 157-164.
20. North, R.A., *P2X3 receptors and peripheral pain mechanisms*. *J Physiol*, 2004. **554**(2): p. 301-308.
21. Cockayne, D.A., et al., *Urinary bladder hyporeflexia and reduced pain-related behaviour in P2X3-deficient mice*. *Nature*, 2000. **407**(6807): p. 1011-5.
22. Vlaskovska, M., et al., *P2X3 Knock-Out Mice Reveal a Major Sensory Role for Urothelially Released ATP*. *J. Neurosci.*, 2001. **21**(15): p. 5670-5677.
23. Weyts, F.A., et al., *Mechanical control of human osteoblast apoptosis and proliferation in relation to differentiation*. *Calcif Tissue Int*, 2003. **72**(4): p. 505-12.
24. Mizuno, S., *A novel method for assessing effects of hydrostatic fluid pressure on intracellular calcium: a study with bovine articular chondrocytes*. *Am J Physiol Cell Physiol*, 2005. **288**(2): p. C329-37.
25. Alenghat, F.J. and D.E. Ingber, *Mechanotransduction: All Signals Point to Cytoskeleton, Matrix, and Integrins*. *Sci. STKE*, 2002. **2002**(119): p. pe6-.
26. Alenghat, F.J., et al., *Global cytoskeletal control of mechanotransduction in kidney epithelial cells*. *Experimental Cell Research*, 2004. **301**(1): p. 23-30.

27. Ingber, D.E., *Mechanosensation through integrins: cells act locally but think globally*. Proc Natl Acad Sci U S A, 2003. **100**(4): p. 1472-4.
28. Burridge, K., et al., *Focal adhesions: transmembrane junctions between the extracellular matrix and the cytoskeleton*. Annu Rev Cell Biol, 1988. **4**: p. 487-525.
29. Sawada, Y. and M.P. Sheetz, *Force transduction by Triton cytoskeletons*. J Cell Biol, 2002. **156**(4): p. 609-15.
30. Li, W., et al., *Integrin and FAK-mediated MAPK activation is required for cyclic strain mitogenic effects in Caco-2 cells*. Am J Physiol Gastrointest Liver Physiol, 2001. **280**(1): p. G75-87.
31. Araki, I., et al., *Roles of mechanosensitive ion channels in bladder sensory transduction and overactive bladder*. International Journal of Urology, 2008. **15**(0): p. 681-687.
32. Yao, X. and C.J. Garland, *Recent Developments in Vascular Endothelial Cell Transient Receptor Potential Channels*. Circ Res, 2005. **97**(9): p. 853-863.
33. Wang, E.C.Y., et al., *Hydrostatic pressure-regulated ion transport in bladder uroepithelium*. Am J Physiol Renal Physiol, 2003. **285**(4): p. F651-663.
34. Guharay, F. and F. Sachs, *Stretch-activated single ion channel currents in tissue-cultured embryonic chick skeletal muscle*. J Physiol, 1984. **352**: p. 685-701.
35. Sackin, H., *Stretch-activated ion channels*. Kidney Int, 1995. **48**(4): p. 1134-1147.

36. Filipovic, D. and H. Sackin, *A calcium-permeable stretch-activated cation channel in renal proximal tubule*. Am J Physiol, 1991. **260**(1 Pt 2): p. F119-29.
37. Lansman, J.B., T.J. Hallam, and T.J. Rink, *Single stretch-activated ion channels in vascular endothelial cells as mechanotransducers?* Nature, 1987. **325**(6107): p. 811-3.
38. Lang, F., et al., *Functional significance of cell volume regulatory mechanisms*. Physiol Rev, 1998. **78**(1): p. 247-306.
39. Niisato, N. and Y. Marunaka, *Osmotransduction Through Volume-Sensitive Cl Channels*, in *Mechanosensitive Ion Channels*, I.K. Andre Kamkin, Editor 2008, Springer. p. 179-202.
40. Niisato, N., Y. Ito, and Y. Marunaka, *Activation of Cl⁻ channel and Na⁺/K⁺/2Cl⁻ cotransporter in renal epithelial A6 cells by flavonoids: genistein, daidzein, and apigenin*. Biochem Biophys Res Commun, 1999. **254**(2): p. 368-71.
41. Baumgarten, C.M. and H.F. Clemo, *Swelling-activated chloride channels in cardiac physiology and pathophysiology*. Prog Biophys Mol Biol, 2003. **82**(1-3): p. 25-42.
42. Kohler, R., et al., *Regulation of pressure-activated channel in intact vascular endothelium of stroke-prone spontaneously hypertensive rats*. Am J Hypertens, 2001. **14**(7 Pt 1): p. 716-21.

43. Roberts, S.R., et al., *Mechanical compression influences intracellular Ca²⁺ signaling in chondrocytes seeded in agarose constructs*. J Appl Physiol, 2001. **90**(4): p. 1385-1391.
44. Rosenbaum, T., et al., *Ca²⁺/Calmodulin Modulates TRPV1 Activation by Capsaicin*. J. Gen. Physiol., 2003. **123**(1): p. 53-62.
45. Birder, L., et al., *Activation of Urothelial Transient Receptor Potential Vanilloid 4 by 4 α -Phorbol 12,13-Didecanoate Contributes to Altered Bladder Reflexes in the Rat*. J Pharmacol Exp Ther, 2007. **323**(1): p. 227-235.
46. Birder, L.A., et al., *Vanilloid receptor expression suggests a sensory role for urinary bladder epithelial cells*. Proceedings of the National Academy of Sciences, 2001. **98**(23): p. 13396-13401.
47. Daly, D., et al., *Bladder afferent sensitivity in wild-type and TRPV1 knockout mice*. The Journal of Physiology, 2007. **583**(2): p. 663-674.
48. Ross, R.A., *Anandamide and vanilloid TRPV1 receptors*. Br J Pharmacol, 2003. **140**(5): p. 790-801.
49. Apostolidis, A., et al., *Capsaicin receptor TRPV1 in urothelium of neurogenic human bladders and effect of intravesical resiniferatoxin*. Urology, 2005. **65**(2): p. 400-405.
50. Birder, L.A., et al, *Altered urinary bladder function in mice lacking the vanilloid receptor*. Nat. Neurosci, 2002. **5**: p. 856-860.

51. Chuang, Y.C., et al., *Analysis of the afferent limb of the vesicovascular reflex using neurotoxins, resiniferatoxin and capsaicin*. *Am J Physiol Regul Integr Comp Physiol*, 2001. **281**(4): p. R1302-10.
52. Guler, A.D., et al., *Heat-Evoked Activation of the Ion Channel, TRPV4*. *J. Neurosci.*, 2002. **22**(15): p. 6408-6414.
53. Delany, N.S., et al., *Identification and characterization of a novel human vanilloid receptor-like protein, VRL-2*. *Physiol Genomics*, 2001. **4**(3): p. 165-74.
54. Nilius, B., et al., *TRPV4 calcium entry channel: a paradigm for gating diversity*. *Am J Physiol Cell Physiol*, 2004. **286**(2): p. C195-205.
55. Stein, R.J., et al., *Cool (TRPM8) and hot (TRPV1) receptors in the bladder and male genital tract*. *J Urol*, 2004. **172**(3): p. 1175-8.
56. Du, S., et al., *Differential expression profile of cold (TRPA1) and cool (TRPM8) receptors in human urogenital organs*. *Urology*, 2008. **72**(2): p. 450-5.
57. Schild, L., et al., *Identification of Amino Acid Residues in the alpha , beta , and gamma Subunits of the Epithelial Sodium Channel (ENaC) Involved in Amiloride Block and Ion Permeation*. *J. Gen. Physiol.*, 1997. **109**(1): p. 15-26.
58. Canessa, C.M., et al., *Amiloride-sensitive epithelial Na⁺ channel is made of three homologous subunits*. *Nature*, 1994. **367**(6462): p. 463-7.
59. Drummond, H.A., F.M. Abboud, and M.J. Welsh, *Localization of beta and gamma subunits of ENaC in sensory nerve endings in the rat foot pad*. *Brain Res*, 2000. **884**(1--2): p. 1-12.

60. Fricke, B., et al., *Epithelial Na⁺ channels and stomatin are expressed in rat trigeminal mechanosensory neurons*. Cell Tissue Res, 2000. **299**(3): p. 327-34.
61. Welsh, M.J., M.P. Price, and J. Xie, *Biochemical Basis of Touch Perception: Mechanosensory Function of Degenerin/Epithelial Na⁺ Channels*. J. Biol. Chem., 2002. **277**(4): p. 2369-2372.
62. Mobasheri, A., C. Dart, and R. Barret-Joley, *Potassium Ion Channels in Articular Chondrocytes*, in *Mechanosensitive Ion Channels*, A. Kamkin and I. Kiseleva, Editors. 2008, Springer. p. 157-178.
63. Mobasheri, A., et al., *Integrins and stretch activated ion channels; putative components of functional cell surface mechanoreceptors in articular chondrocytes*. Cell Biol Int, 2002. **26**(1): p. 1-18.
64. Bonewald, L.F., *Mechanosensation and Transduction in Osteocytes*. Bonekey Osteovision, 2006. **3**(10): p. 7-15.
65. Liedert, A., L. Claes, and A. Ignatius, *Signal Transduction Pathways Involved in Mechanotransduction in Osteoblastic and Mesenchymal Stem Cells*, in *Mechanosensitive Ion Channels*, A. Kamkin and I. Kiseleva, Editors. 2008, Springer. p. 253-265.
66. Davidson, R.M., D.W. Tatakis, and A.L. Auerbach, *Multiple forms of mechanosensitive ion channels in osteoblast-like cells*. Pflugers Arch, 1990. **416**(6): p. 646-51.

67. Kizer, N., X.L. Guo, and K. Hruska, *Reconstitution of stretch-activated cation channels by expression of the alpha-subunit of the epithelial sodium channel cloned from osteoblasts*. Proc Natl Acad Sci U S A, 1997. **94**(3): p. 1013-8.
68. Barakat, A.I., D.K. Lieu, and A. Gojova, *Secrets of the code: Do vascular endothelial cells use ion channels to decipher complex flow signals?* Biomaterials, 2006. **27**(5): p. 671-678.
69. Maroto, R., et al., *TRPC1 forms the stretch-activated cation channel in vertebrate cells*. Nat Cell Biol, 2005. **7**(2): p. 179-85.
70. Muraki, K., et al., *TRPV2 is a component of osmotically sensitive cation channels in murine aortic myocytes*. Circ Res, 2003. **93**(9): p. 829-38.
71. Yao, X., et al., *A protein kinase G-sensitive channel mediates flow-induced Ca(2+) entry into vascular endothelial cells*. Faseb J, 2000. **14**(7): p. 932-8.
72. Althaus, M., et al., *Mechano-sensitivity of epithelial sodium channels (ENaCs): laminar shear stress increases ion channel open probability*. FASEB J., 2007. **21**(10): p. 2389-2399.
73. Apodaca, G., et al., *Disruption of bladder epithelium barrier function after spinal cord injury*. Am J Physiol Renal Physiol, 2003. **284**(5): p. F966-76.
74. Lewis, S.A. and J.R. Lewis, *Kinetics of urothelial ATP release*. Am J Physiol Renal Physiol, 2006. **291**(2): p. F332-340.
75. Novak, I., *ATP as a signaling molecule: the exocrine focus*. News Physiol Sci, 2003. **18**: p. 12-7.

76. Stout, C.E., et al., *Intercellular calcium signaling in astrocytes via ATP release through connexin hemichannels*. J Biol Chem, 2002. **277**(12): p. 10482-8.
77. Reisin, I.L., et al., *The cystic fibrosis transmembrane conductance regulator is a dual ATP and chloride channel*. J Biol Chem, 1994. **269**(32): p. 20584-91.
78. Ferguson, D.R., *Urothelial function*. BJU Int, 1999. **84**(3): p. 235-42.
79. Liedtke, W., et al., *Mammalian TRPV4 (VR-OAC) directs behavioral responses to osmotic and mechanical stimuli in Caenorhabditis elegans*. Proceedings of the National Academy of Sciences, 2003. **100**(90002 November 25, 2003): p. 14531-14536.
80. Suzuki, M., et al., *Impaired pressure sensation in mice lacking TRPV4*. J Biol Chem, 2003. **278**(25): p. 22664-8.
81. Araki, I., et al., *Overexpression of epithelial sodium channels in epithelium of human urinary bladder with outlet obstruction*. Urology, 2004. **64**(6): p. 1255-60.
82. Birder, L.A., et al., *Feline interstitial cystitis results in mechanical hypersensitivity and altered ATP release from bladder urothelium*. Am J Physiol Renal Physiol, 2003. **285**(3): p. F423-9.
83. Ganz, M.L., et al., *Economic costs of overactive bladder in the United States*. Urology, 2010. **75**(3): p. 526-32, 532 e1-18.
84. Streng, T., et al., *Distribution and Function of the Hydrogen Sulfide-Sensitive TRPA1 Ion Channel in Rat Urinary Bladder*. European Urology, 2008. **53**(2): p. 391-400.

85. Yu, W., P. Khandelwal, and G. Apodaca, *Distinct apical and basolateral membrane requirements for stretch-induced membrane traffic at the apical surface of bladder umbrella cells*. Mol Biol Cell, 2009. **20**(1): p. 282-95.
86. Mochizuki, T., et al., *The TRPV4 cation channel mediates stretch-evoked Ca²⁺ influx and ATP release in primary urothelial cell cultures*. J Biol Chem, 2009. **284**(32): p. 21257-64.
87. Nagatomi, J., et al., *Frequency- and duration-dependent effects of cyclic pressure on select bone cell functions*. Tissue Eng, 2001. **7**(6): p. 717-28.
88. Lewis, S.A., *Everything you wanted to know about the bladder epithelium but were afraid to ask*. Am J Physiol Renal Physiol, 2000. **278**(6): p. F867-74.
89. Gevaert, T., et al., *Autonomous contractile activity in the isolated rat bladder is modulated by a TRPV1 dependent mechanism*. NeuroUrol Urodyn, 2007. **26**(3): p. 424-32; discussion 451-3.
90. Birder, L.A., *Urinary bladder urothelium: Molecular sensors of chemical/thermal/mechanical stimuli*. Vascular Pharmacology, 2006. **45**(4): p. 221-226.
91. Lindstrom, S. and L. Mazieres, *Effect of menthol on the bladder cooling reflex in the cat*. Acta Physiol Scand, 1991. **141**(1): p. 1-10.
92. Chopra, B., et al., *Expression and function of bradykinin B1 and B2 receptors in normal and inflamed rat urinary bladder urothelium*. J Physiol, 2005. **562**(Pt 3): p. 859-71.

93. Lee, H.Y., M. Bardini, and G. Burnstock, *Distribution of P2X receptors in the urinary bladder and the ureter of the rat*. J Urol, 2000. **163**(6): p. 2002-7.
94. Matsumoto-Miyai, K., et al., *Extracellular Ca²⁺ regulates the stimulus-elicited ATP release from urothelium*. Auton Neurosci, 2009. **150**(1-2): p. 94-9.
95. Kurzrock, E.A., et al., *Rat urothelium: improved techniques for serial cultivation, expansion, freezing and reconstitution onto acellular matrix*. The Journal of Urology, 2005. **173**(1): p. 281-285.
96. Stover, J. and J. Nagatomi, *Cyclic pressure stimulates DNA synthesis through the PI3K/Akt signaling pathway in rat bladder smooth muscle cells*. Ann Biomed Eng, 2007. **35**(9): p. 1585-94.
97. Daneshgari, F., et al., *Temporal differences in bladder dysfunction caused by diabetes, diuresis, and treated diabetes in mice*. Am J Physiol Regul Integr Comp Physiol, 2006. **290**(6): p. R1728-35.
98. Nakada, Y., et al., *Effects of aniracetam on bladder overactivity in rats with cerebral infarction*. J Pharmacol Exp Ther, 2000. **293**(3): p. 921-8.
99. O'Connor, L.T., Jr., E.D. Vaughan, Jr., and D. Felsen, *In vivo cystometric evaluation of progressive bladder outlet obstruction in rats*. J Urol, 1997. **158**(2): p. 631-5.
100. Ethier, C.R. and C.A. Simmons, *Introductory Biomechanics* 2007, Cambridge, UK: Cambridge University Press.

101. Rabbany, S.Y., J.T. Funai, and A. Noordergraaf, *Pressure generation in a contracting myocyte*. Heart Vessels, 1994. **9**(4): p. 169-74.
102. McCleskey, E.W. and M.S. Gold, *Ion channels of nociception*. Annu Rev Physiol, 1999. **61**: p. 835-56.
103. Caterina, M.J., *Ion Channels and Thermotransduction*, in *Transduction Channels in Sensory Cells*, S. Frings and J. Bradley, Editors. 2004, WILEY-VCH: Weinheim. p. 235-249.
104. Sigurdson, W., A. Ruknudin, and F. Sachs, *Calcium imaging of mechanically induced fluxes in tissue-cultured chick heart: role of stretch-activated ion channels*. Am J Physiol, 1992. **262**(4 Pt 2): p. H1110-5.
105. Petersen, C.C., et al., *Putative capacitance calcium entry channels: expression of Drosophila trp and evidence for the existence of vertebrate homologues*. Biochem J, 1995. **311** (Pt 1): p. 41-4.
106. Birder, L.A., et al., *Beta-adrenoceptor agonists stimulate endothelial nitric oxide synthase in rat urinary bladder urothelial cells*. J Neurosci, 2002. **22**(18): p. 8063-70.
107. Caterina, M.J., et al., *Impaired nociception and pain sensation in mice lacking the capsaicin receptor*. Science, 2000. **288**(5464): p. 306-13.
108. Hamill, O.P., *Twenty odd years of stretch-sensitive channels*. Pflugers Arch, 2006. **453**(3): p. 333-51.

109. Inoue, R., et al., *The transient receptor potential protein homologue TRP6 is the essential component of vascular alpha(1)-adrenoceptor-activated Ca(2+)-permeable cation channel*. *Circ Res*, 2001. **88**(3): p. 325-32.
110. Hosoki, E. and T. Iijima, *Chloride-sensitive Ca²⁺ entry by histamine and ATP in human aortic endothelial cells*. *Eur J Pharmacol*, 1994. **266**(3): p. 213-8.
111. Hosoki, E. and T. Iijima, *Modulation of cytosolic Ca²⁺ concentration by thapsigargin and cyclopiazonic acid in human aortic endothelial cells*. *Eur J Pharmacol*, 1995. **288**(2): p. 131-7.
112. Myers, K.A., et al., *Hydrostatic pressure sensation in cells: integration into the tensegrity model*. *Biochemistry and Cell Biology-Biochimie Et Biologie Cellulaire*, 2007. **85**(5): p. 543-551.
113. Yoshida, M., et al., *Non-neuronal cholinergic system in human bladder urothelium*. *Urology*, 2006. **67**(2): p. 425-430.
114. Namasivayam, Eardley, and Morrison, *Purinergic sensory neurotransmission in the urinary bladder: an in vitro study in the rat*. *BJU International*, 1999. **84**(7): p. 854-860.
115. Olsen, S.M., J.D. Stover, and J. Nagatomi, *Examining the Role of Mechanosensitive Ion Channels in Pressure Mechanotransduction in Rat Bladder Urothelial Cells*. *Ann Biomed Eng*, 2011. **39**(2): p. 688-697.

116. Liedtke, W. and J.M. Friedman, *Abnormal osmotic regulation in trpv4-/- mice*. Proceedings of the National Academy of Sciences, 2003. **100**(23): p. 13698-13703.
117. Strotmann, R., et al., *OTRPC4, a nonselective cation channel that confers sensitivity to extracellular osmolarity*. Nat Cell Biol, 2000. **2**(10): p. 695-702.
118. Mandal, A., M. Shahidullah, and N.A. Delamere, *Hydrostatic Pressure-Induced Release of Stored Calcium in Cultured Rat Optic Nerve Head Astrocytes*. Investigative Ophthalmology & Visual Science, 2010. **51**(6): p. 3129-3138.
119. Boudreault, F. and R. Grygorczyk, *Cell swelling-induced ATP release and gadolinium-sensitive channels*. American Journal of Physiology - Cell Physiology, 2002. **282**(1): p. C219-C226.
120. Wang, Y., et al., *Autocrine signaling through ATP release represents a novel mechanism for cell volume regulation*. Proceedings of the National Academy of Sciences, 1996. **93**(21): p. 12020-12025.
121. Braunstein, G.M., et al., *Cystic Fibrosis Transmembrane Conductance Regulator Facilitates ATP Release by Stimulating a Separate ATP Release Channel for Autocrine Control of Cell Volume Regulation*. Journal of Biological Chemistry, 2001. **276**(9): p. 6621-6630.
122. Hazama, A., et al., *Swelling-Induced, Cfr-Independent Atp Release from a Human Epithelial Cell Line*. The Journal of General Physiology, 1999. **114**(4): p. 525-533.

123. Koyama, T., M. Oike, and Y. Ito, *Involvement of Rho-kinase and tyrosine kinase in hypotonic stress-induced ATP release in bovine aortic endothelial cells*. The Journal of Physiology, 2001. **532**(3): p. 759-769.
124. Hamann, S., et al., *Measurement of Cell Volume Changes by Fluorescence Self-Quenching*. Journal of Fluorescence, 2002. **12**(2): p. 139-145.
125. Tschumperlin, D.J., et al., *Mechanotransduction through growth-factor shedding into the extracellular space*. Nature, 2004. **429**(6987): p. 83-6.
126. Oberleithner, H., et al., *Human Endothelium: Target for Aldosterone*. Hypertension, 2004. **43**(5): p. 952-956.
127. Jakubovicz, D.E., S. Grinstein, and A. Klip, *Cell swelling following recovery from acidification in C6 glioma cells: an in vitro model of postischemic brain edema*. Brain Research, 1987. **435**(1-2): p. 138-146.
128. Kreisberg, J.I., et al., *Protection of cultured renal tubular epithelial cells from anoxic cell swelling and cell death*. Proceedings of the National Academy of Sciences, 1980. **77**(9): p. 5445-5447.
129. Becker, D., et al., *TRPV4 exhibits a functional role in cell-volume regulation*. J Cell Sci, 2005. **118**(11): p. 2435-2440.
130. Myers, K.A., et al., *Hydrostatic pressure sensation in cells: integration into the tensegrity model*. Biochem Cell Biol, 2007. **85**(5): p. 543-51.

131. Rauch, C., et al., *On Some Aspects of the Thermodynamic of Membrane Recycling Mediated by Fluid Phase Endocytosis: Evaluation of Published Data and Perspectives*. Cell Biochemistry and Biophysics, 2010. **56**(2): p. 73-90.
132. Olsen, S.M., J.D. Stover, and J. Nagatomi, *Examining the Role of Mechanosensitive Ion Channels in Pressure Mechanotransduction in Rat Bladder Urothelial Cells*. Ann Biomed Eng, 2010.
133. Boudreault, F. and R. Grygorczyk, *Cell swelling-induced ATP release and gadolinium-sensitive channels*. Am J Physiol Cell Physiol, 2002. **282**(1): p. C219-26.
134. Burnstock, G. and M. Williams, *P2 purinergic receptors: modulation of cell function and therapeutic potential*. J Pharmacol Exp Ther, 2000. **295**(3): p. 862-9.
135. Dubyak, G.R. and C. el-Moatassim, *Signal transduction via P2-purinergic receptors for extracellular ATP and other nucleotides*. Am J Physiol, 1993. **265**(3 Pt 1): p. C577-606.
136. Sun, Y., et al., *Augmented stretch activated adenosine triphosphate release from bladder uroepithelial cells in patients with interstitial cystitis*. J Urol, 2001. **166**(5): p. 1951-6.
137. Sun, Y., et al., *Stretch-activated release of adenosine triphosphate by bladder uroepithelia is augmented in interstitial cystitis*. Urology, 2001. **57**(6 Suppl 1): p. 131.

138. Gevaert, T., et al., *Deletion of the transient receptor potential cation channel TRPV4 impairs murine bladder voiding*. J Clin Invest, 2007. **117**(11): p. 3453–3462.
139. Ohashi, T., et al., *Hydrostatic pressure influences morphology and expression of VE-cadherin of vascular endothelial cells*. Journal of Biomechanics, 2007. **40**(11): p. 2399-2405.
140. Rossi, M.R., et al., *The immortalized UROtsa cell line as a potential cell culture model of human urothelium*. Environ Health Perspect, 2001. **109**(8): p. 801-8.
141. Charrua, A., et al., *Functional Transient Receptor Potential Vanilloid 1 is Expressed in Human Urothelial Cells*. J Urol, 2009. **182**(6): p. 2944-2950.
142. Yamada, T., et al., *TRPV2 activation induces apoptotic cell death in human T24 bladder cancer cells: a potential therapeutic target for bladder cancer*. Urology, 2010. **76**(2): p. 509 e1-7.
143. Sun, Y. and T.C. Chai, *Augmented extracellular ATP signaling in bladder urothelial cells from patients with interstitial cystitis*. Am J Physiol Cell Physiol, 2006. **290**(1): p. C27-34.
144. Hamill, O.P. and D.W. McBride, Jr., *The pharmacology of mechanogated membrane ion channels*. Pharmacol Rev, 1996. **48**(2): p. 231-52.
145. Bell, P.D., et al., *Macula densa cell signaling involves ATP release through a maxi anion channel*. Proceedings of the National Academy of Sciences, 2003. **100**(7): p. 4322-4327.

146. Hanrahan, J.W., W.P. Alles, and S.A. Lewis, *Single anion-selective channels in basolateral membrane of a mammalian tight epithelium*. Proc Natl Acad Sci U S A, 1985. **82**(22): p. 7791-5.